NANOSTRUCTURED SURFACES AND EMERGENT PHYSICAL BEHAVIOR

A Dissertation

Presented to

the Faculty of the Department of Mechanical Engineering

University of Houston

In Partial Fulfillment

of the Requirements for the Degree

Doctor of Philosophy

in Mechanical Engineering

by

Parnia Mohammadi

May 2012

Acknowledgements

It is a pleasure to thank the many people who helped me accomplish this great achievement. First, I would like to express my sincere gratitude to my advisor, Dr. Pradeep Sharma, for his constant support and guidance through this work, for his patience, motivation, enthusiasm, physical intuition and immense knowledge. His guidance helped me throughout the research and writing of this thesis. I also thank him for recommending me for the GK-12 fellowship upon entering the PhD program full time. This fellowship not only provided two years of support for me, but provided training and experience in teaching and professional development.

Besides my advisor, I would like to specially thank Dr. Liping Liu and Dr. Yashashree Kulkarni, for their unconditional support, for their willingness to have long discussions and guidance throughout this work. I am also grateful to the rest of my committee Dr. Lewis Wheeler, Dr. Stanko Brankovic and Dr. Ashutosh Agrawal for their availability and for accepting to be part of my thesis defense committee. I am very thankful to Trina Johnson, in the Department of Mechanical Engineering, for her patient assistance, her encouragement and being such a good friend. I also want to thank Dr. Haleh Ardebili for her useful guidance and advice.

I would like to commend Dr. Fritz Claydon, Dr. Eugene Chiappetta, Dr. Hanadi Rifai, Dr. Stuart Long, Maria Modeleska, Roberto Dimaliwat and all of my GK12 friends, including Rachel, Nathan, Nicole, Lynn, Crystal, Jennifer, Emil, Mansour, Mark, Christiana, Mircea and all the others who helped me through my amazing GK-12 experience.

I would like to acknowledge my labmates Sabri, Ravi, Nikhil, Feng, Gharbi, Prakash, Nejib, Fares, Afif, Swapnil, Fan, Raouf, Tanushree, Farah, Shangjie, Dengke, Shuyin, Mario, Nebiu, Majdi, Rutraparna, Nikhil and Qin for their constant support.

I am forever indebted to my family, in particular, my husband Hossein for his love, patience, emotional support and constant encouragement. This work would not have been possible without his presence and support. Also, I want to specially acknowledge my lovely son Borhan for keeping me busy and for making me a lot of fun.

Finally I want to thank my father Reza, my mother Mina, my sisters Parisa and Dena and my brother Hamid for their endless love and confidence. To my family, I dedicate this work.

NANOSTRUCTURED SURFACES AND EMERGENT PHYSICAL BEHAVIOR

An Abstract

of a

Dissertation

Presented to

the Faculty of the Department of Mechanical Engineering

University of Houston

In Partial Fulfillment

of the Requirements for the Degree

Doctor of Philosophy

in Mechanical Engineering

by

Parnia Mohammadi

May 2012

Abstract

Due to larger surface to volume ratio, surfaces play a significant role at the nanoscale. Surface atoms have different coordination numbers, charge distribution and subsequently different physical, mechanical and chemical properties. These differences are interpreted phenomenologically by postulating the existence of surface energy and acknowledging that the various bulk properties such as elastic modulus, melting temperature, and electromagnetic properties are different for surfaces.

In this dissertation, we consider two types of surfaces: those bounding a three-dimensional entity, and independent two-dimensional deformable surfaces that can be used to represent, for example, graphene sheets, thin films, and lipid bilayers among others.

In this dissertation:

(i) We develop a theoretical framework, complemented by atomistic calculations, that elucidates the effect of roughness on surface energy, stress and surface elasticity. We find that the residual surface stress is hardly affected by roughness while the superficial elastic properties are dramatically altered and, importantly, may also result in a change in its sign; this has significant ramifications in the interpretation of sensing based on frequency measurement changes. In particular, we also comment on the effect of roughness on the generally ignored term that represents the curvature dependence of surface energy, crystalline Tolman's length.

(ii) In the context of independent deformable surfaces, our focus is on electromechanical coupling; in particular, the rapidly emerging topic of flexoelectricity. Recent developments in flexoelectricity, especially in nanostructures, have lead to several interesting notions such as creating piezoelectric substances without using piezoelectric materials, enhanced energy harvesting at the nanoscale among others. In the biological context also, membrane flexoelectricity has been hypothesized to play an important role, e.g., biological mechano-transduction, hearing mechanisms. In this dissertation, we consider a heterogenous flexoelectric membrane, and derive the homogenized flexoelectric, dielectric and elastic response. In particular for purely fluid or lipid type membranes, we obtain exact results—one of very few in homogenization theory. Using quantum mechanical calculations, we also show that graphene can be designed to be pyroelectric, thus providing an avenue to create the thinnest possible thermo-electro-mechanical material.

Table of Contents

List of Figures

Chapter 1: Introduction and Overview

For a cubic piece of copper with 1 nm sides, nearly 64% of atoms reside on the surface. This simple fact makes apparent the enormous role surfaces play at the nanoscale. Surface atoms have different coordination numbers, charge distribution and subsequently different physical, mechanical and chemical properties. These differences are interpreted phenomenologically by postulating the existence of surface energy and acknowledging that the various bulk properties such as elastic modulus (Miller and Shenoy, 2000; Diao et al., 2004; Dingreville et al., 2005), melting temperature (Qi, 2005; Shim et al., 2002), electromagnetic properties (Eliseev et al., 2009; Sharma et al., 2010; Dai et al., 2011) among others are different for surfaces. These differences play an increasing role as the material characteristic size is shrunk smaller and smaller, for example, leading to size-dependency in the elastic modulus of nanostructures. Correspondingly, surface structures also play a significant role in renormalization of materials properties as well as leading to (sometimes) fundamentally new phenomena at the nanoscale. Therefore, one may consider intentionally nanostructuring the surface to design a tailored response.

In this dissertation we consider two types of surfaces: those bounding a three-dimensional entity and independent two-dimensional deformable surfaces that can be used to represent (for example) graphene sheets, thin films, and lipid bilayers among others.

Relating microstructure to properties, electromagnetic, mechanical, thermal and their couplings has been a major focus of mechanics, physics and materials science. The majority of the literature focuses on deriving homogenized constitutive responses for macroscopic composites relating effective properties to various microstructural details. In this dissertation, we depart from the usual practice and consider homogenization of heterogeneous surfaces. Surfaces of real materials, even the most thoroughly polished ones, will typically exhibit random roughness across different lateral length scales. How are the surface properties renormalized due to such roughness? Can the surface roughness be artificially tailored to obtain desired surface characteristics? In the first part of this work, we present theoretical derivations that relate both periodic and random roughness to the effective surface elastic behavior. In parallel to the theoretical calculations, we conduct atomistic simulations to further elucidate the interplay between surface energy and roughness. In particular, we also comment on the effect of roughness on the (generally ignored) term that represents the curvature dependence of surface energy (crystalline Tolman's length).

In the context of independent deformable surfaces, our focus is on electromechanical coupling in particular the rapidly emerging topic of flexoelectricity. Recently, flexoelectricity has attracted a fair amount of attention from both fundamental and applications points of view leading to intensive experimental (Ma and Cross, 2001, 2002, 2003; Catalan et al., 2004; Cross, 2006; Zubko et al. 2007) and theoretical (Sharma et al., 2007; Eliseev et al.

2009a, 2009b, 2011; Maranganti and Sharma, 2009) activity in this topic. Lack of symmetry at surfaces and the capability to support large strain gradient in nanoscale structures enables unusual forms of electromechanical coupling; For example, creating piezoelectric meta-material from a non-piezoelectric material has been investigated experimentally and computationally (Cross and co-workers, 1999, 2006a-c; Sharma et al. 2010, Baskaran et al., 2010). In fact, Chandratre and Sharma (2012) recently showed that predicated on the phenomenon of flexoelectricity, Graphene can be "coaxed" to behave like a piezoelectric material merely by creating holes of certain symmetry. The artificial piezoelectricity thus produced was found to be almost as strong as that of well-known piezoelectric substances such as quartz.

Several other works have appeared on elucidating flexoelectricity in two-dimensional structures (Naumov et al., 2009). Dumitrica et al. (2002) and Kalinin and Meunier (2008) showed that low dimensional systems such as graphene tend to exhibit electronic flexoelectricity, e.g., bending of non polar quantum systems leading to emergence of net dipole moments. Upon bending, redistribution of the electron gas in the normal direction results in the formation of a net dipole moment, and hence flexoelectric coupling. For large radii of curvatures and in the extreme case of closed seamless cylinder, the dipoles (formed) cancel out each other and the net polarization vanishes—which is why non-chiral (dielectric) carbon nanotubes have no dipole moment.

Flexoelectricity in curved structures has also been investigated in soft condensed materials such as liquid crystals and cellular membranes (Petrov et al., 1996, 1998, 2011; Kuczynski and Hoffmann, 2005; Spector, et al., 2006; Harden et al., 2010; Jewell, 2011) pioneered by Meyer (1969). Synthetic and biological flexoelectric membranes are actuators that bend under the action of external electric fields, a phenomenon of interest to the development of emerging adaptive materials as well as biological mechano-transduction. Several works have explored biological implications of membrane flexoelectricity e.g. mechanosensitivity, electromotility and hearing systems (Petrov, 1975, 2002, 2006, 2007; Raphael et al., 2000; Brownell et al., 2001, 2003; Breneman and Rabbitt, 2009).

Flexoelectricity in membranes is fundamentally different from three-dimensional materials (crystalline or otherwise). In the second part of this dissertation, we consider an important emerging problem that is unaddressed so far, what is the renormalized or effective flexoelectric, response of a heterogeneous two-dimensional structure? How do the elastic and dielectric responses alter due to flexoelectricity? The answer to these questions will help interpret the behavior of complex biological membranes, tailoring membranes such as graphene and boron-nitride sheets for various technological applications, energy harvesting for stretchable electronics among others.

In a pyroelectric material, electric polarization is induced due to a change in temperature. Although, pyroelectric effect has been known as a physically observable phenomenon for many centuries, its broad spectrum of potential scientific and technical applications have only emerged recently (Whatmore, 1986; Muralt, 2001; Hadni, 1981). Using a combination of insights from theory and detailed quantum calculations, we demonstrate that graphene can be designed to be pyroelectric thus providing an avenue for the thinnest possible thermo-electro-mechanical material.

Chapter 2: Elastic Homogenization of Rough Surface: General Theory, Theoretical Calculation of Effective Surface Stress and Superficial Elasticity for Periodic Roughness

2.1 Introduction

Due to large surface to volume ratio, phenomena at the nanoscale require consideration of surface energy effects and the latter are frequently used to interpret size-effects in material behavior. A fair amount of literature has appeared that explain various interesting size-effects due to surface energy effects, e.g. nanoinclusions (Sharma et al., 2003, Sharma and Ganti, 2003, Sharma, 2004; Sharma and Ganti, 2004; Duan et al., 2005a, 2005b; He and Li, 2006; Lim et al., 2005; Mi and Kouris, 2007; Sharma and Wheeler, 2007; Tian and Rajapakse, 2007, 2008; Hui and Chen, 2010), quantum dots (Sharma et al., 2002, 2003; Peng et al., 2006), nanoscale beams and plates (Miller and Shenoy, 2000; Jing et al., 2006; Bar et al., 2010; Liu and Rajapakse, 2010), nano particles, wires and films (Streitz et al., 1994; Diao et al., 2003, 2004, 2006; Villain et al., 2004; Dingreville et al., 2005) on sensing and vibration (Lim and He, 2004; Wang and Feng, 2007; Park and Klein, 2008; Park, 2009), composites (Mogilevskaya et al., 2008) and studies on surface properties (Shenoy, 2005; Shodja and Tehranchi, 2010; Mi et al., 2008).

Surface energy effects are usually accounted for via recourse to a theoretical framework proposed by Gurtin and Murdoch (1975, 1978). The surface is treated as a zero-thickness deformable elastic entity possessing non-trivial elasticity as well as a residual stress (the so-called “surface stress”). It is worthwhile to indicate that while fundamentally similar, a parallel line of works exists that are more materials oriented: Cahn (1989), Streitz (1994), Weissmuller and Cahn (1997), Johnson (2000), Voorhees and Johnson (2004) and Cammarata (1994, 2009a, 2009b) among others. The reader is referred to an extensive recent review by Cammarata (2009) on the literature. Steigmann and Ogden (1997) later generalized the Gurtin–Murdoch theory and incorporated curvature dependence on surface energy as well thus resolving some important issues related to the use of Gurtin-Murdoch theory in the context of compressive stress states and for wrinkling type behavior. Some recent works are worth mentioning as they provide clarifications and guidance on some of the theories underlying surface energy effects, e.g. Ru (2010), Mogielvskaya (2008, 2010) and Schiavone and Ru (2009). Huang and co-workers (Wang et al., 2010; Huang and Sun, 2007) have pointed out the importance of residual surface stress on elastic properties of nanostructures and composites.

In this chapter, we make an effort to elucidate the effect of surface roughness on the surface stress and elastic behavior and present theoretical derivations that relate periodic roughness to the effective surface elastic behavior. In particular, in Section 2 we briefly summarize the Gurtin-Murdoch surface elasticity theory. In section 3, we present our general homogenization strategy for a media with deterministic surface roughness. In Section 4, specializing to the 2D case, we present results for periodically rough surfaces.

2.2 Surface Elasticity

The physical system that has been considered is a semi-infinite elastic media that occupies the region $B=\{(x,y,z): y<h(x,z)\}$, where the function $h(x,z)$ describes the surface roughness. We denote the bulk and boundary of the media by B and ∂B, respectively (Figure 2-1). Let $\mathbb{C}$ be the fourth-rank bulk stiffness tensor and assume there is no applied body force. In linearized elasticity, the displacement $u: B\to\mathbb{R}^3$ satisfies the equilibrium equation

$$\mathrm{div}\left[\mathbb{C}\nabla u\right]=0 \quad \text{in } B. \tag{1}$$

These equations will be supplemented by traction boundary conditions on the rough surface, which we describe below in detail.

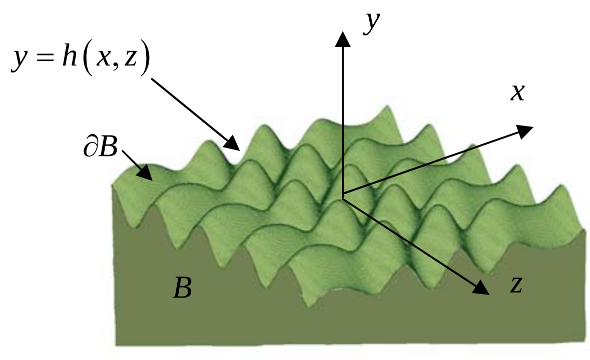

Figure 2-1: Semi-infinite media with bulk B, boundary ∂B and surface roughness profile $y=h(x,z)$.

We employ the linearized surface elasticity theory of Gurtin and Murdoch (Gurtin and Murdoch, 1975; Gurtin et. al., 1998). In this theory the surface is modeled as a deformable elastic membrane that adheres to the bulk material without slipping. Let e_n be the outward unit normal to the surface,

$$\mathbb{P} = \mathbb{I} - e_n \otimes e_n \ , \tag{2}$$

be the projection from $\mathbb{R}^3$ to the subspace orthogonal to e_n, and

$$M_1 = \left\{ M : Me_n = 0, \quad M^T e_n = 0, \quad M \in \mathbb{R}^{3\times 3} \right\} , \tag{3}$$

be the subspace, where surface strains belong to. Then the surface strain ε^s is given by

$$\nabla_s u = (\nabla u)\mathbb{P} , \quad Du = \mathbb{P}\nabla_s u , \quad \varepsilon^s = \mathbb{P}\varepsilon\mathbb{P} = \frac{1}{2}\left(Du + (Du)^T\right) \ \text{ on } \ \partial B , \tag{4}$$

where ∇_s denotes the surface gradient. We remark that the above equations follow from the kinematic assumption that displacements are continuous up to the surface.

Let $\tau^0 \in \mathbb{R}$ be the magnitude of the residual isotropic stress tensor (often referred to as the surface tension), $\mathbb{I}_s = \mathbb{P}\mathbb{I}\mathbb{P}$ be the identity mapping from M_1 to M_1, λ^s and μ^s be the surface elastic constants (Láme parameters), and symmetric matrix $\varepsilon_s^0 \in M_1$ be the residual/eigen surface strain such that

$\mathbb{C}_s\varepsilon_s^0 = -\tau^0\mathbb{I}_s$ on ∂B. We adopt the linear isotropic surface constitutive law from Gurtin and Murduch (1975), equation (8.6),

$$S = \mathbb{C}_s\left(\varepsilon^s - \varepsilon_s^0\right) \text{ on } \partial B, \tag{5}$$

where $\varepsilon_s^0 = \dfrac{-\tau^0}{2\left(\lambda^s + \mu^s\right)}\mathbb{I}_s$, S is the (first) Piola-Kirchhoff surface stress tensor, and $\mathbb{C}_s$ is the isotropic surface elasticity tensor such that for any symmetric $E \in M_1$,

$$\mathbb{C}_s\left(E\right) = \lambda^s Tr\left(E\right)\mathbb{I}_s + 2\mu^s E \text{ on } \partial B. \tag{6}$$

We remark that the surface constitutive law used here (equation 5) is different than Gurtin and Murdoch by a term of $\tau^0\nabla_s u$. This term leads to asymmetry of the surface stress tensor and quite a few works have chosen to ignore its presence completely (as justified in some cases). The reader is referred to Ru (2010), Mogilevskaya et al. (2008) and Huang (2010) for further discussions on this subject. We anticipate that if $\tau^0 \ll \lambda^s, \mu^s$, the effect of this term is negligible. In section 5, we will assess its impact in detail and for the remainder of the calculations, this term will be ignored.

The equilibrium of any sub-surface of ∂B implies that,

$$\left(\mathbb{C}\nabla u\right)e_n = \mathrm{div}_s\left[\mathbb{C}_s\left(\varepsilon^s - \varepsilon_s^0\right)\right] \text{ on } \partial B. \tag{7}$$

The above equation can also be regarded as boundary condition for (1). In summary, equations (1) and (7) form the boundary value problem for linearized elasticity with surface effects.

Further, within a non-consequential constant, the elastic energy contributed by the surface is given by (Gurtin and Murdoch, 1975, equation 9.3 and theorem 9.1),

$$\Gamma[u] = \frac{1}{2}\int_{\partial B}\left[\left(\varepsilon^{s} - \varepsilon_{s}^{0}\right)\cdot\mathbb{C}_{s}\left(\varepsilon^{s} - \varepsilon_{s}^{0}\right)\right]. \tag{8}$$

Below we consider the effective behaviors of a rough surface.

2.3 Homogenization Strategy and Problem Formulation for Deterministic Surface Roughness

In this section we outline our homogenization strategy for a rough surface. We assume the amplitude of the roughness h is small compared with the average distance λ between successive 'peaks' or 'valleys' on the surface, $\delta = \frac{h}{\lambda} \ll 1$. This dimensionless number will be the small parameter used in our subsequent perturbation calculations. The overall half space is subject to a uniform in-plane stress $\sigma = \sigma^{\infty}\hat{\sigma}$, where σ^{∞} is the magnitude of σ and $\hat{\sigma}$ with $|\hat{\sigma}| = 1$ is any plane-stress (xz-plane) tensor. By (1) and (7) our original problem is to solve for $u : B \to \mathbb{R}^{3}$:

$$\begin{cases} \operatorname{div}\left(\mathbb{C}\nabla u\right)=0 & in \quad B, \\ \left(\mathbb{C}\nabla u\right)e_n=\operatorname{div}_s\left[\mathbb{C}_s\left(\varepsilon^s - \varepsilon_s^0\right)\right] & on \quad \partial B, \\ \left(\mathbb{C}\nabla u\right)e_x=\sigma_\infty e_x \quad as & |y|\to\infty. \end{cases} \tag{9}$$

Due to the presence of the non-trivial boundary condition $(9)_2$, we will find the solution via perturbation theory. We assume that the solution to (9) can be expanded as

$$u=u^{(0)}+\delta u^{(1)}+\delta^2 u^{(2)}+\cdots, \tag{10}$$

Inserting (10) into (9), by $(9)_1$ and $(9)_3$ we have

$$\begin{aligned} &\operatorname{div}\left[\mathbb{C}\nabla u^{(i)}\right]=0 \quad i=0,1,2 \qquad \text{in } B^0, \\ &\left(\mathbb{C}\nabla u^{(0)}\right)e_x=\sigma^\infty e_x \qquad \text{as } |y|\to\infty, \\ &\left(\mathbb{C}\nabla u^{(i)}\right)e_x=0 \quad i=1,2,\cdots \quad \text{as } |y|\to\infty, \end{aligned} \tag{11}$$

where $B^0=\{(x,y,z):y<0\}$. We notice that the boundary conditions at the infinity are homogenous unless $i=0$.

The boundary conditions on the rough surface, i.e., $(9)_2$, can be converted to an effective boundary condition on the nominal flat surface ∂B^0. To this end, we assume that the displacement on ∂B can be obtained by extrapolating from the displacement and their derivatives on ∂B^0 through Taylor series expansion. Upon tedious calculations that is outlined in section 2.4, we find the boundary conditions on the nominal flat surface as

$$\left(\mathbb{C}\nabla u^{(i)}\right)e_2 = t^{(i)} \quad i=0,1,2 \quad \text{on } \partial B^0, \tag{12}$$

where the detailed expressions for surface traction $t^{(i)}$ are presented in section 2.4.1 for sinusoidal rough surface. Upon solving (11) and (12) for $u^{(i)}$ $(\mathrm{i}=0,1,2)$, we can find the total elastic energy of the half-space as a function of the applied far field stress,

$$\begin{aligned} E^{act}\left(\sigma^{\infty}\right) &= \frac{1}{2}\int_B \nabla u \cdot \mathbb{C}(\nabla u) + \frac{1}{2}\int_{\partial B}\left(\varepsilon^S - \varepsilon_s^0\right)\cdot \mathbb{C}_s\left(\varepsilon^S - \varepsilon_s^0\right) \\ &= \frac{1}{2}\int_B\left(\nabla u^{(0)} + \delta\nabla u^{(1)} + \delta^2\nabla u^{(2)}\right)\cdot\mathbb{C}\left(\nabla u^{(0)} + \delta\nabla u^{(1)} + \delta^2\nabla u^{(2)}\right) \\ &+ \frac{1}{2}\int_{\partial B}\left[\left(\nabla_s u^{(0)} + \delta\nabla_s u^{(1)} + \delta^2\nabla_s u^{(2)} - \varepsilon^0\right)\cdot\mathbb{C}_s\left(\nabla_s u^{(0)} + \delta\nabla_s u^{(1)} + \delta^2\nabla_s u^{(2)} - \varepsilon^0\right)\right] + O\left(\delta^3\right), \end{aligned} \tag{13}$$

where $u^{(i)}$ $(\mathrm{i}=0,1,2)$, the solution of (9), depends on the far applied stress σ^{∞}, and the first and second term on the right hand side of (13) is the elastic energy contributed by the bulk and surface, respectively.

We will approximate this elastic body with rough surface by a half-space solid with a flat surface where the flat surface has effective properties different from the original rough surface (Figure 2-2). To define the effective properties of the surface, we propose to equate the total elastic energy of the rough-surface half space $\left(E^{act}\right)$ to the total elastic energy of a half space with a nominal “effective” flat surface $\left(E^{eff}\right)$,

$$E^{eff}\left(\sigma^{\infty}\right)=\frac{1}{2}\int_{B^0}\nabla u^{(0)}\cdot\mathbb{C}\left(\nabla u^{(0)}\right)+\frac{1}{2}\int_{\partial B^0}\left(\nabla u^{(0)}-\left(\varepsilon_s^0\right)^{eff}\right)\cdot\mathbb{C}_s{}^{eff}\left(\nabla u^{(0)}-\left(\varepsilon_s^0\right)^{eff}\right), \tag{14}$$

where $\left(\varepsilon_s^0\right)^{eff}$ is the effective surface residual strain and $\mathbb{C}_s{}^{eff}$ is the effective surface elasticity tensor. By

$$E^{act}\left(\sigma^{\infty}\right)=E^{eff}\left(\sigma^{\infty}\right), \tag{15}$$

we can find the effective surface stress and effective surface elastic modulus.

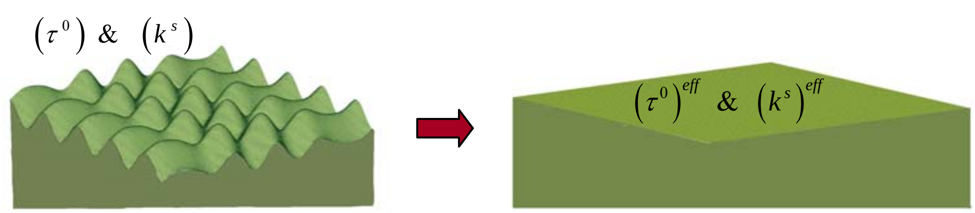

Figure 2-2: The elastic body (a) with rough surface is approximated by a Semi-infinite media (b) with flat surface that has effective properties $\left(\tau^0\right)^{eff}$ & $\left(k^s\right)^{eff}$.

2.4 Solution

2.4.1 General Procedure

We now specialize to two-dimensions. Our work can be readily extended to three dimensions. However, the calculations are quite tedious with relatively little prospects for (additional) novel insights. We will employ two coordinate systems. The first one is the standard Cartesian frame (e_1, e_2) aligned along the nominally flat surface while the second one (e_n, e_s) is the unit normal and unit tangent along the curve. (Figure 2-3)

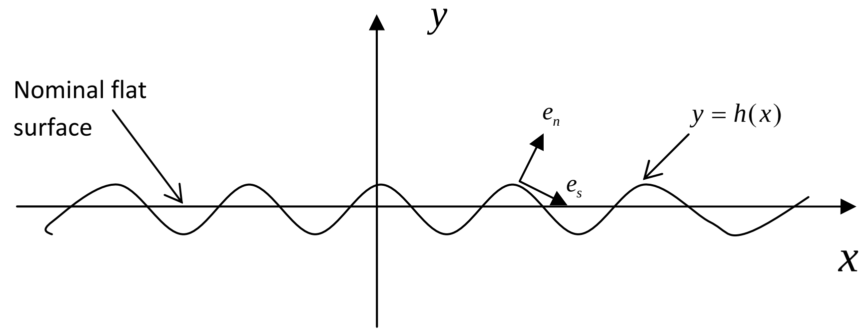

Figure 2-3: A rough surface profile.

If the surface is given by $y = h(x)$, we have the following differential geometry results for plane curves (Frenet formulae):

$$e_s = \frac{e_1 + e_2 h_x}{\sqrt{1+h_x^2}}, \qquad e_n = \frac{-h_x e_1 + e_2}{\sqrt{1+h_x^2}}, \qquad \frac{de_s}{ds} = \kappa e_n, \qquad \frac{de_n}{ds} = -\kappa e_s, \tag{16}$$

where $\kappa = \frac{h_{xx}}{\left(1+h_x^2\right)^{3/2}}$ is the curvature. Let $u : B \to \mathbb{R}^2$ be the displacement. On the surface ∂B, let u_s and u_n be the displacements in the tangential and normal directions,

$$u = u_s e_s + u_n e_n. \tag{17}$$

By (4), the surface strain is given by

$$\varepsilon^s = \varepsilon_{ss} e_s \otimes e_s, \qquad \varepsilon_{ss} = \left(\frac{\partial u_s}{\partial s} - \kappa u_n \right) \tag{18}$$

By (5) and (6), the surface stress is given by

$$S = \tau^o e_s \otimes e_s + k^s \varepsilon_{ss} e_s \otimes e_s, \qquad k^s \equiv \lambda^s + 2\mu^s. \tag{19}$$

We remark that the above surface strain-stress relation is reminiscent of the familiar bulk strain-stress relation for plain strain. By (19), the boundary condition (7) is now re-written as

$$(\mathbb{C}\nabla u) e_n = \left(\tau^o \kappa + k^s \kappa \varepsilon_{ss}\right) e_n + \left(k^s \frac{\partial \varepsilon_{ss}}{\partial s}\right) e_s \qquad \text{on } \partial B \tag{20}$$

Using the following relations, we convert the above boundary condition to Cartesian coordinates,

$$h(x) = \delta h_0(x), \qquad \delta \ll 1 \ ,$$

$$e_s \approx \left(1 - \frac{1}{2}\delta^2 h_{0x}^2\right) e_1 + \delta h_{0x} e_2 \ , \ \ e_n \approx -\delta h_{0x} e_1 + \left(1 - \frac{1}{2}\delta^2 h_{0x}^2\right) e_2 \ , \ \kappa = \delta h_{0xx} \, ,$$

$$\frac{\partial x}{\partial s} = \frac{1}{\sqrt{1+h_x{}^2}} \approx 1 - \frac{1}{2}\delta^2 h_{0x}{}^2 \ , \ \ \frac{\partial y}{\partial s} = \frac{h_x}{\sqrt{1+h_x{}^2}} \approx \delta h_{0x}, \quad h_{0x} = \frac{\partial h_0(x)}{\partial x}, \tag{21}$$

$$u_s \approx \left(1 - \frac{1}{2}\delta^2 h_{0x}^2\right) u_x + \delta u_y h_{ox}, \quad u_n \approx -\delta h_{ox} u_x + \left(1 - \frac{1}{2}\delta^2 h_{0x}^2\right) u_y \, ,$$

$$\varepsilon_{ss} = \varepsilon_{xx} + 2\delta h_{0x} \varepsilon_{xy} + \delta^2 h_{0x}{}^2 \left(\varepsilon_{yy} - \varepsilon_{xx}\right) + O\left(\delta^3\right),$$

$$\frac{\partial \varepsilon_{ss}}{\partial s} \approx \frac{\partial \varepsilon_{ss}}{\partial x}\left(1-\frac{1}{2}\delta^2 h_{0x}{}^2\right)+\frac{\partial \varepsilon_{ss}}{\partial y}\delta h_{0x} = \frac{\partial \varepsilon_{xx}}{\partial x}\left(1-\frac{1}{2}\delta^2 h_{0x}{}^2\right)+2\delta h_{0xx}\varepsilon_{xy}+2\delta h_{0x}\frac{\partial \varepsilon_{xy}}{\partial x}$$
$$+2\delta^2 h_{0x}h_{0xx}\left(\varepsilon_{yy}-\varepsilon_{xx}\right)+\delta^2 h_{0x}{}^2\left(\frac{\partial \varepsilon_{yy}}{\partial x}-\frac{\partial \varepsilon_{xx}}{\partial x}\right)+\frac{\partial \varepsilon_{xx}}{\partial y}\delta h_{0x}+2\delta^2 h_{0x}{}^2\frac{\partial \varepsilon_{xy}}{\partial y}+O\left(\delta^3\right),$$

$$\frac{\partial u_n}{\partial s} \approx -\delta h_{0xx}u_x+\delta h_{0x}\left(-\varepsilon_{xx}+\varepsilon_{yy}\right)-\delta^2 h_{0x}h_{0xx}u_y+\left(1-\frac{1}{2}\delta^2 h_{0x}{}^2\right)\frac{\partial u_y}{\partial x}-\delta^2 h_{0x}{}^2\frac{\partial u_x}{\partial y},$$

$$\frac{\partial \kappa}{\partial s} = \delta h_{0xxx},$$

$$\frac{\partial^2 u_n}{\partial s^2} \approx -\delta h_{0xxx}u_x-2\delta h_{0xx}\varepsilon_{xx}+\delta h_{0xx}\varepsilon_{yy}+\delta h_{0x}\left(-\frac{\partial \varepsilon_{xx}}{\partial x}+\frac{\partial \varepsilon_{yy}}{\partial x}\right)-\delta^2 h_{0xx}{}^2 u_y -$$
$$-\delta^2 h_{0x}h_{0xxx}u_y-2\delta^2 h_{0x}h_{0xx}\varepsilon_{xy}-2\delta^2 h_{0x}h_{0xx}\frac{\partial u_x}{\partial y}-2\delta^2 h_{0x}{}^2\frac{\partial \varepsilon_{xy}}{\partial x}+\frac{\partial^2 u_y}{\partial x^2}+$$
$$+\delta^2\left(h_{0x}\right)^2\left(-\frac{\partial \varepsilon_{xx}}{\partial y}+\frac{\partial \varepsilon_{yy}}{\partial y}\right)+\delta h_{0x}\frac{\partial^2 u_y}{\partial x \partial y}.$$

In regard of the assumption of small-roughness, the displacement on the rough surface may be approximated by

$$\left[u(x,y)\right]_{y=h(x)} = u(x,0)+\delta h_0(x)\left[\frac{\partial u(x,y)}{\partial y}\right]_{y=0}+\frac{1}{2}\delta^2 h_0{}^2(x)\left[\frac{\partial^2 u(x,y)}{\partial y^2}\right]_{y=0}+\cdots, \tag{22}$$

where we have assumed that the Taylor expansion is valid around the surface. Inserting (10) and (22) into (20) and keeping terms up to $O\left(\delta^2\right)$, we find the boundary conditions on the nominal flat surface for $u^{(i)}$ $\left(i=0,1,2\right)$, i.e., the right hand side of (12) as follows.

$$t^{(0)} = \left(t_x{}^{(0)}, t_y{}^{(0)}\right), \qquad t_x{}^{(0)} = k^s \frac{\partial \varepsilon_{xx}{}^{(0)}}{\partial x}, \qquad t_y{}^{(0)} = 0, \tag{23}$$

$$t^{(1)} = \left(t_x{}^{(1)}, t_y{}^{(1)}\right),$$

$$\begin{aligned} t_x{}^{(1)} &= h_{0x}\sigma_{xx}{}^{(0)} - h_0 \frac{\partial \sigma_{xy}{}^{(0)}}{\partial y} + k^s \frac{\partial \varepsilon_{xx}{}^{(1)}}{\partial x} + k^s h_0 \frac{\partial^2 \varepsilon_{xx}{}^{(0)}}{\partial x \partial y} \\ &\quad + 2k^s h_{0xx}\varepsilon_{xy}{}^{(0)} + 2k^s h_{0x} \frac{\partial \varepsilon_{xy}{}^{(0)}}{\partial x} + k^s h_{0x} \frac{\partial \varepsilon_{xx}{}^{(0)}}{\partial y}, \end{aligned} \tag{24}$$

$$t_y{}^{(1)} = h_{0x}\sigma_{yx}{}^{(0)} - h_0 \frac{\partial \sigma_{yy}{}^{(0)}}{\partial y} + \tau^o h_{0xx} + (k^s) h_{0xx}\varepsilon_{xx}{}^{(0)} + (k^s) h_{0x} \frac{\partial \varepsilon_{xx}{}^{(0)}}{\partial x}$$

and

$$t^{(2)} = \left(t_x{}^{(2)}, t_y{}^{(2)}\right),$$

$$\begin{aligned} t_x{}^{(2)} &= h_{0x}\sigma_{xx}{}^{(1)} + h_0 h_{0x} \frac{\partial \sigma_{xx}{}^{(0)}}{\partial y} + \frac{1}{2} h_{0x}^2 \sigma_{xy}{}^{(0)} - h_0 \frac{\partial \sigma_{xy}{}^{(1)}}{\partial y} - \frac{1}{2} h_0{}^2 \frac{\partial^2 \sigma_{xy}{}^{(0)}}{\partial y^2} - \tau^o h_{0x} h_{0xx} \\ &\quad - k^s h_{0x} h_{0xx} \varepsilon_{xx}{}^{(0)} + k^s \frac{\partial \varepsilon_{xx}{}^{(2)}}{\partial x} + k^s h_0 \frac{\partial^2 \varepsilon_{xx}{}^{(1)}}{\partial x \partial y} + \frac{1}{2} k^s \left(h_0\right)^2 \frac{\partial^3 \varepsilon_{xx}{}^{(0)}}{\partial x \partial y^2} - k^s h_{0x}^2 \frac{\partial \varepsilon_{xx}{}^{(0)}}{\partial x} \\ &\quad + 2k^s h_{0xx} \varepsilon_{xy}{}^{(1)} + 2k^s h_{0xx} h_0 \frac{\partial \varepsilon_{xy}{}^{(0)}}{\partial y} + 2k^s h_{0x} \frac{\partial \varepsilon_{xy}{}^{(1)}}{\partial x} + 2k^s h_{0x} h_0 \frac{\partial^2 \varepsilon_{xy}{}^{(0)}}{\partial x \partial y} \\ &\quad + 2k^s h_{0x} h_{0xx} \left(\varepsilon_{yy}{}^{(0)} - \varepsilon_{xx}{}^{(0)}\right) + k^s h_{0x}{}^2 \left(\frac{\partial \varepsilon_{yy}{}^{(0)}}{\partial x} - \frac{\partial \varepsilon_{xx}{}^{(0)}}{\partial x}\right) + 2k^s h_{0x} \frac{\partial \varepsilon_{xx}{}^{(1)}}{\partial y} \\ &\quad + k^s h_{0x} h_0 \frac{\partial^2 \varepsilon_{xx}{}^{(0)}}{\partial y^2} + 4k^s \left(h_{0x}\right)^2 \frac{\partial \varepsilon_{xy}{}^{(0)}}{\partial y}, \end{aligned} \tag{25}$$

$$t_y^{(2)} = h_{0x}\sigma_{yx}^{(1)} + h_{0x}h_0\frac{\partial\sigma_{yx}^{(0)}}{\partial y} + \frac{1}{2}h_{0x}^2\sigma_{yy}^{(0)} - h_0\frac{\partial\sigma_{yy}^{(1)}}{\partial y} - \frac{1}{2}h_0^{\ 2}\frac{\partial^2\sigma_{yy}^{(0)}}{\partial y^2} + k^s h_{0xx}\varepsilon_{xx}^{(1)}$$
$$+k^s h_{0xx}h_0\frac{\partial\varepsilon_{xx}^{(0)}}{\partial y} + 2k^s h_{0x}h_{0xx}\varepsilon_{xy}^{(0)} + h_{0x}k^s\frac{\partial\varepsilon_{xx}^{(1)}}{\partial x} + h_{0x}h_0k^s\frac{\partial^2\varepsilon_{xx}^{(0)}}{\partial x\partial y} + 2k^s h_{0x}h_{0xx}\varepsilon_{xy}^{(0)}$$
$$+2k^s h_{0x}h_{0x}\frac{\partial\varepsilon_{xy}^{(0)}}{\partial x} + k^s h_{0x}h_{0x}\frac{\partial\varepsilon_{xx}^{(0)}}{\partial y} + k^s h_{0x}h_{0x}\frac{\partial\varepsilon_{xx}^{(0)}}{\partial y},$$

where $h_{0x} = \frac{\partial h_0}{\partial x}$, $h_{0xx} = \frac{\partial^2 h_0}{\partial x^2}$, etc. We remark that the elasticity problems (11) and (12) for $u^{(i)}$ $(i = 0,1,2)$ are now the classical Cerruti-Boussinesq half-space problems whose solutions can be found in text books, e.g., Johnson, 1985. Upon specifying the surface roughness profile $h_0(x)$, we can solve (11) and (12) for the elastic fields, compute the total elastic energy (13) and (14) and find the effective properties of the nominal flat surface by using (15). In section 2.4.3, we present the detailed calculations for a sinusoidal surface.

2.4.2 General Procedure for Finding Elastic Fields for Cerruti-Boussinesq Problem Using Airy Stress Function (Asaro and Lubarda, 2006)

In this section, solutions involving general types of loading on half-spaces are considered. Such solutions are developed using Fourier transforms. The media are taken to be elastically isotropic.

Consider a half space defined by $y \le 0$. The loading is specified by

$$\sigma_{xy} = f(x), \qquad \sigma_{yy} = p(x) \qquad \text{on} \quad y = 0, \tag{26}$$

which describes a state of general normal and shear loading on the external surface of the half space.

The nature of the loadings, $f(x)$ and $p(x)$, is such that it produces bounded stresses. Infinitely far into the bulk of the medium the stresses must be bounded, so that

$$\sigma_{\alpha\beta} \not\to \infty \quad \text{as} \quad y \to -\infty . \tag{27}$$

As there are no body forces or temperature gradients, the Airy stress function satisfies the simple form of the biharmonic equation,

$$\nabla^4 \phi = \frac{\partial^4 \phi}{\partial x^4} + 2\frac{\partial^4 \phi}{\partial x^2 \partial y^2} + \frac{\partial^4 \phi}{\partial y^4} = 0 . \tag{28}$$

Introduce the Fourier transform in spatial coordinate x,

$$\Phi(\alpha, y) = \int_{-\infty}^{\infty} \phi(x, y) e^{-i\alpha x} dx, \tag{29}$$

and it's inverse

$$\phi(x, y) = \frac{1}{2\pi} \int_{-\infty}^{\infty} \Phi(\alpha, y) e^{i\alpha x} d\alpha . \tag{30}$$

Apply the Fourier transform to the biharmonic equation (95), it is found that

$$(i\alpha)^4 \Phi + 2(i\alpha)^2 \frac{\partial^2 \Phi}{\partial y^2} + \frac{\partial^4 \Phi}{\partial y^4} = 0 . \tag{31}$$

The acceptable solution for the transform $\Phi(\alpha, y)$, are of the form

$$\Phi(\alpha, y) = (A + By)e^{-|\alpha|y} + (C + Dy)e^{|\alpha|y} . \tag{32}$$

The transform of the stresses are

$$\begin{aligned}
\sigma_{xx} &= \frac{\partial^2 \phi}{\partial y^2} \quad \Rightarrow \quad \int_{-\infty}^{\infty} \frac{\partial^2 \phi}{\partial y^2} e^{-i\alpha x} dx = \frac{\partial^2 \Phi}{\partial y^2}, \\
\sigma_{xy} &= -\frac{\partial^2 \phi}{\partial x \partial y} \quad \Rightarrow \quad \int_{-\infty}^{\infty} -\frac{\partial^2 \phi}{\partial x \partial y} e^{-i\alpha x} dx = -i\alpha \frac{\partial \Phi}{\partial y}, \\
\sigma_{yy} &= \frac{\partial^2 \phi}{\partial x^2} \quad \Rightarrow \quad \int_{-\infty}^{\infty} \sigma_{yy} e^{-i\alpha x} dx = (i\alpha)^2 \Phi(\alpha, y) = -\alpha^2 \Phi(\alpha, y).
\end{aligned} \tag{33}$$

The inverse transform follow immediately as

$$\begin{aligned}
\sigma_{xx} &= \frac{1}{2\pi} \int_{-\infty}^{\infty} \frac{\partial^2 \Phi(\alpha, y)}{\partial y^2} e^{i\alpha x} d\alpha, \\
\sigma_{xy} &= -\frac{1}{2\pi} \int_{-\infty}^{\infty} i\alpha \frac{\partial \Phi(\alpha, y)}{\partial y} e^{i\alpha x} d\alpha, \\
\sigma_{yy} &= -\frac{1}{2\pi} \int_{-\infty}^{\infty} \alpha^2 \Phi(\alpha, y) e^{i\alpha x} d\alpha.
\end{aligned} \tag{34}$$

Next, invoke the boundary conditions specified above and form the Fourier transform of the normal and tangential loading boundary conditions on $y = 0$, we have

$$\int_{-\infty}^{\infty} \sigma_{xy} e^{-i\alpha x} dx = -\int_{-\infty}^{\infty} \frac{\partial^2 \phi}{\partial x \partial y} e^{-i\alpha x} dx = -i\alpha \left[\frac{\partial \Phi(\alpha, y)}{\partial y} \right]_{y=0} = \int_{-\infty}^{\infty} f(x) e^{-i\alpha x} dx = f(\alpha) \tag{35}$$

and

$$\int_{-\infty}^{\infty} \sigma_{yy} e^{-i\alpha x} dx = \int_{-\infty}^{\infty} \frac{\partial^2 \phi}{\partial x^2} e^{-i\alpha x} dx = -\alpha^2 \Phi(\alpha, y = 0) = \int_{-\infty}^{\infty} p(x) e^{-i\alpha x} dx = p(\alpha) . \tag{36}$$

Since the stresses need to be bounded as $y \to -\infty$, it is clear that

$$A = B = 0, \tag{37}$$

whereas the transformed boundary conditions of (102) and (103) require that

$$-i\alpha\left(D+|\alpha|C\right)= f(\alpha) \quad \text{and} \quad -\alpha^2 C = p(\alpha). \tag{38}$$

This leads to

$$C=-\frac{p(\alpha)}{\alpha^2} \quad \text{and} \quad D=-\frac{f(\alpha)}{i\alpha}+\frac{p(\alpha)}{|\alpha|}. \tag{39}$$

The result for $\Phi(\alpha, y)$ is then

$$\Phi(\alpha, y)=\left[-\frac{p(\alpha)}{\alpha^2}+\left(-\frac{f(\alpha)}{i\alpha}+\frac{p(\alpha)}{|\alpha|}\right)y\right]e^{|\alpha|y}. \tag{40}$$

The solution for the stresses is consequently

$$\begin{aligned}
\sigma_{xx}(x,y)&=\frac{1}{2\pi}\int_{-\infty}^{\infty}[f(\alpha)(-2\frac{|\alpha|}{i\alpha}+i\alpha y)+p(\alpha)(1+|\alpha|y)]e^{i\alpha x+|\alpha|y}d\alpha,\\
\sigma_{xy}(x,y)&=\frac{1}{2\pi}\int_{-\infty}^{\infty}[f(\alpha)(1+|\alpha|y)-i\alpha p(\alpha)y]e^{i\alpha x+|\alpha|y}d\alpha,\\
\sigma_{yy}(x,y)&=\frac{1}{2\pi}\int_{-\infty}^{\infty}[-i\alpha f(\alpha)y+p(\alpha)(1-|\alpha|y)]e^{i\alpha x+|\alpha|y}d\alpha.
\end{aligned} \tag{41}$$

2.4.3 Solution for Sinusoidal roughness profile

To fix the idea we first consider a sinusoidal rough surface. Let the surface be given by $h(x)=a\cos kx$ ($\delta = ak << 1$). This rough surface may be regarded as a perturbation of the flat surface $\{(x,y):\ y=0\}$:

$$h(x) = 0 + \frac{ak}{k}\cos kx = \delta h_0, \qquad h_0 = \frac{\cos kx}{k}, \qquad \delta = ak \ll 1. \tag{42}$$

Assume that the far-field stress is given by $\sigma = \sigma^\infty e_1 \otimes e_1$, we solve the different order boundary value problems (11) and (12) for half space with flat surface. By (23), we have the zeroth oreder boundary condition as

$$t_x^{(0)} = k^s \frac{\partial \varepsilon_{xx}^{(0)}}{\partial x} = 0, \qquad t_y^{(0)} = 0. \tag{43}$$

The zeroth order solution would be obtained as

$$\begin{aligned}
&\sigma_{xx}^{(0)} = \sigma^\infty, \qquad \sigma_{xy}^{(0)} = \sigma_{yy}^{(0)} = 0, \\
&\varepsilon_{xx}^{(0)} = \frac{1-\nu^2}{E}\sigma^\infty, \qquad \varepsilon_{xy}^{(0)} = 0, \qquad \varepsilon_{yy}^{(0)} = \frac{-\nu\left(1+\nu\right)}{E}\sigma^\infty.
\end{aligned} \tag{44}$$

By (24), the first order B.C. is

$$\begin{aligned}
&t_x^{(1)} = h_{0x}\sigma_{xx}^{(0)} = -\sigma^\infty \sin kx, \\
&t_y^{(1)} = \tau^o h_{0xx} + k^s h_{0xx}\varepsilon_{xx}^{(0)} = -k\left(\tau^o + k^s\frac{(1-\nu^2)}{E}\sigma^\infty\right)\cos kx,
\end{aligned} \tag{45}$$

and the first order solution is

$$\begin{aligned}
&\sigma_{xx}^{(1)} = \left\{-\sigma^\infty\left(2+ky\right)e^{ky} - k\left(\tau^o + k^s\frac{(1-\nu^2)}{E}\sigma^\infty\right)\left(1+ky\right)e^{ky}\right\}\cos kx, \\
&\sigma_{xy}^{(1)} = \left\{-\sigma^\infty\left(ky+1\right)e^{ky} - k\left(\tau^o + k^s\frac{(1-\nu^2)}{E}\sigma^\infty\right)kye^{ky}\right\}\sin kx,
\end{aligned} \tag{46}$$

$$\sigma_{yy}{}^{(1)} = \left\{ \sigma^\infty \left(ky\right) e^{ky} + k\left(\tau^o + k^s \frac{(1-\nu^2)}{E} \sigma^\infty \right) \left(ky-1\right) e^{ky} \right\} \cos kx,$$

$$\varepsilon_{xx}{}^{(1)} = \frac{1-\nu^2}{E} \left\{ -\sigma^\infty \left(2+ky\right) e^{ky} - k\left(\tau^o + k^s \frac{(1-\nu^2)}{E} \sigma^\infty \right) \left(1+ky\right) e^{ky} \right\} \cos kx$$
$$- \frac{\nu(1+\nu)}{E} \left\{ \sigma^\infty \left(ky\right) e^{ky} + k\left(\tau^o + k^s \frac{(1-\nu^2)}{E} \sigma^\infty \right) \left(ky-1\right) e^{ky} \right\} \cos kx,$$

$$\varepsilon_{yy}{}^{(1)} = -\frac{\nu(1+\nu)}{E} \left\{ -\sigma^\infty \left(2+ky\right) e^{ky} - k\left(\tau^o + k^s \frac{(1-\nu^2)}{E} \sigma^\infty \right) \left(1+ky\right) e^{ky} \right\} \cos kx$$
$$+ \frac{1-\nu^2}{E} \left\{ \sigma^\infty \left(ky\right) e^{ky} + k\left(\tau^o + k^s \frac{(1-\nu^2)}{E} \sigma^\infty \right) \left(ky-1\right) e^{ky} \right\} \cos kx,$$

$$\varepsilon_{xy}{}^{(1)} = \frac{(1+\nu)}{E} \left\{ -\sigma^\infty \left(ky+1\right) e^{ky} - k\left(\tau^o + k^s \frac{(1-\nu^2)}{E} \sigma^\infty \right) k y e^{ky} \right\} \sin kx.$$

Using zeroth and first order solutions at $y=0$, by (25), the second order B.C. is

$$\begin{aligned}
t_x{}^{(2)} = &\left(-\sin kx\right) \left\{ -2\sigma^\infty - k\left(\tau^o + k^s \frac{(1-\nu^2)}{E} \sigma^\infty \right) \right\} \cos kx \\
&- \frac{\cos kx}{k} \left\{ -2\sigma^\infty k - k^2 \left(\tau^o + k^s \frac{(1-\nu^2)}{E} \sigma^\infty \right) \right\} \sin kx \\
&- \tau^o \left(-\sin kx\right)\left(-k\cos kx\right) - k^s \left(-\sin kx\right)\left(-k\cos kx\right) \left(\frac{1-\nu^2}{E} \sigma_\infty \right) \\
&+ k^s \frac{\cos kx}{k} \left\{ 3\frac{(1-\nu^2)}{E} k^2 \sigma^\infty + 2\frac{(1-\nu^2)}{E} k^3 \left(\tau^o + k^s \frac{(1-\nu^2)}{E} \sigma^\infty \right) + \frac{\nu(1+\nu)}{E} k^2 \sigma^\infty \right\} \sin kx \\
&+ 2k^s \left(-k\cos kx\right) \left(-\frac{(1+\nu)}{E} \sigma^\infty \sin kx \right) + 2k^s \left(-\sin kx\right) \left(-\frac{(1+\nu)}{E} k \sigma^\infty \cos kx \right) \\
&+ 2k^s \left(-\sin kx\right)\left(-k\cos kx\right) \left(\frac{-\nu\left(1+\nu\right)}{E} \sigma_\infty - \frac{1-\nu^2}{E} \sigma_\infty \right) \\
&+ k^s \left(-\sin kx\right) \left(-3\frac{(1-\nu^2)}{E} k\sigma^\infty - 2\frac{(1-\nu^2)}{E} k^2 \left(\tau^o + k^s \frac{(1-\nu^2)}{E} \sigma^\infty \right) - \frac{\nu(1+\nu)}{E} k \sigma^\infty \right) \cos kx,
\end{aligned} \tag{47}$$

$$
\begin{aligned}
t_y^{(2)} &= \left(-\sin kx\right)\left(-\sigma^{\infty}\sin kx\right) - \left(\frac{\cos kx}{k}\right)\left(k\sigma^{\infty}\cos kx\right) \\
&\quad + k^s\left(-k\cos kx\right)\left\{-\frac{(1-2\nu)(1+\nu)}{E}k\left(\tau^o + k^s\frac{(1-\nu^2)}{E}\sigma^{\infty}\right) - \sigma^{\infty}\frac{2(1-\nu^2)}{E}\right\}\cos kx \\
&\quad + k^s\left(-\sin kx\right)\left\{\frac{(1-2\nu)(1+\nu)}{E}k^2\left(\tau^o + k^s\frac{(1-\nu^2)}{E}\sigma^{\infty}\right) + \sigma^{\infty}\frac{2(1-\nu^2)}{E}k\right\}\sin kx.
\end{aligned} \tag{48}
$$

More simplifying we would have

$$
t_x^{(2)} = \beta\sin 2kx, \qquad t_y^{(2)} = \gamma\cos 2kx, \tag{49}
$$

with

$$
\begin{aligned}
\beta &= 2\sigma^{\infty} + \frac{1}{2}\tau^o k + \frac{5}{2}\frac{1-\nu^2}{E}k^s k\sigma_{\infty} + 2k^s\frac{(1-\nu^2)}{E}k^2\left(\tau^o + k^s\frac{(1-\nu^2)}{E}\sigma^{\infty}\right) \\
&\quad + \frac{2(1+\nu)}{E}kk^s\sigma^{\infty}, \\
\gamma &= -\sigma^{\infty} + \frac{(1-2\nu)(1+\nu)}{E}k^2k^s\left(\tau^o + k^s\frac{(1-\nu^2)}{E}\sigma^{\infty}\right) + \sigma^{\infty}kk^s\frac{2(1-\nu^2)}{E}.
\end{aligned} \tag{50}
$$

By solving the second order terms we are led to the following results

$$
\begin{aligned}
\sigma_{xx}^{(2)} &= 2\beta\left(1+ky\right)e^{2ky}\cos 2kx + \gamma(1+2ky)e^{2ky}\cos 2kx, \\
\sigma_{yy}^{(2)} &= -2\beta kye^{2ky}\cos 2kx + \gamma(1-2ky)e^{2ky}\cos 2kx, \\
\varepsilon_{xx}^{(2)} &= \frac{1-\nu^2}{E}\left(2\beta\left(1+ky\right)e^{2ky}\cos 2kx + \gamma(1+2ky)e^{2ky}\cos 2kx\right) \\
&\quad - \frac{\nu(1+\nu)}{E}\left(-2\beta kye^{2ky}\cos 2kx + \gamma(1-2ky)e^{2ky}\cos 2kx\right).
\end{aligned} \tag{51}
$$

And at $y = 0$

$$
\begin{aligned}
\left.\varepsilon_{xx}{}^{(2)}\right|_{y=0} &= \frac{(1-2\nu)(1+\nu)}{E}\gamma\cos 2kx + \frac{2(1-\nu^2)}{E}\beta\cos 2kx \\
&= \eta\cos 2kx,
\end{aligned}
\tag{52}
$$

with $\eta = \frac{(1-2\nu)(1+\nu)}{E}\gamma + \frac{2(1-\nu^2)}{E}\beta$. We remark that the energy contributed by strain fields, $\varepsilon_{xy}{}^{(2)}$ and $\varepsilon_{yy}{}^{(2)}$, are negligible compared with δ^2. In order to find the surface stress on $y = h(x)$, we use the transformation law mentioned in section 2.4.1 and Taylor extrapolation that yield ε_{ss} as

$$
\begin{aligned}
\left[\varepsilon_{ss}\right]_{y=h(x)} &= \left[\varepsilon_{xx} + 2\delta h_{0x}\varepsilon_{xy} + \delta^2\left(h_{0x}\right)^2\left(\varepsilon_{yy} - \varepsilon_{xx}\right)\right]_{y=h(x)} = \\
&= \left[\begin{array}{l}
\varepsilon_{xx}{}^{(0)} + \delta\left(\varepsilon_{xx}{}^{(1)} + 2h_{0x}\varepsilon_{xy}{}^{(0)} + h_0\dfrac{\partial\varepsilon_{xx}{}^{(0)}}{\partial y}\right) + \\
\delta^2\left(\begin{array}{l}
h_0\dfrac{\partial\varepsilon_{xx}{}^{(1)}}{\partial y} + \dfrac{1}{2}\left(h_0\right)^2\dfrac{\partial^2\varepsilon_{xx}{}^{(0)}}{\partial y^2} + 2\left(h_{0x}\right)h_0\dfrac{\partial\varepsilon_{xy}{}^{(0)}}{\partial y} \\
-\left(h_{0x}\right)^2\varepsilon_{xx}{}^{(0)} + \varepsilon_{xx}{}^{(2)} + 2h_{0x}\varepsilon_{xy}{}^{(1)} + \left(h_{0x}\right)^2\varepsilon_{yy}{}^{(0)}
\end{array}\right)
\end{array}\right]_{y=0} \\
&= \frac{1-\nu^2}{E}\sigma^\infty + \delta\left\{-\frac{(1-2\nu)(1+\nu)}{E}k\left(\tau^o + k^s\frac{(1-\nu^2)}{E}\sigma^\infty\right) - \sigma^\infty\frac{2(1-\nu^2)}{E}\right\}\cos kx \\
&\quad + \delta^2\left\{\begin{array}{l}
\left(-3\dfrac{(1-\nu^2)}{E}\sigma^\infty - 2\dfrac{(1-\nu^2)}{E}k\left(\tau^o + k^s\dfrac{(1-\nu^2)}{E}\sigma^\infty\right) - \dfrac{\nu(1+\nu)}{E}\sigma^\infty\right)\cos^2 kx \\
+\dfrac{(1+\nu)}{E}\sigma_\infty\sin^2 kx + \eta\cos 2kx
\end{array}\right\}.
\end{aligned}
\tag{53}
$$

As mentioned in section 3, our homogenization scheme requires calculation of the total energy under the action of the applied stress σ^∞. Inserting different order solutions obtained above into (13), we obtain

$$E^{act}\left(\sigma^{\infty}\right)=\frac{1}{2}\left(\frac{1}{\lambda}\right)\int_0^{\lambda}\int_{-\infty}^{h(x)}\begin{pmatrix}\varepsilon^{(0)}\cdot\mathbb{C}\varepsilon^{(0)}+2\delta\varepsilon^{(1)}\cdot\mathbb{C}\varepsilon^{(0)}+\\+\delta^2\left(2\varepsilon^{(2)}\cdot\mathbb{C}\varepsilon^{(0)}+\varepsilon^{(1)}\cdot\mathbb{C}\varepsilon^{(1)}\right)\end{pmatrix}\sqrt{1+\delta^2\sin^2 kx}\,dxdy+$$
$$+\frac{1}{2}\left(\frac{1}{\lambda}\right)\int_0^{\lambda}\left(\left(\varepsilon_{ss}-\varepsilon_{ss}^0\right)\cdot\mathbb{C}_s\left(\varepsilon_{ss}-\varepsilon_{ss}^0\right)\right)\sqrt{1+\delta^2\sin^2 kx}\,dx, \tag{54}$$

where ε_{ss} is given by (53). By (14),

$$E^{eff}\left(\sigma^{\infty}\right)=\frac{1}{2}\left(\frac{1}{\lambda}\right)\int_0^{\lambda}\int_{-\infty}^{0}\varepsilon^{(0)}\cdot\mathbb{C}\varepsilon^{(0)}dydx$$
$$+\frac{1}{\lambda}\int_0^{\lambda}\left(\left(\varepsilon_{xx}{}^{(0)}e_1\otimes e_1-\left(\varepsilon_s^0\right)^{eff}\right)\cdot\mathbb{C}_s{}^{eff}\left(\varepsilon_{xx}{}^{(0)}e_1\otimes e_1-\left(\varepsilon_s^0\right)^{eff}\right)\right)dx, \tag{55}$$

where $\varepsilon_{xx}{}^{(0)}=\dfrac{\left(1-\nu^2\right)}{E}\sigma^{\infty}$ is given by (44). Let

$$\left(\tau^0\right)^{eff}=e_1\otimes e_1\cdot\mathbb{C}_s{}^{eff}\left(\varepsilon_s^0\right)^{eff} \tag{56}$$

and

$$\left(k^s\right)^{eff}=e_1\otimes e_1\cdot\mathbb{C}_s{}^{eff}e_1\otimes e_1\,. \tag{57}$$

Therefore by $E^{act}=E^{eff}$, we have the effective properties of the rough surface given by

$$\left(\tau^0\right)^{eff}=\left(\frac{E}{1-\nu^2}\right)\frac{\partial E^{act}\left(\sigma^{\infty}\right)}{\partial\sigma^{\infty}}\bigg|_{\sigma^{\infty}=0}\quad\text{and}\quad\left(k^s\right)^{eff}=\left(\frac{E}{1-\nu^2}\right)^2\frac{\partial^2E^{act}\left(\sigma^{\infty}\right)}{\left(\partial\sigma^{\infty}\right)^2}\bigg|_{\sigma^{\infty}=0}. \tag{58}$$

Inserting zeroth, first and second order bulk surface stress and strains calculated above into (40), by (54), we obtain

$$\left(\tau^{0}\right)^{eff}=\tau^{o}\left[1+\delta^{2}\left(-\frac{3}{4}-kk^{s}\frac{(1+8\nu)(1+\nu)}{8E}+\frac{(1-2\nu)^{2}(1+\nu)^{2}}{2E^{2}}k^{2}\left(k^{s}\right)^{2}\right)\right], \tag{59}$$

$$\left(k^{s}\right)^{eff}=k^{s}+\delta^{2}\left(\begin{array}{l}-\frac{E}{k\left(1-\nu^{2}\right)}\frac{(9-8\nu)}{8(1-\nu)}+\frac{1}{4}k^{s}+\frac{(1-2\nu)^{2}(1+\nu)^{2}}{2E^{2}}k^{2}\left(k^{s}\right)^{3}+\\ \frac{(1+\nu)}{E}\frac{(-24\nu+7)}{8}k\left(k^{s}\right)^{2}\end{array}\right). \tag{60}$$

If $\frac{kk^{s}}{E}\ll 1$, equations (59) and (60) can be further simplified as

$$\left(\tau^{0}\right)^{eff}=\tau^{o}\left(1-\frac{3}{4}\delta^{2}\right), \tag{61}$$

and

$$\left(k^{s}\right)^{eff}=k^{s}-\delta^{2}\frac{E}{k\left(1-\nu^{2}\right)}\frac{(9-8\nu)}{8(1-\nu)}, \tag{62}$$

respectively.

2.4.4 Effect of Considering Asymmetry Term, $\tau^{0}\nabla_{s}u$, in Effective Surface Stress and Effective Surface Elastic Constant

In this section, the impact of asymmetry term of surface stress $\tau^{0}\nabla_{s}u$ in the effective surface stress and effective surface elastic constant for the case of sinusoidal rough profile would be presented. The surface constitutive law for the considered model problem can be explained as

$$S=\mathbb{C}_s\left(\varepsilon^s - \varepsilon_s^0\right)+\tau^0\nabla_s u \quad \text{on} \quad \partial B, \tag{63}$$

with boundary condition

$$\left(\mathbb{C}\nabla u\right)e_n=\mathrm{div}_s\left[\mathbb{C}_s\left(\varepsilon^s - \varepsilon_s^0\right)+\tau^0\nabla_s u\right] \quad \text{on} \quad \partial B. \tag{64}$$

$\nabla_s u$ that is an out of plane component of surface stress, can be expressed as

$$\nabla_s u=\left(\frac{\partial u_s}{\partial s}-\kappa u_n\right)e_s\otimes e_s+\left(\kappa u_s+\frac{\partial u_n}{\partial s}\right)e_s\otimes e_n \qquad \text{on} \quad \partial B. \tag{65}$$

We remark that

$$\left(\frac{\partial u_s}{\partial s}-\kappa u_n\right)=\varepsilon_{ss}. \tag{66}$$

The surface stress can be expressed as summation of the in-plane and out-of-plane components denoted by σ^S and w^S, respectively,

$$\begin{gathered} S=\sigma^s(e_s\otimes e_s)+w^s(e_s\otimes e_n) \\ \sigma^s=\tau^o+(k^s+\tau^0)\varepsilon_{ss}, \qquad w^s=\tau^0\left(\kappa u_s+\frac{\partial u_n}{\partial s}\right) \end{gathered} \qquad \text{on} \quad \partial B \tag{67}$$

Thus, the boundary condition on ∂B would be explained as

$$\begin{aligned}\left(\mathbb{C}\nabla u\right)e_n=&\left(\tau^o\kappa+\tau^o\frac{\partial\kappa}{\partial s}u_s+\tau^o\kappa\frac{\partial u_s}{\partial s}+\left(k^s+\tau^0\right)\kappa\varepsilon_{ss}+\tau^0\frac{\partial^2 u_n}{\partial s^2}\right)e_n+ \\ &+\left(\left(k^s+\tau^0\right)\frac{\partial\varepsilon_{ss}}{\partial s}-\tau^0\kappa^2u_s-\tau^0\kappa\frac{\partial u_n}{\partial s}\right)e_s.\end{aligned} \tag{68}$$

Below we convert the above boundary condition to Cartesian coordinates. Inserting (10) and (22) into (68) and keeping terms up to $O\left(\delta^2\right)$, we find the boundary conditions on the nominal flat surface for $u^{(i)}$ $(i=0,1,2)$, i.e., the right hand side of (12) as follows.

$$t_x{}^{(0)} = \left(k^s + \tau^0\right)\frac{\partial \varepsilon_{xx}{}^{(0)}}{\partial x}, \qquad t_y{}^{(0)} = \tau^0 \frac{\partial^2 u_y{}^{(0)}}{\partial x^2}, \tag{69}$$

$$\begin{aligned} t_x{}^{(1)} &= h_{0x}\sigma_{xx}{}^{(0)} - h_0 \frac{\partial \sigma_{xy}{}^{(0)}}{\partial y} - \tau^0 h_{0x}\frac{\partial^2 u_y{}^{(0)}}{\partial x^2} + \left(k^s+\tau^0\right)\frac{\partial \varepsilon_{xx}{}^{(1)}}{\partial x} + \left(k^s+\tau^0\right)h_0\frac{\partial^2 \varepsilon_{xx}{}^{(0)}}{\partial x\partial y} \\ &+ 2\left(k^s+\tau^0\right)h_{0xx}\varepsilon_{xy}{}^{(0)} + 2\left(k^s+\tau^0\right)h_{0x}\frac{\partial \varepsilon_{xy}{}^{(0)}}{\partial x} + \left(k^s+\tau^0\right)h_{0x}\frac{\partial \varepsilon_{xx}{}^{(0)}}{\partial y} - \tau^0 h_{0xx}\frac{\partial u_y{}^{(0)}}{\partial x}, \end{aligned}$$

$$\begin{aligned} t_y{}^{(1)} &= h_{0x}\sigma_{yx}{}^{(0)} - h_0\frac{\partial \sigma_{yy}{}^{(0)}}{\partial y} + \tau^o h_{0xx} + (k^s+2\tau^0)h_{0xx}\varepsilon_{xx}{}^{(0)} - 2\tau^0 h_{0xx}\varepsilon_{xx}{}^{(0)} + \tau^0 h_{0xx}\varepsilon_{yy}{}^{(0)} \\ &+ \tau^0 h_{0x}\left(-\frac{\partial \varepsilon_{xx}{}^{(0)}}{\partial x} + \frac{\partial \varepsilon_{yy}{}^{(0)}}{\partial x}\right) + \tau^0\frac{\partial^2 u_y{}^{(1)}}{\partial x^2} + \tau^0 h_0\frac{\partial^3 u_y{}^{(0)}}{\partial x^2\partial y} + \tau^0 h_{0x}\frac{\partial^2 u_y{}^{(0)}}{\partial x\partial y} + \\ &+ \left(k^s+\tau^0\right)h_{0x}\frac{\partial \varepsilon_{xx}{}^{(0)}}{\partial x}, \end{aligned} \tag{70}$$

$$\begin{aligned} t_x{}^{(2)} &= h_{0x}\sigma_{xx}{}^{(1)} + h_0 h_{0x}\frac{\partial \sigma_{xx}{}^{(0)}}{\partial y} + \frac{1}{2}h_{0x}^2\sigma_{xy}{}^{(0)} - h_0\frac{\partial \sigma_{xy}{}^{(1)}}{\partial y} - \frac{1}{2}h_0{}^2\frac{\partial^2 \sigma_{xy}{}^{(0)}}{\partial y^2} - \tau^o h_{0x}h_{0xx} - \\ &\left(k^s+2\tau^0\right)h_{0x}h_{0xx}\varepsilon_{xx}{}^{(0)} + 2\tau^0 h_{0x}h_{0xx}\varepsilon_{xx}{}^{(0)} - \tau^0 h_{0x}h_{0xx}\varepsilon_{yy}{}^{(0)} - \tau^0 h_{0x}h_{0x}\left(-\frac{\partial \varepsilon_{xx}{}^{(0)}}{\partial x} + \frac{\partial \varepsilon_{yy}{}^{(0)}}{\partial x}\right) \\ &- \tau^0 h_{0x}\frac{\partial^2 u_y{}^{(1)}}{\partial x^2} - \tau^0 h_{0x}h_{0x}\frac{\partial^2 u_y{}^{(0)}}{\partial x\partial y} + \left(k^s+\tau^0\right)\frac{\partial \varepsilon_{xx}{}^{(2)}}{\partial x} + \left(k^s+\tau^0\right)h_0\frac{\partial^2 \varepsilon_{xx}{}^{(1)}}{\partial x\partial y} + \\ &+ \frac{1}{2}\left(k^s+\tau^0\right)\left(h_0\right)^2\frac{\partial^3 \varepsilon_{xx}{}^{(0)}}{\partial x\partial y^2} - \left(k^s+\tau^0\right)h_{0x}^2\frac{\partial \varepsilon_{xx}{}^{(0)}}{\partial x} + 2\left(k^s+\tau^0\right)h_{0xx}\varepsilon_{xy}{}^{(1)} + \\ &+ 2\left(k^s+\tau^0\right)h_{0xx}h_0\frac{\partial \varepsilon_{xy}{}^{(0)}}{\partial y} + 2\left(k^s+\tau^0\right)h_{0x}\frac{\partial \varepsilon_{xy}{}^{(1)}}{\partial x} + 2\left(k^s+\tau^0\right)h_{0x}h_0\frac{\partial^2 \varepsilon_{xy}{}^{(0)}}{\partial x\partial y} + \\ &+ 2\left(k^s+\tau^0\right)h_{0x}h_{0xx}\left(\varepsilon_{yy}{}^{(0)} - \varepsilon_{xx}{}^{(0)}\right) + \left(k^s+\tau^0\right)h_{0x}{}^2\left(\frac{\partial \varepsilon_{yy}{}^{(0)}}{\partial x} - \frac{1}{2}\frac{\partial \varepsilon_{xx}{}^{(0)}}{\partial x}\right) + \\ &+ \left(k^s+\tau^0\right)h_{0x}\frac{\partial \varepsilon_{xx}{}^{(1)}}{\partial y} + \left(k^s+\tau^0\right)h_{0x}h_0\frac{\partial^2 \varepsilon_{xx}{}^{(0)}}{\partial y^2} + 2\left(k^s+\tau^0\right)\left(h_{0x}\right)^2\frac{\partial \varepsilon_{xy}{}^{(0)}}{\partial y} \\ &- \tau^0 h_{0x}h_{0xx}\left(-\varepsilon_{xx}{}^{(0)} + \varepsilon_{yy}{}^{(0)}\right) - \tau^0 h_{0xx}\frac{\partial u_y{}^{(1)}}{\partial x} - \tau^0 h_{0xx}h_0\frac{\partial^2 u_y{}^{(0)}}{\partial x\partial y}, \end{aligned} \tag{71}$$

$$
\begin{aligned}
t_y{}^{(2)} &= h_{0x}\sigma_{yx}{}^{(1)} + h_{0x}h_0\frac{\partial \sigma_{yx}{}^{(0)}}{\partial y} + \frac{1}{2}h_{0x}^2\sigma_{yy}{}^{(0)} - h_0\frac{\partial \sigma_{yy}{}^{(1)}}{\partial y} - \frac{1}{2}h_0{}^2\frac{\partial^2 \sigma_{yy}{}^{(0)}}{\partial y^2} \\
&+ \left(k^s + 2\tau^0\right)\left(h_{0xx}\varepsilon_{xx}{}^{(1)} + h_{0xx}h_0\frac{\partial \varepsilon_{xx}{}^{(0)}}{\partial y} + 2h_{0x}h_{0xx}\varepsilon_{xy}{}^{(0)}\right) - 2\tau^0 h_{0xx}\varepsilon_{xx}{}^{(1)} \\
&- 2\tau^0 h_{0xx}h_0\frac{\partial \varepsilon_{xx}{}^{(0)}}{\partial y} + \tau^0 h_{0xx}\varepsilon_{yy}{}^{(1)} + \tau^0 h_{0xx}h_0\frac{\partial \varepsilon_{yy}{}^{(0)}}{\partial y} + \tau^0 h_{0x}\left(-\frac{\partial \varepsilon_{xx}{}^{(1)}}{\partial x} + \frac{\partial \varepsilon_{yy}{}^{(1)}}{\partial x}\right) \\
&+ \tau^0 h_{0x}h_0\left(-\frac{\partial^2 \varepsilon_{xx}{}^{(0)}}{\partial x\partial y} + \frac{\partial^2 \varepsilon_{yy}{}^{(0)}}{\partial x\partial y}\right) - \frac{1}{2}\tau^0 h_{0x}h_{0xx}\frac{\partial u_y{}^{(0)}}{\partial x} - \tau^0 h_{0xx}{}^2 u_y{}^{(0)} - \frac{1}{2}\tau^0\left(h_{0x}{}^2\right)\frac{\partial^2 u_y{}^{(0)}}{\partial x^2} \\
&+ \tau^0\frac{\partial^2 u_y{}^{(2)}}{\partial x^2} + \tau^0 h_0\frac{\partial^3 u_y{}^{(1)}}{\partial x^2\partial y} + \frac{1}{2}\tau^0\left(h_0\right)^2\frac{\partial^4 u_y{}^{(0)}}{\partial x^2\partial y^2} - 2\tau^0 h_{0xx}h_{0x}\varepsilon_{xy}{}^{(0)} - 2\tau^0 h_0 h_{0x}\frac{\partial \varepsilon_{xy}{}^{(0)}}{\partial x} \\
&- 2\tau^0 h_{0x}h_{0xx}\frac{\partial u_x{}^{(0)}}{\partial y} + \tau^0\left(h_{0x}\right)^2\left(-\frac{\partial \varepsilon_{xx}{}^{(0)}}{\partial y} + \frac{\partial \varepsilon_{yy}{}^{(0)}}{\partial y}\right) + \tau^0 h_{0x}\frac{\partial^2 u_y{}^{(1)}}{\partial x\partial y} + \tau^0 h_{0x}h_0\frac{\partial^3 u_y{}^{(0)}}{\partial x\partial y^2} \\
&+ h_{0x}\left(k^s + \tau^0\right)\frac{\partial \varepsilon_{xx}{}^{(1)}}{\partial x} + h_{0x}h_0\left(k^s + \tau^0\right)\frac{\partial^2 \varepsilon_{xx}{}^{(0)}}{\partial x\partial y} + 2\left(k^s + \tau^0\right)h_{0x}h_{0xx}\varepsilon_{xy}{}^{(0)} + \\
&+ 2\left(k^s + \tau^0\right)h_{0x}h_{0x}\frac{\partial \varepsilon_{xy}{}^{(0)}}{\partial x} + \left(k^s + \tau^0\right)h_{0x}h_{0x}\frac{\partial \varepsilon_{xx}{}^{(0)}}{\partial y} - \tau^0 h_{0x}h_{0xx}\frac{\partial u_y{}^{(0)}}{\partial x}.
\end{aligned}
$$

Similar to the previous cases, we proceed to solve the different order boundary value problems.

Zero order boundary conditions are

$$
t_x{}^{(0)} = 0, \qquad t_y{}^{(0)} = 0. \tag{72}
$$

Therefore, zero order solution is

$$
\begin{gathered}
\sigma_{xx}{}^{(0)} = \sigma^\infty, \qquad \sigma_{xy}{}^{(0)} = \sigma_{yy}{}^{(0)} = 0, \\
\varepsilon_{xx}{}^{(0)} = \frac{1-\nu^2}{E}\sigma^\infty, \qquad \varepsilon_{xy}{}^{(0)} = 0, \qquad \varepsilon_{yy}{}^{(0)} = \frac{-\nu\left(1+\nu\right)}{E}\sigma^\infty,
\end{gathered} \tag{73}
$$

first order boundary conditions are written as

$$t_x{}^{(1)} = h_{0x}\sigma_{xx}{}^{(0)} = -\sigma^\infty \sin kx,$$

$$\begin{aligned} t_y{}^{(1)} &= \tau^o h_{0xx} + k^s h_{0xx}\varepsilon_{xx}{}^{(0)} + \tau^0 h_{0xx}\varepsilon_{yy}{}^{(0)} = \\ &= -k\left(\tau^o + k^s\frac{(1-\nu^2)}{E}\sigma^\infty - \tau^o\frac{\nu(1-\nu)}{E}\sigma^\infty\right)\cos kx, \end{aligned} \tag{74}$$

and, subsequently first order solution is obtained as

$$\sigma_{xx}{}^{(1)} = \left\{-\sigma^\infty\left(2+ky\right)e^{ky} - k\left(\tau^o + k^s\frac{(1-\nu^2)}{E}\sigma^\infty - \tau^o\frac{\nu(1-\nu)}{E}\sigma^\infty\right)\left(1+ky\right)e^{ky}\right\}\cos kx$$

$$\sigma_{xy}{}^{(1)} = \left\{-\sigma^\infty\left(ky+1\right)e^{ky} - k\left(\tau^o + k^s\frac{(1-\nu^2)}{E}\sigma^\infty - \tau^o\frac{\nu(1-\nu)}{E}\sigma^\infty\right)kye^{ky}\right\}\sin kx$$

$$\sigma_{yy}{}^{(1)} = \left\{\sigma^\infty\left(ky\right)e^{ky} + k\left(\tau^o + k^s\frac{(1-\nu^2)}{E}\sigma^\infty - \tau^o\frac{\nu(1-\nu)}{E}\sigma^\infty\right)\left(ky-1\right)e^{ky}\right\}\cos kx$$

$$\begin{aligned} \varepsilon_{xx}{}^{(1)} &= \frac{1-\nu^2}{E}\left\{-\sigma^\infty\left(2+ky\right)e^{ky} - k\left(\tau^o + k^s\frac{(1-\nu^2)}{E}\sigma^\infty - \tau^o\frac{\nu(1-\nu)}{E}\sigma^\infty\right)\left(1+ky\right)e^{ky}\right\}\cos kx - \\ &- \frac{\nu(1+\nu)}{E}\left\{\sigma^\infty\left(ky\right)e^{ky} + k\left(\tau^o + k^s\frac{(1-\nu^2)}{E}\sigma^\infty - \tau^o\frac{\nu(1-\nu)}{E}\sigma^\infty\right)\left(ky-1\right)e^{ky}\right\}\cos kx \end{aligned} \tag{75}$$

$$\begin{aligned} \varepsilon_{yy}{}^{(1)} &= -\frac{\nu(1+\nu)}{E}\left\{-\sigma^\infty\left(2+ky\right)e^{ky} - k\left(\tau^o + k^s\frac{(1-\nu^2)}{E}\sigma^\infty - \tau^o\frac{\nu(1-\nu)}{E}\sigma^\infty\right)\left(1+ky\right)e^{ky}\right\}\cos kx + \\ &+ \frac{1-\nu^2}{E}\left\{\sigma^\infty\left(ky\right)e^{ky} + k\left(\tau^o + k^s\frac{(1-\nu^2)}{E}\sigma^\infty - \tau^o\frac{\nu(1-\nu)}{E}\sigma^\infty\right)\left(ky-1\right)e^{ky}\right\}\cos kx \end{aligned}$$

$$\varepsilon_{xy}{}^{(1)} = \frac{(1+\nu)}{E}\left\{-\sigma^\infty\left(ky+1\right)e^{ky} - k\left(\tau^o + k^s\frac{(1-\nu^2)}{E}\sigma^\infty - \tau^o\frac{\nu(1-\nu)}{E}\sigma^\infty\right)kye^{ky}\right\}\sin kx$$

$$\frac{\partial u_y^{(1)}}{\partial x} = \frac{\nu(1+\nu)}{E} k \left\{ -\sigma^\infty \left(\frac{1}{k} + y \right) e^{ky} - k \left(\tau^o + k^s \frac{(1-\nu^2)}{E} \sigma^\infty - \tau^o \frac{\nu(1-\nu)}{E} \sigma^\infty \right) (y) e^{ky} \right\} \sin kx +$$

$$- \frac{1-\nu^2}{E} k \left\{ \sigma^\infty \left(-\frac{1}{k} + y \right) e^{ky} + k \left(\tau^o + k^s \frac{(1-\nu^2)}{E} \sigma^\infty - \tau^o \frac{\nu(1-\nu)}{E} \sigma^\infty \right) \left(-\frac{1}{k} + y \right) e^{ky} \right\} \sin kx$$

$$u_x^{(1)} = \frac{1-\nu^2}{E} \left\{ -\frac{1}{k} \sigma^\infty (2+ky) e^{ky} - \left(\tau^o + k^s \frac{(1-\nu^2)}{E} \sigma^\infty - \tau^o \frac{\nu(1-\nu)}{E} \sigma^\infty \right) (1+ky) e^{ky} \right\} \sin kx -$$

$$- \frac{\nu(1+\nu)}{E} \left\{ \sigma^\infty (y) e^{ky} + \left(\tau^o + k^s \frac{(1-\nu^2)}{E} \sigma^\infty - \tau^o \frac{\nu(1-\nu)}{E} \sigma^\infty \right) (ky-1) e^{ky} \right\} \sin kx.$$

The first order solutions on the boundary $y=0$ are needed in order to find the second order boundary conditions.

$$\varepsilon_{xx}^{(1)} = \left\{ -\frac{(1-2\nu)(1+\nu)}{E} k \left(\tau^o + k^s \frac{(1-\nu^2)}{E} \sigma^\infty - \tau^o \frac{\nu(1-\nu)}{E} \sigma^\infty \right) - \sigma^\infty \frac{2(1-\nu^2)}{E} \right\} \cos kx$$

$$\frac{\partial \varepsilon_{xx}^{(1)}}{\partial x} = \left\{ \frac{(1-2\nu)(1+\nu)}{E} k^2 \left(\tau^o + k^s \frac{(1-\nu^2)}{E} \sigma^\infty - \tau^o \frac{\nu(1-\nu)}{E} \sigma^\infty \right) + \sigma^\infty \frac{2(1-\nu^2)}{E} k \right\} \sin kx$$

$$\frac{\partial \sigma_{xy}^{(1)}}{\partial y} = \left\{ -2\sigma^\infty k - k^2 \left(\tau^o + k^s \frac{(1-\nu^2)}{E} \sigma^\infty - \tau^o \frac{\nu(1-\nu)}{E} \sigma^\infty \right) \right\} \sin kx$$

(76)

$$\sigma_{xx}^{(1)} = \left\{ -2\sigma^\infty - k \left(\tau^o + k^s \frac{(1-\nu^2)}{E} \sigma^\infty - \tau^o \frac{\nu(1-\nu)}{E} \sigma^\infty \right) \right\} \cos kx$$

$$\frac{\partial \varepsilon_{xx}^{(1)}}{\partial y} = -\left\{ 3 \frac{(1-\nu^2)}{E} k \sigma^\infty + 2 \frac{(1-\nu^2)}{E} k^2 \left(\tau^o + k^s \frac{(1-\nu^2)}{E} \sigma^\infty - \tau^o \frac{\nu(1-\nu)}{E} \sigma^\infty \right) + \frac{\nu(1+\nu)}{E} k \sigma^\infty \right\} \cos kx$$

$$\frac{\partial^2 \varepsilon_{xx}^{(1)}}{\partial x \partial y} = \left\{ 3 \frac{(1-\nu^2)}{E} k^2 \sigma^\infty + 2 \frac{(1-\nu^2)}{E} k^3 \left(\tau^o + \frac{(1-\nu^2)}{E} \sigma^\infty - \tau^o \frac{\nu(1-\nu)}{E} \sigma^\infty \right) + \frac{\nu(1+\nu)}{E} k^2 \sigma^\infty \right\} \sin kx$$

$$\sigma_{xy}{}^{(1)} = -\sigma^{\infty} \sin kx$$

$$\varepsilon_{xy}{}^{(1)} = -\frac{(1+\nu)}{E} \sigma^{\infty} \sin kx$$

$$\frac{\partial \varepsilon_{xy}{}^{(1)}}{\partial x} = -\frac{(1+\nu)}{E} k \sigma^{\infty} \cos kx$$

$$\frac{\partial \sigma_{yy}{}^{(1)}}{\partial y} = k\sigma^{\infty} \cos kx$$

$$\frac{\partial u_{y}{}^{(1)}}{\partial x} = -\frac{\nu(1+\nu)}{E} \sigma^{\infty} \sin kx + \frac{1-\nu^2}{E} \left\{ \sigma^{\infty} + k\left(\tau^{o} + \frac{(1-\nu^2)}{E} \sigma^{\infty} - \tau^{o} \frac{\nu(1-\nu)}{E} \sigma^{\infty} \right) \right\} \sin kx$$

$$\varepsilon_{yy}{}^{(1)} = -\frac{\nu(1+\nu)}{E} \left\{ -2\sigma^{\infty} - k\left(\tau^{o} + k^{s} \frac{(1-\nu^2)}{E} \sigma^{\infty} - \tau^{o} \frac{\nu(1-\nu)}{E} \sigma^{\infty} \right) \right\} \cos kx +$$
$$-\frac{1-\nu^2}{E} \left\{ k\left(\tau^{o} + k^{s} \frac{(1-\nu^2)}{E} \sigma^{\infty} - \tau^{o} \frac{\nu(1-\nu)}{E} \sigma^{\infty} \right) \right\} \cos kx.$$

Second order boundary conditions can be written as

$$t_x^{(2)} = \left(-\sin kx\right)\left\{-2\sigma^{\infty} - k\left(\tau^o + k^s \frac{(1-\nu^2)}{E}\sigma^{\infty} - \tau^o \frac{\nu(1-\nu)}{E}\sigma^{\infty}\right)\right\}\cos kx$$
$$-\frac{\cos kx}{k}\left\{-2\sigma^{\infty}k - k^2\left(\tau^o + k^s \frac{(1-\nu^2)}{E}\sigma^{\infty} - \tau^o \frac{\nu(1-\nu)}{E}\sigma^{\infty}\right)\right\}\sin kx - \tau^o\left(-\sin kx\right)\left(-k\cos kx\right)$$
$$+(-3k^s - \tau^0)\left(-\sin kx\right)\left(-k\cos kx\right)\left(\frac{1-\nu^2}{E}\sigma_{\infty}\right) + 2k^s\left(-\sin kx\right)\left(-k\cos kx\right)\left(-\frac{\nu(1-\nu)}{E}\sigma_{\infty}\right)$$
$$+k^s\frac{\cos kx}{k}\left\{3\frac{(1-\nu^2)}{E}k^2\sigma^{\infty} + 2\frac{(1-\nu^2)}{E}k^3\left(\tau^o + k^s \frac{(1-\nu^2)}{E}\sigma^{\infty} - \tau^o \frac{\nu(1-\nu)}{E}\sigma^{\infty}\right) + \frac{\nu(1+\nu)}{E}k^2\sigma^{\infty}\right\}\sin kx \quad (77)$$
$$+2k^s\left(-k\cos kx\right)\left(-\frac{(1+\nu)}{E}\sigma^{\infty}\sin kx\right) + 2k^s\left(-\sin kx\right)\left(-\frac{(1+\nu)}{E}k\sigma^{\infty}\cos kx\right)$$
$$+k^s\left(-\sin kx\right)\left(-3\frac{(1-\nu^2)}{E}k\sigma^{\infty} - 2\frac{(1-\nu^2)}{E}k^2\left(\tau^o + k^s \frac{(1-\nu^2)}{E}\sigma^{\infty} - \tau^o \frac{\nu(1-\nu)}{E}\sigma^{\infty}\right) - \frac{\nu(1+\nu)}{E}k\sigma^{\infty}\right)\cos kx$$
$$-\tau^o\left(k\frac{\nu(1+\nu)}{E}\sigma^{\infty}\sin 2kx - k\frac{1-\nu^2}{E}\left\{\sigma^{\infty} + k\left(\tau^o + k^s \frac{(1-\nu^2)}{E}\sigma^{\infty} - \tau^o \frac{\nu(1-\nu)}{E}\sigma^{\infty}\right)\right\}\sin 2kx\right),$$

$$t_y^{(2)} = \left(-\sin kx\right)\left(-\sigma^{\infty}\sin kx\right) - \left(\frac{\cos kx}{k}\right)\left(k\sigma^{\infty}\cos kx\right)$$
$$+ (k^s - \tau^0)\left(-k\cos kx\right)\left\{-\frac{(1-2\nu)(1+\nu)}{E}k\left(\tau^o + k^s \frac{(1-\nu^2)}{E}\sigma^{\infty} - \tau^o \frac{\nu(1-\nu)}{E}\sigma^{\infty}\right) - \sigma^{\infty}\frac{2(1-\nu^2)}{E}\right\}\cos kx$$
$$+ \tau^o\left(-k\cos kx\right)\begin{pmatrix} -\frac{\nu(1+\nu)}{E}\left\{-2\sigma^{\infty} - k\left(\tau^o + k^s \frac{(1-\nu^2)}{E}\sigma^{\infty} - \tau^o \frac{\nu(1-\nu)}{E}\sigma^{\infty}\right)\right\} + \\ -\frac{1-\nu^2}{E}k\left(\tau^o + k^s \frac{(1-\nu^2)}{E}\sigma^{\infty} - \tau^o \frac{\nu(1-\nu)}{E}\sigma^{\infty}\right) \end{pmatrix}\cos kx +$$
$$+ \tau^o\left(-\sin kx\right)\begin{pmatrix} -\frac{\nu(1+\nu)}{E}\left\{-2\sigma^{\infty} - k\left(\tau^o + k^s \frac{(1-\nu^2)}{E}\sigma^{\infty} - \tau^o \frac{\nu(1-\nu)}{E}\sigma^{\infty}\right)\right\} + \\ -\frac{1-\nu^2}{E}k\left(\tau^o + k^s \frac{(1-\nu^2)}{E}\sigma^{\infty} - \tau^o \frac{\nu(1-\nu)}{E}\sigma^{\infty}\right) \end{pmatrix}\left(-k\sin kx\right)$$
$$+ \tau^o\left(\frac{\cos kx}{k}\right)\begin{pmatrix} -\frac{\nu(1+\nu)}{E}\left\{-2\sigma^{\infty} - k\left(\tau^o + k^s \frac{(1-\nu^2)}{E}\sigma^{\infty} - \tau^o \frac{\nu(1-\nu)}{E}\sigma^{\infty}\right)\right\} + \\ -\frac{1-\nu^2}{E}\left\{k\left(\tau^o + k^s \frac{(1-\nu^2)}{E}\sigma^{\infty} - \tau^o \frac{\nu(1-\nu)}{E}\sigma^{\infty}\right)\right\} \end{pmatrix}\left(-k^2\cos kx\right) + \quad (78)$$
$$+ \tau^o\left(-\sin kx\right)\begin{pmatrix} -\frac{\nu(1+\nu)}{E}\left\{-2\sigma^{\infty} - k\left(\tau^o + k^s \frac{(1-\nu^2)}{E}\sigma^{\infty} - \tau^o \frac{\nu(1-\nu)}{E}\sigma^{\infty}\right)\right\} + \\ -\frac{1-\nu^2}{E}\left\{k\left(\tau^o + k^s \frac{(1-\nu^2)}{E}\sigma^{\infty} - \tau^o \frac{\nu(1-\nu)}{E}\sigma^{\infty}\right)\right\} \end{pmatrix}\left(-k\sin kx\right)$$
$$+ (k^s - \tau^o)\left(-\sin kx\right)\left\{\frac{(1-2\nu)(1+\nu)}{E}k^2\left(\tau^o + k^s \frac{(1-\nu^2)}{E}\sigma^{\infty} - \tau^o \frac{\nu(1-\nu)}{E}\sigma^{\infty}\right) + \sigma^{\infty}\frac{2(1-\nu^2)}{E}k\right\}\sin kx.$$

By more simplifying we would have

$$t_x^{(2)} = \beta \sin 2kx,$$

$$\beta = \begin{pmatrix} 2\sigma^\infty + \frac{1}{2}k\tau^o + \left(\frac{5}{2}k^s + \frac{7}{2}\tau^0\right)k\frac{(1-\nu^2)}{E}\sigma^\infty + \left(k^s + \tau^0\right)k\frac{-\nu(1-\nu)+2(1+\nu)}{E}\sigma^\infty + \\ \frac{(1-\nu^2)}{E}\begin{pmatrix} k^2(2k^s+3\tau^o)\tau^o + k^s(2k^s+3\tau^o)k^2\frac{(1-\nu^2)}{E}\sigma^\infty - \\ -\tau^o(2k^s+3\tau^o)k^2\frac{\nu(1-\nu)}{E}\sigma^\infty \end{pmatrix} - \frac{\nu(1+\nu)}{E}k^s k\sigma^\infty \end{pmatrix}, \tag{79}$$

$$t_y^{(2)} = \gamma \cos 2kx,$$

$$\gamma = \begin{pmatrix} -\sigma^\infty + k^s\left\{\frac{(1-2\nu)(1+\nu)}{E}k^2\left(\tau^o + k^s\frac{(1-\nu^2)}{E}\sigma^\infty - \tau^o\frac{\nu(1-\nu)}{E}\sigma^\infty\right) - \sigma^\infty k\frac{2(1-\nu^2)}{E}\right\} \\ -2\tau^o\begin{pmatrix} -\frac{\nu(1+\nu)}{E}k\left\{-2\sigma^\infty - k\left(\tau^o + k^s\frac{(1-\nu^2)}{E}\sigma^\infty - \tau^o\frac{\nu(1-\nu)}{E}\sigma^\infty\right)\right\} + \\ -\frac{1-\nu^2}{E}k^2\left(\tau^o + k^s\frac{(1-\nu^2)}{E}\sigma^\infty - \tau^o\frac{\nu(1-\nu)}{E}\sigma^\infty\right) \end{pmatrix} \end{pmatrix}. \tag{80}$$

By solving the second order terms we are lead to the following results:

$$\begin{aligned} &\sigma_{xx}^{(2)} = 2\beta\left(1+ky\right)e^{2ky}\cos 2kx + \gamma(1+2ky)e^{2ky}\cos 2kx \\ &\sigma_{yy}^{(2)} = -2\beta kye^{2ky}\cos 2kx + \gamma(1-2ky)e^{2ky}\cos 2kx \\ &\varepsilon_{xx}^{(2)} = \frac{1-\nu^2}{E}\left(2\beta\left(1+ky\right)e^{2ky}\cos 2kx + \gamma(1+2ky)e^{2ky}\cos 2kx\right) - \\ &\frac{\nu(1+\nu)}{E}\left(-2\beta kye^{2ky}\cos 2kx + \gamma(1-2ky)e^{2ky}\cos 2kx\right), \end{aligned} \tag{81}$$

and at $y = 0$

$$\begin{aligned} &\varepsilon_{xx}^{(2)}\Big|_{y=0} = \frac{(1-2\nu)(1+\nu)}{E}\gamma\cos 2kx + \frac{2(1-\nu^2)}{E}\beta\cos 2kx = \eta\cos 2kx \\ &\text{with} \\ &\eta = \frac{(1-2\nu)(1+\nu)}{E}\gamma + \frac{2(1-\nu^2)}{E}\beta. \end{aligned} \tag{82}$$

In order to find the surface stress on $y = h(x)$, we use the transformation law in section 2.4.1 and Taylor extrapolation that yield ε_{ss} as

$$
\begin{aligned}
&[\varepsilon_{ss}]_{y=h(x)} = \left[\varepsilon_{xx} + 2\delta h_{0x}\varepsilon_{xy} + \delta^2 (h_{0x})^2 (\varepsilon_{yy} - \varepsilon_{xx})\right]_{y=h(x)} = \\
&\left[\begin{array}{l}
\varepsilon_{xx}{}^{(0)} + \delta\left(\varepsilon_{xx}{}^{(1)} + 2h_{0x}\varepsilon_{xy}{}^{(0)} + h_0 \dfrac{\partial \varepsilon_{xx}{}^{(0)}}{\partial y}\right) + \\
\delta^2 \left(\begin{array}{l} h_0 \dfrac{\partial \varepsilon_{xx}{}^{(1)}}{\partial y} + \dfrac{1}{2}(h_0)^2 \dfrac{\partial^2 \varepsilon_{xx}{}^{(0)}}{\partial y^2} + 2(h_{0x}) h_0 \dfrac{\partial \varepsilon_{xy}{}^{(0)}}{\partial y} - (h_{0x})^2 \varepsilon_{xx}{}^{(0)} + \varepsilon_{xx}{}^{(2)} + \\ 2h_{0x}\varepsilon_{xy}{}^{(1)} + (h_{0x})^2 \varepsilon_{yy}{}^{(0)} \end{array}\right)
\end{array}\right]_{y=0} \\
&= \frac{1-\nu^2}{E}\sigma^\infty + \delta\left\{-\frac{(1-2\nu)(1+\nu)}{E} k\left(\tau^o + k^s \frac{(1-\nu^2)}{E}\sigma^\infty - \tau^o \frac{\nu(1-\nu)}{E}\sigma^\infty\right) - \sigma^\infty \frac{2(1-\nu^2)}{E}\right\}\cos kx + \\
&+\delta^2 \left\{\begin{array}{l} -3\dfrac{(1-\nu^2)}{E}\sigma^\infty - 2\dfrac{(1-\nu^2)}{E} k\left(\tau^o + k^s \dfrac{(1-\nu^2)}{E}\sigma^\infty - \tau^o \dfrac{\nu(1-\nu)}{E}\sigma^\infty\right) - \dfrac{\nu(1+\nu)}{E}\sigma^\infty \cos^2 kx \\ + \dfrac{(1+\nu)}{E}\sigma_\infty \sin^2 kx + \eta \cos 2kx \end{array}\right\}.
\end{aligned}
\tag{83}
$$

Proceeding similarly as in for previous parts we calculate the total energy of the rough half space and then find the effective surface stress and effective surface elastic constant as below. The detail calculations are not presented here.

$$
(\tau^0)^{eff} = \tau^o - \delta^2 \tau^o \left(\begin{array}{l} \dfrac{3}{4} + kk^s \dfrac{(1+8\nu)(1+\nu)}{8E} - k\tau^o \left(\dfrac{\nu(3-\nu)}{8E}\right) - \\ -\dfrac{(1-2\nu)^2(1+\nu)^2}{2E^2} k^2 (k^s)^2 + -\dfrac{(1-2\nu)^2(1+\nu)^2}{E^2} k^2 \tau^o \dfrac{\nu}{2(1+\nu)} \end{array}\right), \tag{84}
$$

If $\dfrac{kk^s}{E} \ll 1$, equations (84) can be further simplified as

$$
(\tau^0)^{eff} = \tau^o \left(1 - \frac{3}{4}\delta^2\right) \tag{85}
$$

and

$$\left(k^s\right)^{eff} = k^s +$$
$$+\delta^2\left(\begin{array}{l} -\dfrac{E}{k(1-\nu^2)}\left[\dfrac{9-8\nu}{8(1-\nu)}\right]+\dfrac{1}{4}k^s+k(k^s)^2\dfrac{(1+\nu)}{E}\left[\dfrac{-24\nu+7}{8}\right]+k(\tau^o)^2\left[\dfrac{\nu^2\left(7-8\nu\right)}{8E\left(1+\nu\right)}\right] \\ +k^s\tau^o k\left[-\dfrac{\nu(7-12\nu)}{4E}\right]+\dfrac{(1-2\nu)^2(1+\nu)^2}{2E^2}k^2k^s\left((k^s)^2+\left(\tau^o\right)^2\nu^2-2k^s\dfrac{\nu}{(1+\nu)}\tau^o\right)\end{array}\right). \qquad (86)$$

Again, if $\dfrac{kk^s}{E} \ll 1$, equations (86) can be further simplified as

$$\left(k^s\right)^{eff} = k^s + \delta^2\left(-\frac{E}{k(1-\nu^2)}\left[\frac{9-8\nu}{8(1-\nu)}\right]\right). \qquad (87)$$

As is observed from the result, effect of asymmetry term, $\tau^0\nabla_s u$, in effective surface stress and effective surface elastic constant is negligible.

Chapter 3: Elastic Homogenization of Rough Surface with Random Roughness Profile: Theoretical Calculation of Effective Surface Stress and Superficial Elasticity

3.1 Introduction

This chapter is focused on the determination of the surface stress and surface elastic constant for a surface with random roughness profile. In particular, in section 2, the homogenization strategy is presented following with the solution in section 3.

3.2 Homogenization Strategy and Problem Formulation

The displacement field, $u_i (i = x, y, z)$, in general, has two components, its average $\langle u_i \rangle$ over the ensemble of realization of the surface roughness and its fluctuation component Qu_i (Eguiluz and Maradudin, 1983a, 1983b). Due to the randomness of the surface profile, it is useful to introduce the linear operators P (called "smoothing operator", Eguiluz and Maradudin, 1983) and Q such that

$$Pu^{(i)} = \left\langle u^{(i)} \right\rangle, \qquad P + Q = 1, \qquad u^{(i)} \equiv \left(P + Q\right) u^{(i)} = \left\langle u^{(i)} \right\rangle + Qu^{(i)}. \tag{88}$$

We further assume that the random roughness satisfies that for a constant $\eta > 0$,

$$Ph(x) = 0, \qquad Ph^2(x) = \eta^2, \tag{89}$$

where η is the standard deviation of the roughness.

Following a similar procedure for the deterministic roughness profile, the overall half space is subjected to a uniform in-plane stress $\sigma = \sigma^{\infty}\hat{\sigma}$. Using perturbation theory and converting the boundary conditions on the rough surface to an effective boundary condition on the nominal flat surface ∂B^0, we find the boundary conditions on the nominal flat surface as

$$\left(\mathbb{C}\nabla u^{(i)}\right)e_2 = t^{(i)} \quad i = 0,1,2 \quad \text{on } \partial B^0, \tag{90}$$

where the detailed expressions for surface traction $t^{(i)}$ are presented in section 3.3.1 for random rough surface. Direct calculations show that the average field of displacement satisfies an effective problem that is formally similar to the flat surface problem. We remark that the fluctuation $Qu^{(i)}$ is at the order of $\delta Pu^{(i)} \quad \forall\ i = 0,1,2,\cdots$, which will be repeatedly used below. Therefore, we have

$$div\left(\mathbb{C}\left\langle\nabla u^{(i)}\right\rangle\right) = 0 \quad i = 0,1,2 \quad \text{in } B^0, \tag{91}$$

with ensemble average of boundary conditions

$$\left(\mathbb{C}\left\langle\nabla u^{(i)}\right\rangle\right).e_2 = \left\langle t^{(i)}\right\rangle \quad i = 0,1,2 \quad \text{on } \partial B^0. \tag{92}$$

To solve these boundary value problems as will be seen later, we need to find the Q-terms which similarly satisfy the equilibrium equations,

$$div\left(\mathbb{C}Q\left(\nabla u^{(i)}\right)\right) = 0 \quad i = 0,1,2 \quad \text{in } B^0, \tag{93}$$

with boundary conditions,

$$\left(\mathbb{C}Q\left(\nabla u^{(i)}\right)\right)e_2 = Q\left(t^{(i)}\right) \quad i=0,1,2 \quad \text{on } \partial B^0 . \tag{94}$$

Upon solving (91) and (92) for $\left\langle u^{(i)}\right\rangle$ (i=0,1,2) and (93) and (94) for $Qu^{(i)}$ (i=0,1,2), the displacement field $u^{(i)} = \left\langle u^{(i)}\right\rangle + Qu^{(i)}$ (i=0,1,2) is obtained and the total elastic energy of the half-space (13) can be calculated as a function of the applied far field stress. To define the effective surface properties of the surface, we propose to equate the ensemble average of the total elastic energy of the half space with rough surface, $\left\langle E^{act}\left(\sigma^\infty\right)\right\rangle$, with the total elastic energy of a half space with a nominal "effective" flat surface, $E^{eff}\left(\sigma^\infty\right)$ (See equation 14), endowed with effective surface stress and surface elasticity constants:

$$E^{eff}\left(\sigma^\infty\right) = \left\langle E^{act}\left(\sigma^\infty\right)\right\rangle . \tag{95}$$

The above equation will enable us to find the effective surface stress and effective surface elastic constants in a similar manner as for nonrandom cases.

3.3 Solution to the Boundary Value Problem

3.3.1. General Procedure

The general procedure presented in section 2.4.1 for nonrandom surface roughness is applicable for case of random roughness as well. The boundary conditions on the nominal flat surface for $u^{(i)}$ $(i=0,1,2)$, i.e., the right hand side of (90) are presented as (23)-(25). Applying operator P to equations (23)-(25) and assuming that $h=\delta h_0,\ h_0\sim 1$ lead to the following results

$$\left\langle t_x{}^{(0)}\right\rangle = k^s\frac{\partial\left\langle \varepsilon_{xx}{}^{(0)}\right\rangle}{\partial x},\qquad \left\langle t_y{}^{(0)}\right\rangle = 0, \tag{96}$$

$$\begin{aligned}\left\langle t_x{}^{(1)}\right\rangle ={}& -P\left[h_0\frac{\partial Q\sigma_{xy}{}^{(0)}}{\partial y}\right]+P\left[h_{0x}Q\sigma_{xx}{}^{(0)}\right]+k^s\frac{\partial\left\langle \varepsilon_{xx}{}^{(1)}\right\rangle}{\partial x}+k^sP\left[h_0\frac{\partial^2 Q\varepsilon_{xx}{}^{(0)}}{\partial x\partial y}\right]+\\ &+2k^sP\left[h_{0xx}Q\varepsilon_{xy}{}^{(0)}\right]+2k^sP\left[h_{0x}\frac{\partial Q\varepsilon_{xy}{}^{(0)}}{\partial x}\right]+k^sP\left[h_{0x}\frac{\partial Q\varepsilon_{xx}{}^{(0)}}{\partial y}\right],\end{aligned} \tag{97}$$

$$\left\langle t_y{}^{(1)}\right\rangle = -P\left[h_0\frac{\partial Q\sigma_{yy}{}^{(0)}}{\partial y}\right]+P\left[h_{0x}Q\sigma_{yx}{}^{(0)}\right]+\tau^o\left\langle h_{0xx}\right\rangle+k^sP\left[h_{0xx}Q\varepsilon_{xx}{}^{(0)}\right]+k^sP\left[h_{0x}\frac{\partial Q\varepsilon_{xx}{}^{(0)}}{\partial x}\right],$$

$$\begin{aligned}\left\langle t_x{}^{(2)}\right\rangle ={}& P\left[h_{0x}Q\sigma_{xx}{}^{(1)}\right]+P\left[h_0h_{0x}\right]\frac{\partial\left\langle \sigma_{xx}{}^{(0)}\right\rangle}{\partial y}+\frac{1}{2}P\left[h_{0x}h_{0x}\right]\left\langle \sigma_{xy}{}^{(0)}\right\rangle-P\left[h_0\frac{\partial Q\sigma_{xy}{}^{(1)}}{\partial y}\right]-\\ &-\frac{1}{2}\eta^2\frac{\partial^2\left\langle \sigma_{xy}{}^{(0)}\right\rangle}{\partial y^2}-\tau^oP\left[h_{0x}h_{0xx}\right]-k^sP\left[h_{0x}h_{0xx}\right]\left\langle \varepsilon_{xx}{}^{(0)}\right\rangle+k^s\frac{\partial\left\langle \varepsilon_{xx}{}^{(2)}\right\rangle}{\partial x}+k^sP\left[h_0\frac{\partial^2 Q\varepsilon_{xx}{}^{(1)}}{\partial x\partial y}\right]\\ &+\frac{1}{2}\eta^2k^s\frac{\partial^3\left\langle \varepsilon_{xx}{}^{(0)}\right\rangle}{\partial x\partial y^2}-k^sP\left[h_{0x}h_{0x}\right]\frac{\partial\left\langle \varepsilon_{xx}{}^{(0)}\right\rangle}{\partial x}+2k^sP\left[h_{0xx}Q\varepsilon_{xy}{}^{(1)}\right]+2k^sP\left[h_{0xx}h_0\right]\frac{\partial\left\langle \varepsilon_{xy}{}^{(0)}\right\rangle}{\partial y}\\ &+2k^sP\left[h_{0x}\frac{\partial Q\varepsilon_{xy}{}^{(1)}}{\partial x}\right]+2k^sP\left[h_{0x}h_0\right]\frac{\partial^2\left\langle \varepsilon_{xy}{}^{(0)}\right\rangle}{\partial x\partial y}+2k^sP\left[h_{0x}h_{0xx}\right]\left(\left\langle \varepsilon_{yy}{}^{(0)}\right\rangle-\left\langle \varepsilon_{xx}{}^{(0)}\right\rangle\right)+\\ &+k^sP\left[h_{0x}h_{0x}\right]\left(\frac{\partial\left\langle \varepsilon_{yy}{}^{(0)}\right\rangle}{\partial x}-\frac{1}{2}\frac{\partial\left\langle \varepsilon_{xx}{}^{(0)}\right\rangle}{\partial x}\right)+k^sP\left[h_{0x}\frac{\partial Q\varepsilon_{xx}{}^{(1)}}{\partial y}\right]+k^sP\left[h_0h_{0x}\right]\frac{\partial^2\left\langle \varepsilon_{xx}{}^{(0)}\right\rangle}{\partial y^2}+\\ &+2k^sP\left[h_{0x}h_{0x}\right]\frac{\partial\left\langle \varepsilon_{xy}{}^{(0)}\right\rangle}{\partial y},\end{aligned} \tag{98}$$

$$\left\langle t_y{}^{(2)}\right\rangle = -P\left[h_0 \frac{\partial Q\sigma_{yy}{}^{(1)}}{\partial y}\right] - \frac{1}{2}\eta^2 \frac{\partial^2 \left\langle \sigma_{yy}{}^{(0)}\right\rangle}{\partial y^2} + P\left[h_{0x} Q\sigma_{yx}{}^{(1)}\right] + P\left[h_0 h_{0x} \frac{\partial Q\sigma_{yx}{}^{(0)}}{\partial y}\right] +$$
$$+ k^s P\left[h_{0xx} Q\varepsilon_{xx}{}^{(1)}\right] + k^s P\left[h_{0x} \frac{\partial Q\varepsilon_{xx}{}^{(1)}}{\partial x}\right] + 2k^s\varepsilon^2 \frac{\partial \left\langle \varepsilon_{xy}{}^{(0)}\right\rangle}{\partial x} + k^s\varepsilon^2 \frac{\partial \left\langle \varepsilon_{xx}{}^{(0)}\right\rangle}{\partial y} +$$
$$k^s P\left[h_{0xx} h_0 \frac{\partial Q\varepsilon_{xx}{}^{(0)}}{\partial y}\right] + 2k^s P\left[h_{0x} h_{0xx} Q\varepsilon_{xy}{}^{(0)}\right] + k^s P\left[h_{0x} h_0 \frac{\partial^2 Q\varepsilon_{xx}{}^{(0)}}{\partial x \partial y}\right] +$$
$$+ 2k^s P\left[h_{0x} h_{0xx} Q\varepsilon_{xy}{}^{(0)}\right].$$

Equation (92) with $\left\langle t^{(i)}\right\rangle$ given by (96)-(98) prescribe the traction boundary conditions for $\left\langle u^{(i)}\right\rangle$ on the average, nominal surface. The average displacement $\left\langle u^{(i)}\right\rangle$ can then be obtained by solving (91) and (92) which are again the classical Cerruti-Boussinesq half-space problems. From (97) and (98) we observe that in order to find the average displacement $\left\langle u^{(1)}\right\rangle$ $\left(\left\langle u^{(2)}\right\rangle\right)$, we have to a priori find the fluctuation $Qu^{(0)}$ $\left(Qu^{(1)}\right)$. The fluctuations $Qu^{(i)}$ satisfy the boundary value problems (93) and (94). To find the right hand side of (94), we act on (23)-(25) with the operator Q. The results are as follows,

$$Qt_x{}^{(0)} = k^s \frac{\partial Q\varepsilon_{xx}{}^{(0)}}{\partial x}, \qquad Qt_y{}^{(0)} = 0, \tag{99}$$

$$Qt_x{}^{(1)} = -h_0 \frac{\partial \left\langle \sigma_{xy}{}^{(0)}\right\rangle}{\partial y} + h_{0x}\left\langle \sigma_{xx}{}^{(0)}\right\rangle + k^s \frac{\partial Q\varepsilon_{xx}{}^{(1)}}{\partial x} + k^s h_0 \frac{\partial^2 \left\langle \varepsilon_{xx}{}^{(0)}\right\rangle}{\partial x \partial y} + 2k^s h_{0xx}\left\langle \varepsilon_{xy}{}^{(0)}\right\rangle$$
$$+ 2k^s h_{0x} \frac{\partial \left\langle \varepsilon_{xy}{}^{(0)}\right\rangle}{\partial x} + k^s h_{0x} \frac{\partial \left\langle \varepsilon_{xx}{}^{(0)}\right\rangle}{\partial y},$$

(100)

$$Qt_y{}^{(1)} = -h_0 \frac{\partial \left\langle \sigma_{yy}{}^{(0)}\right\rangle}{\partial y} + h_{0x}\left\langle \sigma_{yx}{}^{(0)}\right\rangle + \tau^o h_{0xx} + k^s h_{0xx}\left\langle \varepsilon_{xx}{}^{(0)}\right\rangle + k^s h_{0x} \frac{\partial \left\langle \varepsilon_{xx}{}^{(0)}\right\rangle}{\partial x},$$

$$
\begin{aligned}
Qt_x^{(2)} &= h_{0x}Q\sigma_{xx}^{(1)} + h_{0x}\left\langle \sigma_{xx}^{(1)}\right\rangle + h_{0x}h_0\frac{\partial\left\langle \sigma_{xx}^{(0)}\right\rangle}{\partial y} + \frac{1}{2}\left(h_{0x}\right)^2\left\langle \sigma_{xy}^{(0)}\right\rangle - h_0\frac{\partial\left\langle \sigma_{xy}^{(1)}\right\rangle}{\partial y} \\
&- h_0\frac{\partial Q\sigma_{xy}^{(1)}}{\partial y} - \frac{1}{2}\left(h_0\right)^2\frac{\partial^2\left\langle \sigma_{xy}^{(0)}\right\rangle}{\partial y^2} - \tau^o h_{0x}h_{0xx} - k^s h_{0x}h_{0xx}\left\langle \varepsilon_{xx}^{(0)}\right\rangle + k^s\frac{\partial Q\varepsilon_{xx}^{(2)}}{\partial x} + \\
&+ k^s h_0\frac{\partial^2\left\langle \varepsilon_{xx}^{(1)}\right\rangle}{\partial x\partial y} + k^s h_0\frac{\partial^2 Q\varepsilon_{xx}^{(1)}}{\partial x\partial y} + \frac{1}{2}k^s\left(h_0\right)^2\frac{\partial^3\left\langle \varepsilon_{xx}^{(0)}\right\rangle}{\partial x\partial y^2} - k^s\left(h_{0x}\right)^2\frac{\partial\left\langle \varepsilon_{xx}^{(0)}\right\rangle}{\partial x} + \\
&+ 2k^s h_{0xx}\left\langle \varepsilon_{xy}^{(1)}\right\rangle + 2k^s h_{0xx}Q\varepsilon_{xy}^{(1)} + 2k^s h_{0xx}h_0\frac{\partial\left\langle \varepsilon_{xy}^{(0)}\right\rangle}{\partial y} + 2k^s h_{0x}\frac{\partial\left\langle \varepsilon_{xy}^{(1)}\right\rangle}{\partial x} + 2k^s h_{0x}\frac{\partial Q\varepsilon_{xy}^{(1)}}{\partial x} \\
&+ 2k^s h_0 h_{0x}\frac{\partial^2 Q\varepsilon_{xy}^{(0)}}{\partial x\partial y} + 2k^s h_{0x}h_{0xx}\left(\left\langle \varepsilon_{yy}^{(0)}\right\rangle - \left\langle \varepsilon_{xx}^{(0)}\right\rangle\right) + k^s\left(h_{0x}\right)^2\left(\frac{\partial\left\langle \varepsilon_{yy}^{(0)}\right\rangle}{\partial x} - \frac{1}{2}\frac{\partial\left\langle \varepsilon_{xx}^{(0)}\right\rangle}{\partial x}\right) \\
&+ k^s h_{0x}\frac{\partial\left\langle \varepsilon_{xx}^{(1)}\right\rangle}{\partial y} + k^s h_{0x}\frac{\partial Q\varepsilon_{xx}^{(1)}}{\partial y} + k^s h_{0x}h_0\frac{\partial^2\left\langle \varepsilon_{xx}^{(0)}\right\rangle}{\partial y^2} + 2k^s\left(h_{0x}\right)^2\frac{\partial\left\langle \varepsilon_{xy}^{(0)}\right\rangle}{\partial y},
\end{aligned}
\tag{101}
$$

$$
\begin{aligned}
Qt_y^{(2)} &= h_{0x}Q\sigma_{yx}^{(1)} + h_{0x}\left\langle \sigma_{yx}^{(1)}\right\rangle + h_{0x}h_0\frac{\partial\left\langle \sigma_{yx}^{(0)}\right\rangle}{\partial y} + \frac{1}{2}h_{0x}^2\left\langle \sigma_{yy}^{(0)}\right\rangle - h_0\frac{\partial\left\langle \sigma_{yy}^{(1)}\right\rangle}{\partial y} - h_0\frac{\partial Q\sigma_{yy}^{(1)}}{\partial y} \\
&- \frac{1}{2}h_0^{\,2}\frac{\partial^2\left\langle \sigma_{yy}^{(0)}\right\rangle}{\partial y^2} + k^s h_{0xx}\left\langle \varepsilon_{xx}^{(1)}\right\rangle + k^s h_{0xx}Q\varepsilon_{xx}^{(1)} + k^s h_{0xx}h_0\frac{\partial\left\langle \varepsilon_{xx}^{(0)}\right\rangle}{\partial y} + 2k^s h_{0x}h_{0xx}\left\langle \varepsilon_{xy}^{(0)}\right\rangle \\
&+ k^s h_{0x}\frac{\partial\left\langle \varepsilon_{xx}^{(1)}\right\rangle}{\partial x} + k^s h_{0x}\frac{\partial Q\varepsilon_{xx}^{(1)}}{\partial x} + h_{0x}h_0 k^s\frac{\partial^2\left\langle \varepsilon_{xx}^{(0)}\right\rangle}{\partial x\partial y} + 2k^s h_{0x}h_{0xx}\left\langle \varepsilon_{xy}^{(0)}\right\rangle + \\
&+ 2k^s h_{0x}h_{0x}\frac{\partial\left\langle \varepsilon_{xy}^{(0)}\right\rangle}{\partial x} + k^s h_{0x}h_{0x}\frac{\partial\left\langle \varepsilon_{xx}^{(0)}\right\rangle}{\partial y}.
\end{aligned}
$$

Below we present the detailed calculations for a random surface roughness with Gaussian distribution.

3.3.2. Solution for the Random Roughness Profile

Similar to the nonrandom rough surface, we assume that a far-field stress $\sigma = \sigma^{\infty} e_1 \otimes e_1$ is applied on the half-space. Then with the following sequence, we solve the different order boundary value problems (91) and (92) for $\left\langle u^{(i)}\right\rangle$ and (93) and (94) for $Qu^{(i)}$ using the approach explained in section

2.4.2. Solving (91) and (92) for $i=0$ with the right hand side of (92) given by (96), we obtain $\left\langle u^{(0)} \right\rangle$, then solving (93), (94) for $i=0$ with the right hand side of (94) given by (99), we obtain $Qu^{(0)}$. Similarly, solving (91) and (92) for $i=1$ with the right hand side of (92) given by (93), we obtain $\left\langle u^{(1)} \right\rangle$ and solving (93), (94) for $i=1$ with the right hand side of (94) given by (100), we obtain $Qu^{(1)}$. Again, solving (91) and (92) for $i=2$ with the right hand side of (92) given by (98), we obtain $\left\langle u^{(2)} \right\rangle$ and solving (93), (94) for $i=2$ with the right hand side of (94) given by (101), we obtain $Qu^{(2)}$.

By (96), we have the zeroth order boundary condition for average terms as

$$\left\langle t_x{}^{(0)} \right\rangle = k^s \frac{\partial \left\langle \varepsilon_{xx}{}^{(0)} \right\rangle}{\partial x} = 0, \qquad \left\langle t_y{}^{(0)} \right\rangle = 0 \qquad \text{on} \quad \partial B^0. \tag{102}$$

Zeroth order solution for average terms are

$$\left\langle \sigma_{xx}{}^{(0)} \right\rangle = \sigma^\infty, \qquad \left\langle \sigma_{xy}{}^{(0)} \right\rangle = \left\langle \sigma_{yy}{}^{(0)} \right\rangle = 0 \qquad \text{in } B^0 \tag{103}$$

$$\left\langle \varepsilon_{xx}{}^{(0)} \right\rangle = \frac{1-\nu^2}{E}\sigma^\infty, \qquad \left\langle \varepsilon_{yy}{}^{(0)} \right\rangle = \frac{-\nu\left(1+\nu\right)}{E}\sigma^\infty, \qquad \left\langle \varepsilon_{xy}{}^{(0)} \right\rangle = 0 \qquad \text{in } B^0. \tag{104}$$

The boundary condition for Q-terms (99) would be rewritten as

$$Qt_x{}^{(0)} = 0, \qquad Qt_y{}^{(0)} = 0 \qquad \text{on} \quad \partial B^0. \tag{105}$$

The zeroth order solution for Q-terms are obtained as

$$Q\sigma_{xx}{}^{(0)} = Q\sigma_{xy}{}^{(0)} = Q\sigma_{yy}{}^{(0)} = 0 \qquad \text{in } B^0. \tag{106}$$

By (97), we have the first order boundary condition for average terms as

$$\left\langle t_x{}^{(1)} \right\rangle = 0, \qquad \left\langle t_y{}^{(1)} \right\rangle = 0 \qquad \text{on } \partial B^0, \tag{107}$$

and the first order solution for average terms is

$$\left\langle \sigma^{(1)} \right\rangle = 0. \qquad \text{in } B^0 \tag{108}$$

$$\left\langle \varepsilon_{xx}{}^{(1)} \right\rangle = \left\langle \varepsilon_{xy}{}^{(1)} \right\rangle = \left\langle \varepsilon_{yy}{}^{(1)} \right\rangle = 0. \qquad \text{in } B^0. \tag{109}$$

Similarly, using first order boundary condition for Q-terms (100),

$$Qt_x{}^{(1)} = h_{0x}\sigma^\infty, \qquad Qt_y{}^{(1)} = \left[\tau^o + \frac{(1-\nu^2)}{E}(k^s - \tau^o)\sigma^\infty \right] h_{0xx} \qquad \text{on } \partial B^0, \tag{110}$$

first order solution for Q-terms are obtained as follows,

$$Q\sigma_{xx}{}^{(1)}(x,y) = \frac{1}{2\pi}\int_{-\infty}^{\infty} \left[f(\alpha)\left(-2\frac{|\alpha|}{i\alpha} + i\alpha y \right) + p(\alpha)\left(1 + |\alpha| y\right) \right] e^{i\alpha x + |\alpha| y} d\alpha,$$

$$Q\sigma_{xy}{}^{(1)}(x,y) = \frac{1}{2\pi}\int_{-\infty}^{\infty} \left[f(\alpha)\left(1 + |\alpha| y\right) - i\alpha p(\alpha) y \right] e^{i\alpha x + |\alpha| y} d\alpha,$$

$$Q\sigma_{yy}{}^{(1)}(x,y) = \frac{1}{2\pi}\int_{-\infty}^{\infty} \left[-i\alpha f(\alpha) y + p(\alpha)\left(1 - |\alpha| y\right) \right] e^{i\alpha x + |\alpha| y} d\alpha, \tag{111}$$

$$Q\varepsilon_{xy}{}^{(1)}(x,y) = \frac{(1+\nu)}{E} Q\sigma_{xy}{}^{(1)}(x,y) = \frac{(1+\nu)}{2\pi E}\int_{-\infty}^{\infty} \left[f(\alpha)\left(1 + |\alpha| y\right) - i\alpha p(\alpha) y \right] e^{i\alpha x + |\alpha| y} d\alpha,$$

$$\frac{\partial Q\varepsilon_{xy}{}^{(1)}(x,y)}{\partial x} = \frac{(1+\nu)}{2\pi E}\int_{-\infty}^{\infty} \left[f(\alpha)(i\alpha)\left(1 + |\alpha| y\right) + \alpha^2 p(\alpha) y \right] e^{i\alpha x + |\alpha| y} d\alpha,$$

$$Q\varepsilon_{xx}{}^{(1)}(x,y)=\frac{1-\nu^2}{E}Q\sigma_{xx}{}^{(1)}(x,y)-\frac{\nu(1+\nu)}{E}Q\sigma_{yy}{}^{(1)}(x,y)=$$
$$\frac{1-\nu^2}{E}\frac{1}{2\pi}\int_{-\infty}^{\infty}\left[f(\alpha)\left(-2\frac{|\alpha|}{i\alpha}+i\alpha y\right)+p(\alpha)\left(1+|\alpha|y\right)\right]e^{i\alpha x+|\alpha|y}d\alpha$$
$$-\frac{\nu(1+\nu)}{E}\frac{1}{2\pi}\int_{-\infty}^{\infty}\left[-i\alpha f(\alpha)y+p(\alpha)\left(1-|\alpha|y\right)\right]e^{i\alpha x+|\alpha|y}d\alpha,$$

$$\frac{\partial Q\sigma_{xy}{}^{(1)}(x,y)}{\partial y}=\frac{1}{2\pi}\int_{-\infty}^{\infty}\left[f(\alpha)\left(2|\alpha|+\alpha^2 y\right)-i\alpha p(\alpha)\left(1+|\alpha|y\right)\right]e^{i\alpha x+|\alpha|y}d\alpha,$$

$$\frac{\partial Q\sigma_{yy}{}^{(1)}(x,y)}{\partial y}=\frac{1}{2\pi}\int_{-\infty}^{\infty}\left[-i\alpha f(\alpha)\left(1+|\alpha|y\right)+p(\alpha)\left(-\alpha^2 y\right)\right]e^{i\alpha x+|\alpha|y}d\alpha,$$

$$\frac{\partial Q\varepsilon_{xx}{}^{(1)}(x,y)}{\partial y}=\frac{1-\nu^2}{E}\frac{1}{2\pi}\int_{-\infty}^{\infty}\left[i\alpha f(\alpha)\left(3+|\alpha|y\right)+p(\alpha)\left(2|\alpha|+\alpha^2 y\right)\right]e^{i\alpha x+|\alpha|y}d\alpha$$
$$-\frac{\nu(1+\nu)}{E}\frac{1}{2\pi}\int_{-\infty}^{\infty}\left[-i\alpha f(\alpha)\left(1+|\alpha|y\right)-p(\alpha)\left(\alpha^2 y\right)\right]e^{i\alpha x+|\alpha|y}d\alpha,$$

$$\frac{\partial^2 Q\varepsilon_{xx}{}^{(1)}(x,y)}{\partial x\partial y}=\frac{1-\nu^2}{E}\frac{1}{2\pi}\int_{-\infty}^{\infty}\left[-\alpha^2 f(\alpha)\left(3+|\alpha|y\right)+(i\alpha)p(\alpha)\left(2|\alpha|+\alpha^2 y\right)\right]e^{i\alpha x+|\alpha|y}d\alpha$$
$$-\frac{\nu(1+\nu)}{E}\frac{1}{2\pi}\int_{-\infty}^{\infty}\left[\alpha^2 f(\alpha)\left(1+|\alpha|y\right)-p(\alpha)(i\alpha^3 y)\right]e^{i\alpha x+|\alpha|y}d\alpha$$

where $f(\alpha)=\sigma_\infty(i\alpha)h_0(\alpha)$ and $p(\alpha)=\left(\tau^o+\frac{(1-\nu^2)}{E}(k^s-\tau^o)\sigma^\infty\right)(i\alpha)^2h_0(\alpha)$.

Consequently, by calculating (111) at $y=0$, the second order B.C. (98) on average fields are rewritten as

$$\begin{aligned}\left\langle t_y{}^{(2)}\right\rangle&=\sigma_\infty P\left[h_0h_{0xx}(x)\right]+\sigma_\infty P\left[h_{0x}h_{0x}(x)\right]-2\sigma_\infty\frac{1-\nu^2}{E}k^sP\left[\frac{1}{2\pi}h_{0xx}\int_{-\infty}^{\infty}|\alpha|h_0(\alpha)e^{i\alpha x}d\alpha\right]\\&+\frac{(1+\nu)(1-2\nu)}{E}k^s\left(\tau^o+\frac{(1-\nu^2)}{E}k^s\sigma^\infty\right)P\left[h_{0xx}(x)h_{0xx}(x)\right]\\&-2\frac{1-\nu^2}{E}k^s\sigma_\infty P\left[\frac{1}{2\pi}h_{0x}\int_{-\infty}^{\infty}i\alpha|\alpha|h_0(\alpha)e^{i\alpha x}d\alpha\right]+\\&+\frac{(1+\nu)(1-2\nu)}{E}k^s\left(\tau^o+\frac{(1-\nu^2)}{E}k^s\sigma^\infty\right)P\left[h_{0x}(x)h_{0xxx}(x)\right]\end{aligned}\tag{112}$$

$$
\begin{aligned}
\left\langle t_x^{(2)}\right\rangle = & P\left[-2\sigma_\infty \frac{1}{2\pi}h_{0x}\int_{-\infty}^{\infty}|\alpha|h_0(\alpha)e^{i\alpha x}d\alpha+\left(\tau^o+\frac{(1-\nu^2)}{E}k^s\sigma^\infty\right)h_{0x}h_{0xx}(x)\right] \\
& -P\left[2\sigma_\infty \frac{1}{2\pi}h_0\int_{-\infty}^{\infty}i\alpha|\alpha|h_0(\alpha)e^{i\alpha x}d\alpha-\left(\tau^o+\frac{(1-\nu^2)}{E}k^s\sigma^\infty\right)h_0h_{0xxx}(x)\right]-\tau^o P\left[h_{0x}h_{0xx}\right] \\
& -k^s P\left[h_{0x}h_{0xx}\right]\frac{1-\nu^2}{E}\sigma_\infty+3k^s\frac{1-\nu^2}{E}\sigma_\infty P\left[h_0(x)h_{0xxx}(x)\right]- \\
& -2k^s\frac{1-\nu^2}{E}\left(\tau^o+\frac{(1-\nu^2)}{E}k^s\sigma^\infty\right)P\left[\frac{1}{2\pi}h_0\int_{-\infty}^{\infty}i\alpha^3|\alpha|h_0(\alpha)e^{i\alpha x}d\alpha\right]+ \\
& +k^s\frac{\nu(1+\nu)}{E}\sigma_\infty P\left[h_0(x)h_{0xxx}(x)\right]+2k^s\frac{(1+\nu)}{E}\sigma_\infty P\left[h_{0xx}(x)h_{0x}(x)\right]+ \\
& +2k^s\frac{(1+\nu)}{E}\sigma_\infty P\left[h_{0x}(x)h_{0xx}(x)\right]+2k^s P\left[h_{0x}(x)h_{0xx}(x)\right]\left(-\frac{\nu(1+\nu)}{E}\sigma_\infty-\frac{1-\nu^2}{E}\sigma_\infty\right) \\
& +3k^s\frac{1-\nu^2}{E}\sigma_\infty P\left[h_{0x}(x)h_{0xx}(x)\right] \\
& -2k^s\frac{1-\nu^2}{E}\left(\tau^o+\frac{(1-\nu^2)}{E}k^s\sigma^\infty\right)P\left[\frac{1}{2\pi}h_{0x}\int_{-\infty}^{\infty}\alpha^2|\alpha|h_0(\alpha)e^{i\alpha x}d\alpha\right] \\
& +k^s\frac{\nu(1+\nu)}{E}\sigma_\infty P\left[h_{0x}(x)h_{0xx}(x)\right].
\end{aligned}
\tag{113}
$$

By replacing $h_0(x)$ by its Fourier integral representation $h_0(x)=\frac{1}{2\pi}\int_{-\infty}^{\infty}h_0(\xi)e^{i\xi x}d\xi$,

(112) and (113) would be rewritten as

$$
\begin{aligned}
< t_y^{(2)} >= & \sigma_\infty\left\langle h_0(x)h_{0xx}(x)\right\rangle+\sigma_\infty\left\langle h_{0x}(x)h_{0x}(x)\right\rangle \\
& -2\sigma_\infty k^s\frac{1-\nu^2}{E}\left(\frac{1}{2\pi}\right)^2 P\left[\int_{-\infty}^{\infty}(i\beta)^2h_0(\beta)e^{i\beta x}d\beta\int_{-\infty}^{\infty}|\alpha|h_0(\alpha)e^{i\alpha x}d\alpha\right] \\
& +\frac{(1+\nu)(1-2\nu)}{E}k^s\left(\tau^o+\frac{(1-\nu^2)}{E}k^s\sigma^\infty\right)\left\langle h_{0xx}(x)h_{0xx}(x)\right\rangle \\
& -P\left[2\sigma_\infty\frac{1-\nu^2}{E}k^s\left(\frac{1}{2\pi}\right)^2\int_{-\infty}^{\infty}(i\beta)h_0(\beta)e^{i\beta x}d\beta\int_{-\infty}^{\infty}i\alpha|\alpha|h_0(\alpha)e^{i\alpha x}d\alpha\right]+ \\
& +\frac{(1+\nu)(1-2\nu)}{E}k^s\left(\tau^o+\frac{(1-\nu^2)}{E}k^s\sigma^\infty\right)\left\langle h_{0x}(x)h_{0xxx}(x)\right\rangle
\end{aligned}
\tag{114}
$$

$$
\begin{aligned}
< t_x^{(2)} >= &-P\left[2\sigma_\infty\left(\frac{1}{2\pi}\right)^2\int_{-\infty}^{\infty}(i\beta)h_0(\beta)e^{i\beta x}d\beta\int_{-\infty}^{\infty}|\alpha|h_0(\alpha)e^{i\alpha x}d\alpha\right]+\\
&+\left(\tau^o+\frac{(1-\nu^2)}{E}k^s\sigma^\infty\right)\langle h_{0x}(x)h_{0xx}(x)\rangle-\\
&-P\left[2\sigma_\infty\left(\frac{1}{2\pi}\right)^2\int_{-\infty}^{\infty}h_0(\beta)e^{i\beta x}d\beta\int_{-\infty}^{\infty}(i\alpha)|\alpha|h_0(\alpha)e^{i\alpha x}d\alpha\right]\\
&+\left(\tau^o+\frac{(1-\nu^2)}{E}k^s\sigma^\infty\right)\langle h_0(x)h_{0xxx}(x)\rangle-\tau^o\langle h_{0x}(x)h_{0xx}(x)\rangle\\
&-k^s\frac{1-\nu^2}{E}\sigma_\infty\langle h_{0x}(x)h_{0xx}(x)\rangle+3\frac{1-\nu^2}{E}\sigma_\infty k^s\langle h_0(x)h_{0xxx}(x)\rangle\\
&-2\frac{1-\nu^2}{E}k^s\left(\tau^o+\frac{(1-\nu^2)}{E}k^s\sigma^\infty\right)P\left[\left(\frac{1}{2\pi}\right)^2\int_{-\infty}^{\infty}h_0(\beta)e^{i\beta x}d\beta\int_{-\infty}^{\infty}i\alpha^3|\alpha|h_0(\alpha)e^{i\alpha x}d\alpha\right]\\
&+\frac{\nu(1+\nu)}{E}\sigma_\infty k^s\langle h_0(x)h_{0xxx}(x)\rangle+\frac{2(1+\nu)}{E}\sigma_\infty k^s\langle h_{0xx}(x)h_{0x}(x)\rangle+\\
&+\frac{2(1+\nu)}{E}\sigma_\infty k^s\langle h_{0x}(x)h_{0xx}(x)\rangle+2k^s\langle h_{0xx}(x)h_{0x}(x)\rangle\left(-\frac{\nu(1+\nu)}{E}\sigma_\infty-\frac{1-\nu^2}{E}\sigma_\infty\right)\\
&+3\sigma_\infty\frac{1-\nu^2}{E}k^s\langle h_{0x}(x)h_{0xx}(x)\rangle+\frac{\nu(1+\nu)}{E}\sigma_\infty k^s\langle h_{0x}(x)h_{0xx}(x)\rangle\\
&-2\frac{1-\nu^2}{E}k^s\left(\tau^o+\frac{(1-\nu^2)}{E}k^s\sigma^\infty\right)P\left[\left(\frac{1}{2\pi}\right)^2\int_{-\infty}^{\infty}(i\beta)h_0(\beta)e^{i\beta x}\int_{-\infty}^{\infty}\alpha^2|\alpha|h_0(\alpha)e^{i\alpha x}d\alpha\right].
\end{aligned}
\tag{115}
$$

We should note here that in order to solve second order boundary value problems we must specify the nature of the randomness of the surface. For that purpose we introduce the surface height correlation function W

$$
\langle h_0(x)h_0(x')\rangle=\eta^2W(|x-x'|)\,. \tag{116}
$$

where η is the root-mean-square departure of the surface from flatness and $W(0)=1$.

If $h_0(x)$ with Fourier integral representation of

$$h_0(x) = \frac{1}{2\pi}\int_{-\infty}^{\infty} h_0(\xi)e^{i\xi x}d\xi \ , \tag{117}$$

be a zero-mean Gaussian random function, then, its Fourier coefficient $h_0(\xi)$ is also a zero-mean Gaussian random variable and possesses the properties (Maradudin, 2007),

$$\begin{aligned} &\langle h_0(\xi)\rangle = 0, \\ &\langle h_0(\xi)h_0(\xi')\rangle = (2\pi)\eta^2 g(\xi)\delta(\xi+\xi'), \end{aligned} \tag{118}$$

where $g(\xi)$ is the one-dimensional Fourier transform of the surface height autocorrelation function $W(|x|)$,

$$g(\xi) = \int_{-\infty}^{\infty} W(|x|)e^{-i\xi x}dx \ . \tag{119}$$

Here $W(|x|)$ and hence $g(\xi)$ will be assumed to be Gaussian in form

$$\begin{aligned} &W(|x|) = e^{(-x^2/a^2)}, \\ &g(\xi) = \sqrt{\pi}ae^{(-a^2\xi^2/4)}. \end{aligned} \tag{120}$$

The characteristic length a is the transverse correlation length of the surface roughness. It is a measure of the average distance between successive ‘peaks’ or ‘valleys’ on the surface.

Also, if $h'(x) = L_1 h(x)$ and $h''(x) = L_2 h(x)$ and L_1 and L_2 be two linear and homogeneous operators, then (Sveshnikov, 1978)

$$\left\langle h'(x)\right\rangle = L_1 \left\langle h(x)\right\rangle,$$

$$\left\langle h_0'(x)h_0'(x'))\right\rangle = L_{1x}L_{1x'}W\left|(x-x')\right|, \tag{121}$$

$$\left\langle (L_1 h_0(x))(L_2 h_0(x'))\right\rangle = L_{1x}L_{2x'}W\left|(x-x')\right|.$$

Here the first equation is the expectation value of random variable $h'(x)$, the second equation is the autocorrelation function of a random variable $h'(x)$, and the third equation is the mutual or cross correlation function of two random variables $h'(x)$ and $h''(x)$. As an example, to calculate $\left\langle h_0(x)h_{0xxx}(x')\right\rangle$, $L_1 = 1$ and $L_2 = \frac{d^3}{dx^3}$, then

$$\left\langle h_0(x)h_{0xxx}(x')\right\rangle = \frac{d^3}{dx'^3}W\left|x-x'\right| = \frac{d^3}{dx'^3}e^{\frac{-\left|x-x'\right|^2}{a^2}}. \tag{122}$$

Therefore, we obtain

$$\left\langle h_0(x)h_{0xxx}(x)\right\rangle = 0, \qquad \left\langle h_{0x}(x)h_{0xx}(x)\right\rangle = 0,$$

$$\left\langle h_{0x}(x)h_{0x}(x)\right\rangle = \frac{2\eta^2}{a^2}, \qquad \left\langle h_0(x)h_{0xx}(x)\right\rangle = -\frac{2\eta^2}{a^2}, \tag{123}$$

$$\left\langle h_{0xx}(x)h_{0xx}(x)\right\rangle = \frac{12\eta^2}{a^4}, \qquad \left\langle h_{0x}(x)h_{0xxx}(x)\right\rangle = -12\frac{\eta^2}{a^4}.$$

The second order boundary condition (114) and (115) can be rewritten as

$$
\begin{aligned}
< t_x{}^{(2)} > = & -2\sigma_\infty \left(\frac{1}{2\pi}\right)^2 (2\pi)\eta^2 \int_{-\infty}^{\infty}\int_{-\infty}^{\infty} i\beta \left|\alpha\right| g(\alpha)\delta(\alpha+\beta)e^{i(\alpha+\beta)x} d\alpha d\beta \\
& -2\sigma_\infty \left(\frac{1}{2\pi}\right)^2 (2\pi)\eta^2 \int_{-\infty}^{\infty}\int_{-\infty}^{\infty} i\alpha \left|\alpha\right| g(\alpha)\delta(\alpha+\beta)e^{i(\alpha+\beta)x} d\alpha d\beta \\
& -2\frac{1-\nu^2}{E}k^s\left(\tau^o + \frac{(1-\nu^2)}{E}k^s\sigma^\infty\right)\left(\frac{1}{2\pi}\right)^2 (2\pi)\eta^2 \int_{-\infty}^{\infty}\int_{-\infty}^{\infty} i\alpha^3 \left|\alpha\right| g(\alpha)\delta(\alpha+\beta)e^{i(\alpha+\beta)x} d\alpha d\beta \\
& -2\frac{1-\nu^2}{E}k^s\left(\tau^o + \frac{(1-\nu^2)}{E}k^s\sigma^\infty\right)\left(\frac{1}{2\pi}\right)^2 (2\pi)\eta^2 \int_{-\infty}^{\infty}\int_{-\infty}^{\infty} (i\beta)\alpha^2 \left|\alpha\right| g(\alpha)\delta(\alpha+\beta)e^{i(\alpha+\beta)x} d\alpha d\beta .
\end{aligned}
\tag{124}
$$

$$
\begin{aligned}
< t_y{}^{(2)} > = & -2\sigma_\infty k^s \frac{1-\nu^2}{E}\left(\frac{1}{2\pi}\right)^2 (2\pi)\eta^2 \int_{-\infty}^{\infty}\int_{-\infty}^{\infty} (i\beta)^2 \left|\alpha\right| g(\alpha)\delta(\alpha+\beta)e^{i(\alpha+\beta)x} d\alpha d\beta \\
& -2\sigma_\infty \frac{1-\nu^2}{E}k^s\left(\frac{1}{2\pi}\right)^2 (2\pi)\eta^2 \int_{-\infty}^{\infty}\int_{-\infty}^{\infty} (i\beta)(i\alpha) \left|\alpha\right| g(\alpha)\delta(\alpha+\beta)e^{i(\alpha+\beta)x} d\alpha d\beta
\end{aligned}
\tag{125}
$$

By more simplifying we would have

$$
< t_x{}^{(2)} > = 0 , \qquad < t_y{}^{(2)} > = 0 \qquad \text{on } \partial B^0 \tag{126}
$$

and the second order solution for average stresses would be obtained as

$$
< \sigma^{(2)} > = 0 \tag{127}
$$

$$
\left\langle \varepsilon_{xx}{}^{(2)} \right\rangle = \left\langle \varepsilon_{xy}{}^{(2)} \right\rangle = \left\langle \varepsilon_{yy}{}^{(2)} \right\rangle = 0. \qquad \text{in } B^0 . \tag{128}
$$

We also need to find the second order solution for Q-terms. The second order boundary conditions for Q-terms (101) would be rewritten as

$$
\begin{aligned}
Qt_x^{(2)} &= h_{0x}\left(-2\sigma_\infty \frac{1}{2\pi}\int_{-\infty}^{\infty}|\alpha|h_0(\alpha)e^{i\alpha x}d\alpha + \left(\tau^o + \frac{(1-\nu^2)}{E}k^s\sigma^\infty\right)h_{0xx}(x)\right) \\
&\quad - h_0\left(2\sigma_\infty \frac{1}{2\pi}\int_{-\infty}^{\infty} i\alpha|\alpha|h_0(\alpha)e^{i\alpha x}d\alpha - \left(\tau^o + \frac{(1-\nu^2)}{E}k^s\sigma^\infty\right)h_{0xxx}(x)\right) \\
&\quad - \tau^o h_{0x}h_{0xx} - k^s h_{0x}h_{0xx}\frac{(1-\nu^2)}{E}\sigma^\infty \\
&\quad + k^s h_0\left(\begin{array}{l} 3\frac{1-\nu^2}{E}\sigma_\infty h_{0xxx}(x) - 2\frac{1-\nu^2}{E}\left(\tau^o + \frac{(1-\nu^2)}{E}k^s\sigma^\infty\right)\frac{1}{2\pi}\int_{-\infty}^{\infty} i\alpha^3|\alpha|h_0(\alpha)e^{i\alpha x}d\alpha + \\ + \frac{\nu(1+\nu)}{E}\sigma_\infty h_{0xxx}(x) \end{array}\right) \\
&\quad + 2k^s h_{0xx}\left(\frac{(1+\nu)}{E}\sigma_\infty h_{0x}(x)\right) + 2k^s h_{0x}\left(\frac{(1+\nu)}{E}\sigma_\infty h_{0xx}(x)\right) + 2k^s h_{0x}h_{0xx}\left(-\frac{\nu(1+\nu)}{E}\sigma_\infty - \frac{(1-\nu^2)}{E}\sigma^\infty\right) \\
&\quad + k^s h_{0x}\left(\begin{array}{l} 3\sigma_\infty\frac{1-\nu^2}{E}h_{0xx}(x) - 2\frac{1-\nu^2}{E}\left(\tau^o + \frac{(1-\nu^2)}{E}k^s\sigma^\infty\right)\frac{1}{2\pi}\int_{-\infty}^{\infty}\alpha^2|\alpha|h_0(\alpha)e^{i\alpha x}d\alpha + \\ + \sigma_\infty\frac{\nu(1+\nu)}{E}h_{0xx}(x) \end{array}\right)
\end{aligned}
\tag{129}
$$

$$
\begin{aligned}
Qt_y^{(2)} &= h_{0x}(x)Q\sigma_{yx}^{(1)} + h_0(x)\sigma_\infty h_{0xx}(x) + \\
&\quad + k^s h_{0xx}(x)\left(-2\sigma_\infty\frac{1-\nu^2}{E}\frac{1}{2\pi}\int_{-\infty}^{\infty}|\alpha|h_0(\alpha)e^{i\alpha x}d\alpha + \frac{(1+\nu)(1-2\nu)}{E}\left(\tau^o + \frac{(1-\nu^2)}{E}k^s\sigma^\infty\right)h_{0xx}(x)\right) \\
&\quad + k^s h_{0x}(x)\left(-2\frac{1-\nu^2}{E}\frac{\sigma_\infty}{2\pi}\int_{-\infty}^{\infty} i\alpha|\alpha|h_0(\alpha)e^{i\alpha x}d\alpha + \frac{(1+\nu)(1-2\nu)}{E}\left(\tau^o + \frac{(1-\nu^2)}{E}k^s\sigma^\infty\right)h_{0xxx}(x)\right).
\end{aligned}
\tag{130}
$$

The solutions for the second order Q-terms are obtained as

$$Q\sigma_{xx}^{(2)}(x,y) = \frac{1}{2\pi}\int_{-\infty}^{\infty}\left[f(\alpha)\left(-2\frac{|\alpha|}{i\alpha} + i\alpha y\right) + p(\alpha)\left(1+|\alpha|y\right)\right]e^{i\alpha x+|\alpha|y}d\alpha$$

$$Q\sigma_{xy}^{(2)}(x,y) = \frac{1}{2\pi}\int_{-\infty}^{\infty}\left[f(\alpha)\left(1+|\alpha|y\right) - i\alpha p(\alpha)y\right]e^{i\alpha x+|\alpha|y}d\alpha$$

$$Q\sigma_{yy}^{(2)}(x,y) = \frac{1}{2\pi}\int_{-\infty}^{\infty}\left[-i\alpha f(\alpha)y + p(\alpha)\left(1-|\alpha|y\right)\right]e^{i\alpha x+|\alpha|y}d\alpha$$

$$Q\varepsilon_{xy}^{(2)}(x,y) = \frac{(1+\nu)}{E}Q\sigma_{xy}^{(1)}(x,y) = \frac{(1+\nu)}{2\pi E}\int_{-\infty}^{\infty}\left[f(\alpha)\left(1+|\alpha|y\right) - i\alpha p(\alpha)y\right]e^{i\alpha x+|\alpha|y}d\alpha$$

$$
\begin{aligned}
Q\varepsilon_{xx}{}^{(2)}(x,y) = \frac{1-\nu^2}{E} Q\sigma_{xx}{}^{(1)}(x,y) - \frac{\nu(1+\nu)}{E} Q\sigma_{yy}{}^{(1)}(x,y) = \\
\frac{1-\nu^2}{E}\frac{1}{2\pi}\int_{-\infty}^{\infty}\left[f(\alpha)\left(-2\frac{|\alpha|}{i\alpha}+i\alpha y\right)+p(\alpha)\left(1+|\alpha|y\right)\right] e^{i\alpha x+|\alpha|y} d\alpha - \\
-\frac{\nu(1+\nu)}{E}\frac{1}{2\pi}\int_{-\infty}^{\infty}\left[-i\alpha f(\alpha)y+p(\alpha)\left(1-|\alpha|y\right)\right] e^{i\alpha x+|\alpha|y} d\alpha,
\end{aligned}
\tag{131}
$$

where $f(\alpha)$ and $p(\alpha)$ are the Fourier transform of (129) and (130), respectively. By using the relations in section 2.4.1 and performing the Taylor series extrapolation, the surface strain on the rough surface is obtained as

$$
\begin{aligned}
\left[\varepsilon_{ss}\right]_{y=h(x)} &= \left[\varepsilon_{xx}+2\delta h_{0x}\varepsilon_{xy}+\delta^2\left(h_{0x}\right)^2\left(\varepsilon_{yy}-\varepsilon_{xx}\right)\right]_{y=h(x)} = \\
&= \left[\begin{array}{l}
\varepsilon_{xx}{}^{(0)}+\delta\left(\varepsilon_{xx}{}^{(1)}+2h_{0x}\varepsilon_{xy}{}^{(0)}+h_0\dfrac{\partial\varepsilon_{xx}{}^{(0)}}{\partial y}\right)+ \\
\delta^2\left(\begin{array}{l}
h_0\dfrac{\partial\varepsilon_{xx}{}^{(1)}}{\partial y}+\dfrac{1}{2}\left(h_0\right)^2\dfrac{\partial^2\varepsilon_{xx}{}^{(0)}}{\partial y^2}+2\left(h_{0x}\right)h_0\dfrac{\partial\varepsilon_{xy}{}^{(0)}}{\partial y} \\
-\left(h_{0x}\right)^2\varepsilon_{xx}{}^{(0)}+\varepsilon_{xx}{}^{(2)}+2h_{0x}\varepsilon_{xy}{}^{(1)}+\left(h_{0x}\right)^2\varepsilon_{yy}{}^{(0)}
\end{array}\right)
\end{array}\right]_{y=0} \\
&= \left[\begin{array}{l}
\left\langle\varepsilon_{xx}{}^{(0)}\right\rangle+\delta\left(Q\varepsilon_{xx}{}^{(1)}\right)+ \\
\delta^2\left(h_0\dfrac{\partial Q\varepsilon_{xx}{}^{(1)}}{\partial y}-\left(h_{0x}\right)^2\left\langle\varepsilon_{xx}{}^{(0)}\right\rangle+Q\varepsilon_{xx}{}^{(2)}+2h_{0x}Q\varepsilon_{xy}{}^{(1)}+\left(h_{0x}\right)^2\left\langle\varepsilon_{yy}{}^{(0)}\right\rangle\right)
\end{array}\right]_{y=0}
\end{aligned}
\tag{132}
$$

and gives us

$$
\begin{aligned}
\left[\varepsilon_{ss}\right]_{y=h(x)} &= \\
&= \frac{1-\nu^2}{E}\sigma^\infty+\delta\left(\begin{array}{l}
\left\{\dfrac{1}{2\pi}\displaystyle\int_{-\infty}^{\infty}-2|\alpha|\sigma_\infty h_0(\alpha)e^{i\alpha x}d\alpha+\left[\tau^o+\dfrac{(1-\nu^2)}{E}k^s\sigma^\infty\right]h_{0xx}(x)\right\}\dfrac{(1-\nu^2)}{E}+ \\
+\left\{\tau^o+\dfrac{(1-\nu^2)}{E}k^s\sigma^\infty h_{0xx}(x)\right\}\dfrac{-\nu(1+\nu)}{E}
\end{array}\right) \\
&+\delta^2\left(\begin{array}{l}
h_0(x)\left[\begin{array}{l}
3\sigma_\infty\dfrac{1-\nu^2}{E}h_{0xx}(x)-2\dfrac{1-\nu^2}{E}\left(\tau^o+\dfrac{(1-\nu^2)}{E}k^s\sigma^\infty\right)\dfrac{1}{2\pi}\displaystyle\int_{-\infty}^{\infty}\alpha^2|\alpha|h_0(\alpha)e^{i\alpha x}d\alpha \\
+\sigma_\infty\dfrac{\nu(1+\nu)}{E}h_{0xx}(x)
\end{array}\right] \\
-\left(h_{0x}\right)^2\dfrac{(1-\nu^2)}{E}\sigma^\infty+Q\varepsilon_{xx}{}^{(2)}+2h_{0x}(x)\dfrac{(1+\nu)}{E}\sigma_\infty h_{0x}(x)+\left(h_{0x}\right)^2\dfrac{-\nu(1+\nu)}{E}\sigma^\infty
\end{array}\right).
\end{aligned}
\tag{133}
$$

Similar to the sinusoidal rough surface, our homogenization scheme requires calculation of the total energy under the action of the applied stress σ^{∞}. In order to find the effective surface stress and effective surface elastic constant we make the ensemble average of total energy of the half space with rough surface equal to energy of a half space with flat surface and effective surface constants.

$$\left\langle E^{act}\left(\sigma^{\infty}\right)\right\rangle = E^{eff}\left(\sigma^{\infty}\right). \tag{134}$$

Then the effective surface stress and the effective surface elastic constant would be extracted from

$$\left(\tau^{0}\right)^{eff} = \left(\frac{E}{1-\nu^{2}}\right)\frac{\partial\left\langle E^{act}\right\rangle\left(\sigma^{\infty}\right)}{\partial\sigma^{\infty}}\Bigg|_{\sigma^{\infty}=0} \quad \text{and} \quad \left(k^{s}\right)^{eff} = \left(\frac{E}{1-\nu^{2}}\right)^{2}\frac{\partial^{2}\left\langle E^{act}\right\rangle\left(\sigma^{\infty}\right)}{\left(\partial\sigma^{\infty}\right)^{2}}\Bigg|_{\sigma^{\infty}=0}. \tag{135}$$

Using the total strain fields as $\varepsilon_{ij} = \left\langle \varepsilon_{ij}\right\rangle + Q\varepsilon_{ij}\ i, j = x, y$ and inserting into (13) we can find the ensemble average of the total energy,

$$\begin{aligned}\left\langle E^{act}\left(\sigma^{\infty}\right)\right\rangle &= \frac{1}{2}P\left[\int_{-\infty}^{h(x)}\left(\varepsilon^{(0)}+\delta\varepsilon^{(1)}+\delta^{2}\varepsilon^{(2)}\right).\mathbb{C}\left(\varepsilon^{(0)}+\delta\varepsilon^{(1)}+\delta^{2}\varepsilon^{(2)}\right)dy\right] \\ &\quad + \frac{1}{2}P\left[\left(\varepsilon_{ss}-\varepsilon_{ss}^{0}\right)\cdot\mathbb{C}_{s}\left(\varepsilon_{ss}-\varepsilon_{ss}^{0}\right)\right].\end{aligned} \tag{136}$$

For calculating $\left(\tau^{0}\right)^{eff}$ we need to consider the energy terms up to first order of σ^{∞} and we call it E'. For simplicity of presenting the proceeding calculation, we split E' into two parts,

$$E'_{bulk} = \left(E'_{bulk}\right)_{1} + \left(E'_{bulk}\right)_{2} \tag{137}$$

$$
\left(E'_{bulk}\right)_1 = \frac{1}{2}\delta P\int_{-\infty}^{h(x)}\left(\begin{array}{l} 2\left\{\frac{1}{2\pi}\int_{-\infty}^{\infty}\left[\tau^o (i\alpha)^2 h_0(\alpha)\left(1+|\alpha| y\right)\right]e^{i\alpha x+|\alpha|y}d\alpha\right\}\times\frac{(1-\nu^2)}{E}\sigma^{\infty}+ \\ +2\left\{\frac{1}{2\pi}\int_{-\infty}^{\infty}\left[\tau^o (i\alpha)^2 h_0(\alpha)\left(1-|\alpha| y\right)\right]e^{i\alpha x+|\alpha|y}d\alpha\right\}\times\frac{-\nu(1+\nu)}{E}\sigma^{\infty} \end{array}\right)dy +
$$

$$
\frac{\delta^2}{2}\int_{-\infty}^{h(x)}P\left(\begin{array}{l}
\frac{(1-\nu^2)}{E}\left(\frac{1}{2\pi}\right)^2\int_{-\infty}^{\infty}\sigma_{\infty}(i\beta)h_0(\beta)\left(-2\frac{|\beta|}{i\beta}+i\beta y\right)e^{i\beta x+|\beta|y}d\beta\times\int_{-\infty}^{\infty}\tau^o(i\alpha)^2h_0(\alpha)\left(1+|\alpha|y\right)e^{i\alpha x+|\alpha|y}d\alpha+ \\
-\frac{\nu(1+\nu)}{E}\left(\frac{1}{2\pi}\right)^2\int_{-\infty}^{\infty}\sigma_{\infty}(i\beta)h_0(\beta)\left(-2\frac{|\beta|}{i\beta}+i\beta y\right)e^{i\beta x+|\beta|y}d\beta\times\int_{-\infty}^{\infty}\tau^o(i\alpha)^2h_0(\alpha)\left(1-|\alpha|y\right)e^{i\alpha x+|\alpha|y}d\alpha \\
+\frac{(1-\nu^2)}{E}\left(\frac{1}{2\pi}\right)^2\frac{(1-\nu^2)}{E}k^s\int_{-\infty}^{\infty}\sigma_{\infty}(i\beta)^2h_0(\beta)\left(1+|\beta|y\right)e^{i\beta x+|\beta|y}d\beta\times\int_{-\infty}^{\infty}\tau^o(i\alpha)^2h_0(\alpha)\left(1+|\alpha|y\right)e^{i\alpha x+|\alpha|y}d\alpha+ \\
-\frac{\nu(1+\nu)}{E}\left(\frac{1}{2\pi}\right)^2\frac{(1-\nu^2)}{E}k^s\int_{-\infty}^{\infty}\sigma_{\infty}(i\beta)^2h_0(\beta)\left(1+|\beta|y\right)e^{i\beta x+|\beta|y}d\beta\times\int_{-\infty}^{\infty}\tau^o(i\alpha)^2h_0(\alpha)\left(1-|\alpha|y\right)e^{i\alpha x+|\alpha|y}d\alpha \\
+\left(\frac{1}{2\pi}\right)^2\frac{(1-\nu^2)}{E}\int_{-\infty}^{\infty}\left[\tau^o(i\alpha)^2h_0(\alpha)\left(1+|\alpha|y\right)\right]e^{i\alpha x+|\alpha|y}d\alpha\times\int_{-\infty}^{\infty}\sigma_{\infty}(i\beta)h_0(\beta)\left(-2\frac{|\beta|}{i\beta}+i\beta y\right)e^{i\beta x+|\beta|y}d\beta+ \\
+\left(\frac{1}{2\pi}\right)^2\frac{(1-\nu^2)}{E}\int_{-\infty}^{\infty}\left[\tau^o(i\alpha)^2h_0(\alpha)\left(1+|\alpha|y\right)\right]e^{i\alpha x+|\alpha|y}d\alpha\times\frac{(1-\nu^2)}{E}k^s\int_{-\infty}^{\infty}\sigma_{\infty}(i\beta)^2h_0(\beta)\left(1+|\beta|y\right)e^{i\beta x+|\beta|y}d\beta \\
+2\left(\frac{1}{2\pi}\right)^2\frac{-\nu(1+\nu)}{E}\int_{-\infty}^{\infty}\left[\tau^o(i\alpha)^2h_0(\alpha)\left(1+|\alpha|y\right)\right]e^{i\alpha x+|\alpha|y}d\alpha\times\int_{-\infty}^{\infty}-\sigma_{\infty}(i\beta)^2h_0(\beta)ye^{i\beta x+|\beta|y}d\beta+ \\
2\left(\frac{1}{2\pi}\right)^2\frac{-\nu(1+\nu)}{E}\int_{-\infty}^{\infty}\left[\tau^o(i\alpha)^2h_0(\alpha)\left(1+|\alpha|y\right)\right]e^{i\alpha x+|\alpha|y}d\alpha\times\frac{(1-\nu^2)}{E}k^s\int_{-\infty}^{\infty}\sigma_{\infty}(i\beta)^2h_0(\beta)\left(1-|\beta|y\right)e^{i\beta x+|\beta|y}d\beta \\
+\left(\frac{1}{2\pi}\right)^2\frac{(1-\nu^2)}{E}\int_{-\infty}^{\infty}\left[\tau^o(i\alpha)^2h_0(\alpha)\left(1-|\alpha|y\right)\right]e^{i\alpha x+|\alpha|y}d\alpha\times\int_{-\infty}^{\infty}-\sigma_{\infty}(i\beta)^2h_0(\beta)ye^{i\beta x+|\beta|y}d\beta+ \\
\left(\frac{1}{2\pi}\right)^2\frac{(1-\nu^2)}{E}\int_{-\infty}^{\infty}\left[\tau^o(i\alpha)^2h_0(\alpha)\left(1-|\alpha|y\right)\right]e^{i\alpha x+|\alpha|y}d\alpha\times\frac{(1-\nu^2)}{E}k^s\int_{-\infty}^{\infty}\sigma_{\infty}(i\beta)^2h_0(\beta)\left(1-|\beta|y\right)e^{i\beta x+|\beta|y}d\beta \\
\left(\frac{1}{2\pi}\right)^2\frac{-\nu(1+\nu)}{E}\int_{-\infty}^{\infty}\left[\tau^o(i\alpha)^2h_0(\alpha)\left(1-|\alpha|y\right)\right]e^{i\alpha x+|\alpha|y}d\alpha\times\int_{-\infty}^{\infty}\sigma_{\infty}(i\beta)h_0(\beta)\left(-2\frac{|\beta|}{i\beta}+i\beta y\right)e^{i\beta x+|\beta|y}d\beta+ \\
\left(\frac{1}{2\pi}\right)^2\frac{-\nu(1+\nu)}{E}\int_{-\infty}^{\infty}\left[\tau^o(i\alpha)^2h_0(\alpha)\left(1-|\alpha|y\right)\right]e^{i\alpha x+|\alpha|y}d\alpha\times\frac{(1-\nu^2)}{E}k^s\int_{-\infty}^{\infty}\sigma_{\infty}(i\beta)^2h_0(\beta)\left(1+|\beta|y\right)e^{i\beta x+|\beta|y}d\beta \\
+\left(\frac{1}{2\pi}\right)^2\frac{(1-\nu^2)}{E}\int_{-\infty}^{\infty}\left[\tau^o(i\alpha)^2h_0(\alpha)\left(1-|\alpha|y\right)\right]e^{i\alpha x+|\alpha|y}d\alpha\times\int_{-\infty}^{\infty}-\sigma_{\infty}(i\beta)^2h_0(\beta)ye^{i\beta x+|\beta|y}d\beta+ \\
\left(\frac{1}{2\pi}\right)^2\frac{(1-\nu^2)}{E}\int_{-\infty}^{\infty}\left[\tau^o(i\alpha)^2h_0(\alpha)\left(1-|\alpha|y\right)\right]e^{i\alpha x+|\alpha|y}d\alpha\times\frac{(1-\nu^2)}{E}k^s\int_{-\infty}^{\infty}\sigma_{\infty}(i\beta)^2h_0(\beta)\left(1-|\beta|y\right)e^{i\beta x+|\beta|y}d\beta \\
+\frac{(1+\nu)}{E}\left(\frac{1}{2\pi}\right)^2\left(2\tau^o\frac{(1-\nu^2)}{E}k^s\sigma^{\infty}\right)\int_{-\infty}^{\infty}(i\beta)^3h_0(\beta)ye^{i\beta x+|\beta|y}d\beta\times\int_{-\infty}^{\infty}(i\alpha)^3h_0(\alpha)ye^{i\alpha x+|\alpha|y}d\alpha+ \\
-2\frac{(1+\nu)}{E}\left(\frac{1}{2\pi}\right)^2\int_{-\infty}^{\infty}\sigma_{\infty}(i\beta)h_0(\beta)\left(1+|\beta|y\right)e^{i\beta x+|\beta|y}d\beta\times\int_{-\infty}^{\infty}\tau^o(i\alpha)^3h_0(\alpha)ye^{i\alpha x+|\alpha|y}d\alpha
\end{array}\right). \quad (138)
$$

More simplifying,

$$
\left(E'_{bulk}\right)_1 = \frac{1}{2}\delta\int_{-\infty}^{h(x)} P\begin{pmatrix} 2\left\{\frac{1}{2\pi}\int_{-\infty}^{\infty}\left[\tau^o(i\alpha)^2 h_0(\alpha)\left(1+|\alpha|y\right)\right]e^{i\alpha x+|\alpha|y}d\alpha\right\}\times\frac{(1-\nu^2)}{E}\sigma^{\infty} + \\ +2\left\{\frac{1}{2\pi}\int_{-\infty}^{\infty}\left[\tau^o(i\alpha)^2 h_0(\alpha)\left(1-|\alpha|y\right)\right]e^{i\alpha x+|\alpha|y}d\alpha\right\}\times\frac{-\nu(1+\nu)}{E}\sigma^{\infty} \end{pmatrix}dy +
$$

$$
\delta^2\int_{-\infty}^{h(x)} P\left(\begin{array}{l}
\frac{(1-\nu^2)}{E}\left(\frac{1}{2\pi}\right)^2\int_{-\infty}^{\infty}\sigma_{\infty}(i\beta)h_0(\beta)\left(-2\frac{|\beta|}{i\beta}+i\beta y\right)e^{i\beta x+|\beta|y}d\beta\int_{-\infty}^{\infty}\tau^o(i\alpha)^2 h_0(\alpha)\left(1+|\alpha|y\right)e^{i\alpha x+|\alpha|y}d\alpha + \\
+\frac{-\nu(1+\nu)}{E}\left(\frac{1}{2\pi}\right)^2\int_{-\infty}^{\infty}\sigma_{\infty}(i\beta)h_0(\beta)\left(-2\frac{|\beta|}{i\beta}+i\beta y\right)e^{i\beta x+|\beta|y}d\beta\int_{-\infty}^{\infty}\tau^o(i\alpha)^2 h_0(\alpha)\left(1-|\alpha|y\right)e^{i\alpha x+|\alpha|y}d\alpha \\
+\frac{(1-\nu^2)}{E}\left(\frac{1}{2\pi}\right)^2\frac{(1-\nu^2)}{E}k^s\int_{-\infty}^{\infty}\sigma_{\infty}(i\beta)^2 h_0(\beta)\left(1+|\beta|y\right)e^{i\beta x+|\beta|y}d\beta\int_{-\infty}^{\infty}\tau^o(i\alpha)^2 h_0(\alpha)\left(1+|\alpha|y\right)e^{i\alpha x+|\alpha|y}d\alpha + \\
+2\frac{-\nu(1+\nu)}{E}\left(\frac{1}{2\pi}\right)^2\frac{(1-\nu^2)}{E}k^s\int_{-\infty}^{\infty}\sigma_{\infty}(i\beta)^2 h_0(\beta)\left(1+|\beta|y\right)e^{i\beta x+|\beta|y}d\beta\int_{-\infty}^{\infty}\tau^o(i\alpha)^2 h_0(\alpha)\left(1-|\alpha|y\right)e^{i\alpha x+|\alpha|y}d\alpha \\
+\left(\frac{1}{2\pi}\right)^2\frac{-\nu(1+\nu)}{E}\int_{-\infty}^{\infty}\left[\tau^o(i\alpha)^2 h_0(\alpha)\left(1+|\alpha|y\right)\right]e^{i\alpha x+|\alpha|y}d\alpha\int_{-\infty}^{\infty}-\sigma_{\infty}(i\beta)^2 h_0(\beta)ye^{i\beta x+|\beta|y}d\beta + \\
+\left(\frac{1}{2\pi}\right)^2\frac{(1-\nu^2)}{E}\int_{-\infty}^{\infty}\left[\tau^o(i\alpha)^2 h_0(\alpha)\left(1-|\alpha|y\right)\right]e^{i\alpha x+|\alpha|y}d\alpha\int_{-\infty}^{\infty}-\sigma_{\infty}(i\beta)^2 h_0(\beta)ye^{i\beta x+|\beta|y}d\beta + \\
\left(\frac{1}{2\pi}\right)^2\frac{(1-\nu^2)}{E}\frac{(1-\nu^2)}{E}k^s\int_{-\infty}^{\infty}\left[\tau^o(i\alpha)^2 h_0(\alpha)\left(1-|\alpha|y\right)\right]e^{i\alpha x+|\alpha|y}d\alpha\int_{-\infty}^{\infty}\sigma_{\infty}(i\beta)^2 h_0(\beta)\left(1-|\beta|y\right)e^{i\beta x+|\beta|y}d\beta \\
+\frac{(1+\nu)}{E}\left(\frac{1}{2\pi}\right)^2\left(\tau^o\frac{(1-\nu^2)}{E}k^s\sigma^{\infty}\right)\int_{-\infty}^{\infty}(i\beta)^3 h_0(\beta)ye^{i\beta x+|\beta|y}d\beta\int_{-\infty}^{\infty}(i\alpha)^3 h_0(\alpha)ye^{i\alpha x+|\alpha|y}d\alpha + \\
-\frac{(1+\nu)}{E}\left(\frac{1}{2\pi}\right)^2\int_{-\infty}^{\infty}\sigma_{\infty}(i\beta)h_0(\beta)\left(1+|\beta|y\right)e^{i\beta x+|\beta|y}d\beta\int_{-\infty}^{\infty}\tau^o(i\alpha)^3 h_0(\alpha)ye^{i\alpha x+|\alpha|y}d\alpha
\end{array}\right)dy. \tag{139}
$$

Calculating the integration in y direction and doing the ensemble average in x direction would yield

$$
\begin{aligned}
\left\langle E'_{bulk}\right\rangle_1 = \delta P & \left(\begin{array}{l} \frac{1}{2\pi}\delta h_0(x)\int_{-\infty}^{\infty}\left[\tau^o(i\alpha)^2 h_0(\alpha)\right]e^{i\alpha x}d\alpha\frac{(1-\nu^2)}{E}\sigma^{\infty} + \\ +\left\{\frac{1}{2\pi}\int_{-\infty}^{\infty}\left[\tau^o(i\alpha)^2 h_0(\alpha)\left(\frac{2}{|\alpha|}+\delta h_0(x)\right)\right]e^{i\alpha x}d\alpha\right\}\frac{-\nu(1+\nu)}{E}\sigma^{\infty} \end{array} \right) + \\
\delta^2\int_{-\infty}^{h(x)} P & \left(\begin{array}{l}
+\frac{(1-\nu^2)}{E}\sigma_{\infty}\tau^o\left(\frac{1}{2\pi}\right)^2\int_{-\infty}^{\infty}\int_{-\infty}^{\infty} i\beta\left(-2\frac{|\beta|}{i\beta}+i\beta y\right)(i\alpha)^2\left(1+|\alpha|y\right)g(\alpha)\delta(\alpha+\beta)e^{i(\alpha+\beta)x+(|\alpha|+|\beta|)y}d\alpha d\beta + \\
+\frac{-\nu(1+\nu)}{E}\sigma_{\infty}\tau^o\left(\frac{1}{2\pi}\right)^2\int_{-\infty}^{\infty}\int_{-\infty}^{\infty} i\beta\left(-2\frac{|\beta|}{i\beta}+i\beta y\right)(i\alpha)^2\left(1-|\alpha|y\right)g(\alpha)\delta(\alpha+\beta)e^{i(\alpha+\beta)x+(|\alpha|+|\beta|)y}d\alpha d\beta \\
+\frac{(1-\nu^2)}{E}\frac{(1-\nu^2)}{E}k^s\sigma_{\infty}\tau^o\left(\frac{1}{2\pi}\right)^2\int_{-\infty}^{\infty}\int_{-\infty}^{\infty}(i\beta)^2\left(1+|\beta|y\right)(i\alpha)^2\left(1+|\alpha|y\right)g(\alpha)\delta(\alpha+\beta)e^{i(\alpha+\beta)x+(|\alpha|+|\beta|)y}d\alpha d\beta + \\
\frac{-2\nu(1+\nu)}{E}\frac{(1-\nu^2)}{E}k^s\sigma_{\infty}\tau^o\left(\frac{1}{2\pi}\right)^2\int_{-\infty}^{\infty}\int_{-\infty}^{\infty}(i\beta)^2\left(1+|\beta|y\right)(i\alpha)^2\left(1-|\alpha|y\right)g(\alpha)\delta(\alpha+\beta)e^{i(\alpha+\beta)x+(|\alpha|+|\beta|)y}d\alpha d\beta \\
+\frac{\nu(1+\nu)}{E}\sigma_{\infty}\tau^o\left(\frac{1}{2\pi}\right)^2\int_{-\infty}^{\infty}\int_{-\infty}^{\infty}(i\beta)^2 y(i\alpha)^2\left(1+|\alpha|y\right)g(\alpha)\delta(\alpha+\beta)e^{i(\alpha+\beta)x+(|\alpha|+|\beta|)y}d\alpha d\beta \\
-\frac{(1-\nu^2)}{E}\sigma_{\infty}\tau^o\left(\frac{1}{2\pi}\right)^2\int_{-\infty}^{\infty}\int_{-\infty}^{\infty}(i\beta)^2 y(i\alpha)^2\left(1-|\alpha|y\right)g(\alpha)\delta(\alpha+\beta)e^{i(\alpha+\beta)x+(|\alpha|+|\beta|)y}d\alpha d\beta \\
+\frac{(1-\nu^2)}{E}\frac{(1-\nu^2)}{E}k^s\sigma_{\infty}\tau^o\left(\frac{1}{2\pi}\right)^2\int_{-\infty}^{\infty}\int_{-\infty}^{\infty}(i\beta)^2\left(1-|\beta|y\right)(i\alpha)^2\left(1-|\alpha|y\right)g(\alpha)\delta(\alpha+\beta)e^{i(\alpha+\beta)x+(|\alpha|+|\beta|)y}d\alpha d\beta \\
+\frac{(1+\nu)^2}{E^2}\left(\tau^o\frac{(1-\nu^2)}{E}k^s\sigma^{\infty}\right)\left(\frac{1}{2\pi}\right)^2\int_{-\infty}^{\infty}\int_{-\infty}^{\infty}(i\beta)^3(i\alpha)^3 y^2 g(\alpha)\delta(\alpha+\beta)e^{i(\alpha+\beta)x+(|\alpha|+|\beta|)y}d\alpha d\beta \\
-\frac{(1+\nu)^2}{E^2}\left(\frac{1}{2\pi}\right)^2\sigma_{\infty}\tau^o\int_{-\infty}^{\infty}\int_{-\infty}^{\infty}(i\beta)\left(1+|\beta|y\right)(i\alpha)^3 y g(\alpha)\delta(\alpha+\beta)e^{i(\alpha+\beta)x+(|\alpha|+|\beta|)y}d\alpha d\beta
\end{array} \right) dy.
\end{aligned}
\tag{140}
$$

After doing some algebra we get to

$$
\begin{aligned}
\left\langle E'_{bulk}\right\rangle_1 = {} & \delta^2\tau^o\sigma^{\infty}\left(\frac{-2(1+\nu)(1-2\nu)-2\nu\left(1+\nu\right)+2(1-\nu^2)}{E}\right)\left(\frac{\eta^2}{a^2}\right)+ \\
& +\delta^2\left(3\frac{(1-\nu^2)}{E}\frac{(1-\nu^2)}{E}-\frac{\nu\left(1+\nu\right)}{E}\frac{(1-\nu^2)}{E}\right)k^s\sigma_{\infty}\tau^o\left(\frac{1}{\sqrt{\pi}}\right)\left(\frac{4\eta^2}{a^3}\right) \\
& +\delta^2\frac{(1+\nu)}{E}\left(\tau^o\frac{(1-\nu^2)}{E}k^s\sigma^{\infty}\right)\left(\frac{1}{\sqrt{\pi}}\right)\left(\frac{2\eta^2}{a^3}\right).
\end{aligned}
\tag{141}
$$

Similarly,

$$
\left\langle E'_{bulk}\right\rangle_2 = \frac{1}{2}\int_{-\infty}^{h(x)}\left\langle Q\sigma_{xx}{}^{(2)}.\left\langle\varepsilon_{xx}{}^{(0)}\right\rangle\right\rangle+\left\langle Q\sigma_{yy}{}^{(2)}.\left\langle\varepsilon_{yy}{}^{(0)}\right\rangle\right\rangle+\left\langle Q\varepsilon_{xx}{}^{(2)}.\left\langle\sigma_{xx}{}^{(0)}\right\rangle\right\rangle dy, \tag{142}
$$

where

$$Q\sigma_{xx}{}^{(2)}(\alpha,y)=\left[f(\alpha)\left(-2\frac{|\alpha|}{i\alpha}+i\alpha y\right)+p(\alpha)\left(1+|\alpha|y\right)\right]e^{|\alpha|y}=$$

$$\left(\frac{1}{2\pi}\right)\left\{\begin{array}{l}-2\sigma_\infty\int_{-\infty}^{\infty}i(\alpha-\beta)h_0(\alpha-\beta)|\beta|h_0(\beta)d\beta\\ -2\sigma_\infty\int_{-\infty}^{\infty}h_0(\alpha-\beta)(i\beta)|\beta|h_0(\beta)d\beta+\tau^o\int_{-\infty}^{\infty}h_0(\alpha-\beta)(i\beta)^3h_0(\beta)d\beta\\ +\left(\frac{(4-\nu)(1+\nu)}{E}+\frac{(1-\nu^2)}{E}\right)k^s\sigma^\infty\int_{-\infty}^{\infty}i(\alpha-\beta)h_0(\alpha-\beta)(i\beta)^2h_0(\beta)d\beta\\ +\left(4\frac{1-\nu^2}{E}+\frac{\nu(1+\nu)}{E}\right)k^s\sigma_\infty\int_{-\infty}^{\infty}h_0(\alpha-\beta)(i\beta)^3h_0(\beta)d\beta-\\ -2\frac{1-\nu^2}{E}k^s\left(\tau^o+\frac{(1-\nu^2)}{E}k^s\sigma^\infty\right)\int_{-\infty}^{\infty}h_0(\alpha-\beta)(i\beta^3)|\beta|h_0(\beta)d\beta\\ -2\frac{1-\nu^2}{E}\left(\tau^o+\frac{(1-\nu^2)}{E}k^s\sigma^\infty\right)k^s\int_{-\infty}^{\infty}i(\alpha-\beta)h_0(\alpha-\beta)(\beta^2)|\beta|h_0(\beta)d\beta\end{array}\right\}\left(-2\frac{|\alpha|}{i\alpha}+i\alpha y\right)e^{|\alpha|y}$$

$$+\left(\frac{1}{2\pi}\right)\left\{\begin{array}{l}\sigma_\infty\int_{-\infty}^{\infty}i(\alpha-\beta)h_0(\alpha-\beta)(i\beta)h_0(\beta)d\beta+\sigma_\infty\int_{-\infty}^{\infty}h_0(\alpha-\beta)(i\beta)^2h_0(\beta)d\beta-\\ -2\sigma_\infty\frac{1-\nu^2}{E}k^s\int_{-\infty}^{\infty}i^2(\alpha-\beta)^2h_0(\alpha-\beta)|\beta|h_0(\beta)d\beta+\\ \frac{(1+\nu)(1-2\nu)}{E}k^s\left(\tau^o+\frac{(1-\nu^2)}{E}k^s\sigma^\infty\right)\int_{-\infty}^{\infty}i^2(\alpha-\beta)^2h_0(\alpha-\beta)(i\beta)^2h_0(\beta)d\beta\\ -2\frac{1-\nu^2}{E}k^s\sigma_\infty\int_{-\infty}^{\infty}i(\alpha-\beta)h_0(\alpha-\beta)(i\beta)|\beta|h_0(\beta)d\beta\\ +\frac{(1+\nu)(1-2\nu)}{E}k^s\left(\tau^o+\frac{(1-\nu^2)}{E}k^s\sigma^\infty\right)\int_{-\infty}^{\infty}i(\alpha-\beta)h_0(\alpha-\beta)(i\beta)^3h_0(\beta)d\beta\end{array}\right\}\left(1+|\alpha|y\right)e^{|\alpha|y},\tag{143}$$

$$Q\sigma_{yy}{}^{(2)}(\alpha,y)=\left[-i\alpha f(\alpha)y+p(\alpha)\left(1-\left|\alpha\right|y\right)\right]e^{|\alpha|y}=$$

$$\left(\frac{1}{2\pi}\right)\left\{\begin{array}{l}
-2\sigma_{\infty}\int_{-\infty}^{\infty}i(\alpha-\beta)h_0(\alpha-\beta)\left|\beta\right|h_0(\beta)d\beta-2\sigma_{\infty}\int_{-\infty}^{\infty}h_0(\alpha-\beta)\left(i\beta\right)\left|\beta\right|h_0(\beta)d\beta+\\
+\tau^{o}\int_{-\infty}^{\infty}h_0(\alpha-\beta)\left(i\beta\right)^3h_0(\beta)d\beta+\\
+\left(\frac{(4-\nu)(1+\nu)}{E}+\frac{(1-\nu^2)}{E}\right)k^s\sigma^{\infty}\int_{-\infty}^{\infty}i\left(\alpha-\beta\right)h_0(\alpha-\beta)\left(i\beta\right)^2h_0(\beta)d\beta\\
+\left(4\frac{1-\nu^2}{E}+\frac{\nu(1+\nu)}{E}\right)k^s\sigma_{\infty}\int_{-\infty}^{\infty}h_0(\alpha-\beta)\left(i\beta\right)^3h_0(\beta)d\beta-\\
-2\frac{1-\nu^2}{E}k^s\left(\tau^{o}+\frac{(1-\nu^2)}{E}k^s\sigma^{\infty}\right)\int_{-\infty}^{\infty}h_0(\alpha-\beta)\left(i\beta^3\right)\left|\beta\right|h_0(\beta)d\beta\\
-2\frac{1-\nu^2}{E}\left(\tau^{o}+\frac{(1-\nu^2)}{E}k^s\sigma^{\infty}\right)k^s\int_{-\infty}^{\infty}i(\alpha-\beta)h_0(\alpha-\beta)\left(\beta^2\right)\left|\beta\right|h_0(\beta)d\beta
\end{array}\right\}\left(-i\alpha y\right)e^{|\alpha|y}+$$

$$\left(\frac{1}{2\pi}\right)\left\{\begin{array}{l}
\sigma_{\infty}\int_{-\infty}^{\infty}i(\alpha-\beta)h_0(\alpha-\beta)\left(i\beta\right)h_0(\beta)d\beta+\sigma_{\infty}\int_{-\infty}^{\infty}h_0(\alpha-\beta)\left(i\beta\right)^2h_0(\beta)d\beta-\\
-2\sigma_{\infty}\frac{1-\nu^2}{E}k^s\frac{1}{2\pi}\int_{-\infty}^{\infty}i^2(\alpha-\beta)^2h_0(\alpha-\beta)\left|\beta\right|h_0(\beta)d\beta\\
+\frac{(1+\nu)(1-2\nu)}{E}k^s\left[\tau^{o}+\frac{(1-\nu^2)}{E}k^s\sigma^{\infty}\right]\int_{-\infty}^{\infty}i^2(\alpha-\beta)^2h_0(\alpha-\beta)\left(i\beta\right)^2h_0(\beta)d\beta\\
-2\frac{1-\nu^2}{E}k^s\sigma_{\infty}\frac{1}{2\pi}\int_{-\infty}^{\infty}i(\alpha-\beta)h_0(\alpha-\beta)\left(i\beta\right)\left|\beta\right|h_0(\beta)d\beta\\
+\frac{(1+\nu)(1-2\nu)}{E}k^s\left[\tau^{o}+\frac{(1-\nu^2)}{E}k^s\sigma^{\infty}\right]\int_{-\infty}^{\infty}i(\alpha-\beta)h_0(\alpha-\beta)\left(i\beta\right)^3h_0(\beta)d\beta
\end{array}\right\}\left(1-\left|\alpha\right|y\right)e^{|\alpha|y}. \tag{144}$$

More simplifying we would have

$$
\begin{aligned}
&\left\langle E'_{bulk}\right\rangle_2=\frac{(1-\nu^2)}{E}\sigma_\infty\left(\frac{1}{2\pi}\right)^2\times\\
&\times\int_{-\infty}^{h(x)}\int_{-\infty}^{\infty}\left\{\begin{array}{l}
\left\{\begin{array}{l}
\tau^o(2\pi)\eta^2\delta(\alpha)\sqrt{\pi}a\int_{-\infty}^{\infty}(i\beta)^3e^{(-a^2\beta^2/4)}d\beta+\\
-2\dfrac{1-\nu^2}{E}k^s\tau^o(2\pi)\eta^2\delta(\alpha)\sqrt{\pi}a\int_{-\infty}^{\infty}(i\beta^3)|\beta|e^{(-a^2\beta^2/4)}d\beta\\
-2\dfrac{1-\nu^2}{E}\tau^ok^s(2\pi)\eta^2\delta(\alpha)\sqrt{\pi}a\int_{-\infty}^{\infty}i(\alpha-\beta)(\beta^2)|\beta|e^{(-a^2\beta^2/4)}d\beta
\end{array}\right\}\delta(\alpha)\left(-2\dfrac{|\alpha|}{i\alpha}+i\alpha y\right)\\
\left\{\begin{array}{l}
+\dfrac{(1+\nu)(1-2\nu)}{E}k^s\tau^o(2\pi)\eta^2\delta(\alpha)\sqrt{\pi}a\int_{-\infty}^{\infty}i^2(\alpha-\beta)^2(i\beta)^2e^{(-a^2\beta^2/4)}d\beta\\
+\dfrac{(1+\nu)(1-2\nu)}{E}k^s\tau^o(2\pi)\eta^2\delta(\alpha)\sqrt{\pi}a\int_{-\infty}^{\infty}i(\alpha-\beta)(i\beta)^3e^{(-a^2\beta^2/4)}d\beta
\end{array}\right\}\delta(\alpha)(1+|\alpha|y)e^{|\alpha|y}
\end{array}\right\}e^{i\alpha x+|\alpha|y}d\alpha\\
&-\frac{\nu(1+\nu)}{E}\sigma_\infty\left(\frac{1}{2\pi}\right)^2\times\\
&\times\int_{-\infty}^{\infty}\left\{\begin{array}{l}
\left\{\begin{array}{l}
\tau^o(2\pi)\eta^2\delta(\alpha)\sqrt{\pi}a\int_{-\infty}^{\infty}h_0(\alpha-\beta)(i\beta)^3h_0(\beta)d\beta+\\
-2\dfrac{1-\nu^2}{E}k^s\tau^o(2\pi)\eta^2\delta(\alpha)\sqrt{\pi}a\int_{-\infty}^{\infty}(i\beta^3)|\beta|e^{(-a^2\beta^2/4)}d\beta\\
-2\dfrac{1-\nu^2}{E}\tau^ok^s(2\pi)\eta^2\delta(\alpha)\sqrt{\pi}a\int_{-\infty}^{\infty}i(\alpha-\beta)(\beta^2)|\beta|e^{(-a^2\beta^2/4)}d\beta
\end{array}\right\}\delta(\alpha)(-i\alpha y)+\\
\left\{\begin{array}{l}
+\dfrac{(1+\nu)(1-2\nu)}{E}k^s\tau^o(2\pi)\eta^2\delta(\alpha)\sqrt{\pi}a\int_{-\infty}^{\infty}i^2(\alpha-\beta)^2(i\beta)^2e^{(-a^2\beta^2/4)}d\beta\\
+\dfrac{(1+\nu)(1-2\nu)}{E}k^s\tau^o(2\pi)\eta^2\delta(\alpha)\sqrt{\pi}a\int_{-\infty}^{\infty}i(\alpha-\beta)(i\beta)^3e^{(-a^2\beta^2/4)}d\beta
\end{array}\right\}\delta(\alpha)(1-|\alpha|y)
\end{array}\right\}e^{i\alpha x+|\alpha|y}d\alpha,
\end{aligned}
\tag{145}
$$

and finally we get

$$
\begin{aligned}
&\left\langle E'_{bulk}\right\rangle_2=\frac{(1-\nu^2)}{E}\sigma_\infty\left(\frac{1}{2\pi}\right)\int_{-\infty}^{h(x)}\int_{-\infty}^{\infty}\left\{\begin{array}{l}
\eta^2\left\{-2\dfrac{1-\nu^2}{E}\tau^ok^s\sqrt{\pi}a\left(\dfrac{16i\alpha}{a^4}\right)\right\}\delta(\alpha)\left(-2\dfrac{|\alpha|}{i\alpha}+i\alpha y\right)+\\
\left\{\begin{array}{l}
\dfrac{(1+\nu)(1-2\nu)}{E}k^s\tau^o\sqrt{\pi}a\left(\dfrac{8\sqrt{\pi}\left(3+\dfrac{a^2\alpha^2}{2}\right)}{a^5}\right)\\
+\dfrac{(1+\nu)(1-2\nu)}{E}k^s\tau^o\sqrt{\pi}a\left(\dfrac{-24\sqrt{\pi}}{a^5}\right)
\end{array}\right\}\delta(\alpha)(1+|\alpha|y)e^{|\alpha|y}
\end{array}\right\}e^{i\alpha x+|\alpha|y}d\alpha\\
&-\frac{\nu(1+\nu)}{E}\sigma_\infty\left(\frac{1}{2\pi}\right)\int_{-\infty}^{h(x)}\int_{-\infty}^{\infty}\eta^2\delta(\alpha)\left\{\begin{array}{l}
-2\dfrac{1-\nu^2}{E}\tau^ok^s\sqrt{\pi}a\left(\dfrac{16i\alpha}{a^4}\right)\delta(\alpha)(-i\alpha y)+\\
\left\{\begin{array}{l}
\dfrac{(1+\nu)(1-2\nu)}{E}k^s\tau^o\sqrt{\pi}a\left(\dfrac{8\sqrt{\pi}\left(3+\dfrac{a^2\alpha^2}{2}\right)}{a^5}\right)\\
+\dfrac{(1+\nu)(1-2\nu)}{E}k^s\tau^o\sqrt{\pi}a\left(\dfrac{-24\sqrt{\pi}}{a^5}\right)
\end{array}\right\}\delta(\alpha)(1-|\alpha|y)
\end{array}\right\}e^{i\alpha x+|\alpha|y}d\alpha=\\
&=0
\end{aligned}
\tag{146}
$$

Similarly we calculate energy contribution of surface stress and surface strain and show the result as

$$\begin{aligned}\left\langle E'(surface)\right\rangle = &\frac{1-\nu^2}{E}\tau^o\sigma^\infty + \delta^2\sigma_\infty\left[\frac{2(1-\nu^2)}{E}\right]\tau^o\left(-\frac{2\eta^2}{a^2}\right)+\\ &+\delta^2\tau^o\left[\left(\frac{1}{\sqrt{\pi}}\right)\sigma^\infty k^s\frac{(1-2\nu)(1+\nu)^2(1-\nu)-2(1-\nu^2)^2}{E^2}\left(\frac{16\eta^2}{a^3}\right)\right]\\ &+\delta^2\tau^o\left(k^s\right)^2\sigma^\infty\frac{(1-\nu^2)(1+\nu)^2\left((1-\nu)(1-3\nu)+\nu^2\right)}{E^3}\left(\frac{12\eta^2}{a^4}\right).\end{aligned} \tag{147}$$

At the end, the effective surface tension is obtained as

$$\begin{aligned}\left(\tau^0\right)^{eff} &= \left(\frac{E}{1-\nu^2}\right)\frac{\partial\left\langle E'\right\rangle\left(\sigma^\infty\right)}{\partial\sigma^\infty}\Bigg|_{\sigma^\infty=0} =\\ &= \tau^o-\delta^2\tau^o\left(\begin{array}{l}\dfrac{4\eta^2}{a^2}+\dfrac{1}{\sqrt{\pi}}\left(k^s\right)\dfrac{(1+8\nu)(1+\nu)}{E}\left(\dfrac{2\eta^2}{a^3}\right)-\\ \left(k^s\right)^2\sigma^\infty\dfrac{(1+\nu)^2(1-2\nu)^2}{E^2}\left(\dfrac{12\eta^2}{a^4}\right)\end{array}\right).\end{aligned} \tag{148}$$

In order to calculate the effective surface elasticity constant, we precede similarly as for finding effective surface stress except that this time we consider only the energy terms that are second order in σ^∞. The detail calculation is not shown here. The final result would be obtained as

$$\begin{aligned}\left(k^s\right)^{eff} &= \left(\frac{E}{1-\nu^2}\right)^2\frac{\partial^2\left\langle E''\right\rangle\left(\sigma^\infty\right)}{\left(\partial\sigma^\infty\right)^2}\Bigg|_{\sigma^\infty=0}\\ &\left(k^s\right)+\delta^2\left(\begin{array}{l}-\dfrac{(9-8\nu)E}{4(1-\nu)(1-\nu^2)}\left(\dfrac{1}{\sqrt{\pi}}\right)\left(\dfrac{\eta^2}{a}\right)+\left(k^s\right)\left(\dfrac{8\eta^2}{a^2}\right)\\ +\dfrac{(-57\nu+11)(1+\nu)}{4E}\left(k^s\right)^2\left(\dfrac{1}{\sqrt{\pi}}\right)\left(\dfrac{\eta^2}{a^3}\right)+\dfrac{(1-2\nu)^2(1+\nu)^2}{E}\left(k^s\right)^3\left(\dfrac{6\eta^2}{a^4}\right)\end{array}\right).\end{aligned} \tag{149}$$

If $\frac{k^s}{aE} \ll 1$, equations (148) and (149) can be further simplified as

$$\left(\tau^0\right)^{eff} = \tau^o\left(1-\delta^2\frac{4\eta^2}{a^2}\right), \tag{150}$$

$$\left(k^s\right)^{eff} = \left(k^s\right)-\delta^2\frac{(9-8\nu)E}{4(1-\nu)\left(1-\nu^2\right)}\left(\frac{1}{\sqrt{\pi}}\right)\left(\frac{\eta^2}{a}\right). \tag{151}$$

Chapter 4: Atomistic Calculations, Results and Discussion

4.1 Atomistic Calculation

Computational modeling of materials is an increasingly important branch in the field of material science and is emerging as a powerful complementary approach to theoretical and experimental methods. Atomistic simulation that explicitly consider every individual atom and molecule and the interaction between them, generate information at the microscopic level, including atomic positions and velocities. The interatomic interaction may be considered with various degrees of accuracy and this variability stems from the quantum mechanical motion and interaction of electrons. The most two common approaches in atomistic simulations are using empirical representations and ab initio (first principal calculation) quantum mechanical methods. The rigorous computational method by quantum calculation is based on solving Schrodinger's equation for atoms and molecules while accounting the electronic structure of each atom. This method is extremely expensive and can be used only for small number of atoms. In the latter simulation approach, the forces between atoms are derived from empirical inter-atomic potentials that are obtained from fitting material properties from experimental data or QM calculations. This simulation method is much less sophisticated and relatively inexpensive compared to first principal calculations. The analytical functional form for the interatomic potential energy of N atoms in general is postulated as

$$V\left(\{r_i\}\right) = V\left(r_1, r_2, r_3, \ldots, r_N\right) = \\ = \underbrace{\sum_{i<j} \phi\left(\left|r_i - r_j\right|\right)}_{two-body\text{ part}} + \underbrace{\sum_{i<j<k} V_3\left(r_i, r_j, r_k\right)}_{three-body\text{ part}} + \underbrace{\sum_{i<j<k<l} V_4\left(r_i, r_j, r_k, r_l\right)}_{four-body\text{ part}} + \ldots, \tag{152}$$

where r_i is the position vector of atom i, the two-body (pair-wise) potential ϕ describes dependence of the potential energy on the distances between pairs of atoms in the system and the many-body part provides dependence on the geometry of the atomic arrangement/bonding. Pair-wise potential function can only describe inter-atomic potential with reasonable accuracy for relatively few materials e.g. noble gases and ionic crystals, but for the materials in the solid state, it does not give the adequate description of all the properties. So the best choice of a potential for simulations of solid state materials is a many-body potential. The form of potential that is common for metals is based on the embedded atom method (EAM) model. The EAM interatomic potential has the mathematical form of

$$U = \sum_{i}^{N} \left\{ \frac{1}{2} \sum_{\substack{i,j \\ i \neq j}}^{N} \phi_{ij}(r_{ij}) + F_i\left(\bar{\rho}_i\right) \right\}, \\ \bar{\rho}_i = \sum_{i \neq j} \rho_j\left(r_{ij}\right). \tag{153}$$

The first term in this equation represents the usual pair wise interaction between atoms i and j separated by a distance $r_{ij} = \left|r_i - r_j\right|$ and accounting for the effect of core electrons. $\bar{\rho}_i$ is the local density of bonding electrons supplied by the atoms neighboring with atom i. Function $\rho\left(r\right)$ represents the contribution of an atom to the electron density field. Finally, $F_i\left(\bar{\rho}_i\right)$ is an embedding function defining the energy required to embed atom i into an environment with electron density $\bar{\rho}_i$.

The force on an atom is the negative derivative of the potential function with respect to its position, i.e.,

$$f_j = -\frac{\partial V\left(\{r_i\}\right)}{\partial r_j}. \tag{154}$$

The major approaches to update atomic positions based on the calculated inter-atomic forces can be classified into Molecular Statics (MS), Molecular Dynamics (MD) and Monte Carlo (MC) simulations. In the case of Molecular Statics (MS) which is used in this part of our work, the energy minimization and the relaxed configuration of atoms are found using gradient methods (e.g. Steepest Descent, Conjugate Gradient).

As discussed earlier, surface roughness will affect the surface stiffness of the material and analytical expressions for effective surface stress and effective surface elastic constant were presented earlier chapters for deterministic and random roughness profiles, respectively. As a complementary analysis to theoretical result, we carry out atomistic simulations of nano-cantilever beams of both flat and rough surfaces and assess the change in the surface stress and the surface elastic constant. Then, the simulation results are compared to the theoretical predictions and in the final sections, a discussion on the implication of this work is presented.

4.1.1 Atomistic Simulation of the nanowire

We have chosen silver (Ag) nanowires as our model system and the tension calculations were performed using the LAMMPS molecular dynamics software (Plimpton, 1995). We simulate the interatomic interaction using embedded atom method (EAM) potential and the Silver parameterization developed by Williams et al. (2006).

We consider two configurations. Both configurations are nanowires that are $\langle 100 \rangle$ axially oriented and have a square cross sectional area with side a and lateral nominal surfaces oriented in $[001]$ and $[010]$ directions. The first nanowire configuration is characterized by flat surfaces while both the top and bottom surfaces of the second nanowire configuration are corrugated (Figure 4-1). The surface roughness is created such that it has zero mean value with the latter coinciding with the flat surface of the first configuration. The surface roughness profile has amplitude of 0.215 nm and wave length of 1.636 nm and is kept the same while the thickness and width of the nanowires (a) is changed from 1.6 to 6 nm. Molecular static simulations are performed on the nanowire and effective Young's elastic moduli of the nanowires are computed under tensile loading.

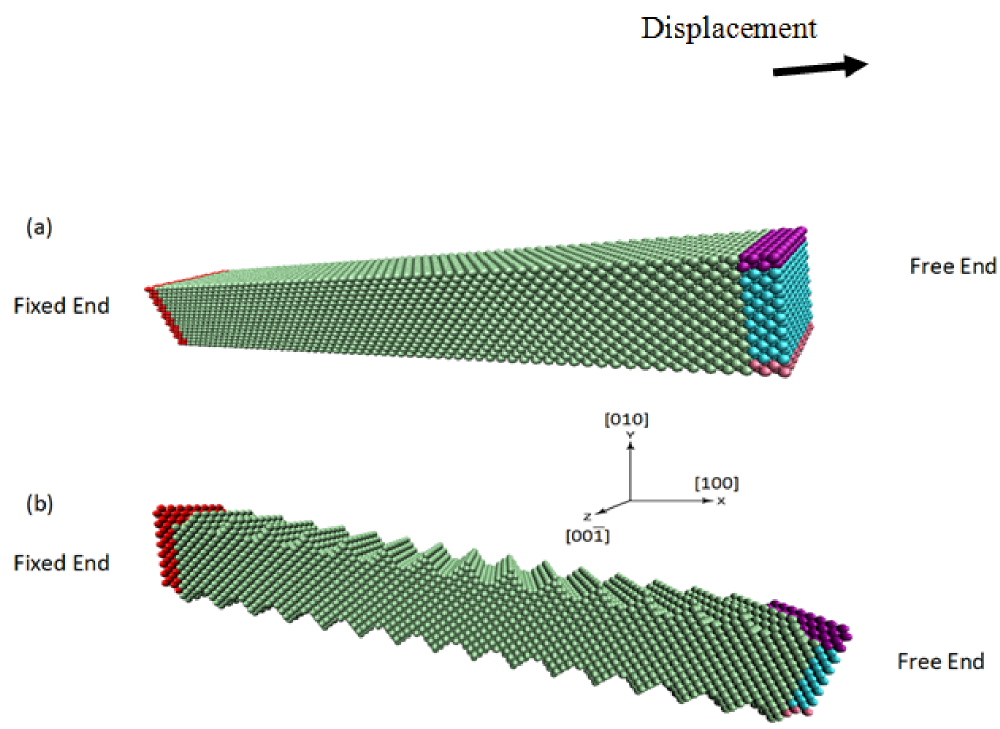

Figure 4-1: Schematic representation of the two nanowire configuration.

The nanowires are initially created based on the silver atom configuration corresponding to a perfect fcc bulk crystal. In order to consider the contribution of free surfaces, the boundary conditions in all directions are chosen to be non-periodic. The nanowire geometry is then relaxed to a local minimum energy state at zero K temperature using the conjugate gradient method. The atoms on or close to the surface change their equilibrium position during this process.

Atomistic simulation of the uniaxial tensile of nanowires have been studied by several researchers (Diao et al., 2004, Liang et al., 2005, McDowell et al., 2008, Chhapadia et al., 2011). In order to determine the effective Young's modulus of the wire under tension, we followed the energy method proposed by Diao et al. (2004). One end of the nanowire is kept fixed while the other end is strained axially up to 1.2%. The strain application is accomplished in six increments starting with zero and with an increment of 0.2%. Upon each incremental strain application, the free end is kept fixed and the nanowire is relaxed again. The change in the total potential energy of the system is equal to the work done due to the axial force which causes tensile strain,

$$\Delta \mathrm{U} = \int_0^{\Delta l} F\, d\left(\Delta l\right) = \int_0^{\varepsilon} S\, \sigma\, l\, d\varepsilon = \int_0^{\varepsilon} V\, \sigma\, d\varepsilon, \tag{155}$$

where $\Delta \mathrm{U}$ is the strain energy of the system, S is the cross section area of the wire after initial relaxation, F is the axial load applied which is balanced by the axial stress σ ($F = S\sigma$), $\varepsilon = dl / l$ is the axial strain, and l and V are the length and volume of the nanowire, respectively. If σ and V be expanded in terms of strain ε, the change of total potential energy of the nanowire can be written in terms of elastic Young's modulus and strain (Diao et al., 2004) as follows:

$$\frac{\Delta \mathrm{U}}{\mathrm{V}_0} = E\left[\frac{1}{2}\varepsilon^2 + \frac{1}{3}\xi\varepsilon^3\right], \tag{156}$$

where V_0 is the initial volume of the nanowire, E is the Young's modulus before applying strain ($\varepsilon = 0$) and ξ is a constant. From the atomistic simulations we calculate the quantity $\frac{\Delta \mathrm{U}}{\mathrm{V}_0}$ at each loading step, which is then fitted as a cubic polynomial function of strain. Then the effective elastic modulus of the beam E_{eff} that includes the free surface effects is determined from the quadratic term coefficient.

Figures 4-2 present our results. We observe that the wire with rough surface has a lower Young's modulus compared to the wire with flat surface. Therefore our simulation results prove that surface corrugation causes softening in the wire.

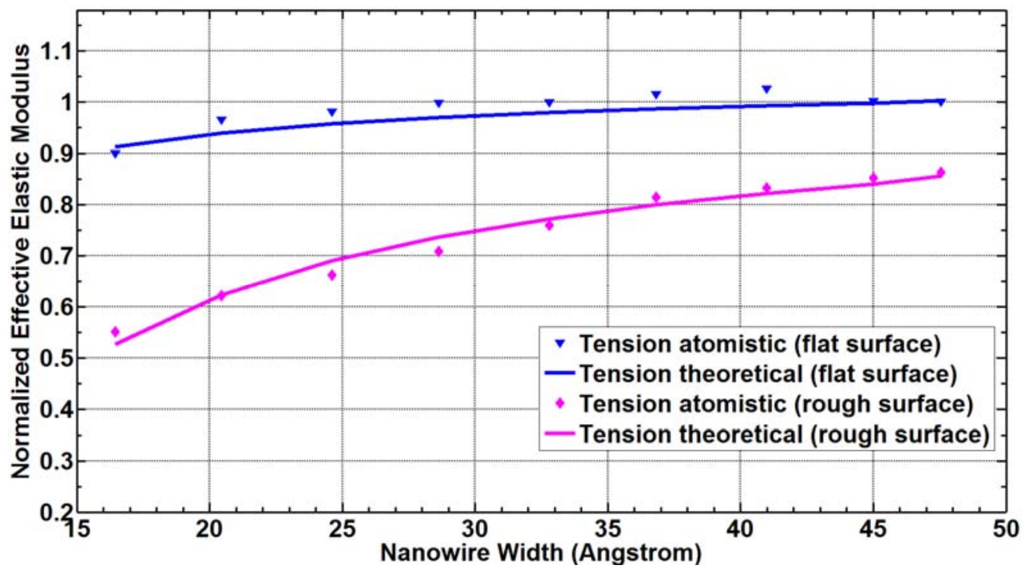

Figure 4-2: Normalized effective elastic modulus of nanowires with flat surface and rough surface.

4.1.2 Simulation Result

The continuum model that predicts the deviation of elastic property of a nanobar, E_{eff}, from that of conventional continuum mechanics, E, in tension can be expressed as (Miller and Shenoy, 2000),

$$\frac{E_{\mathrm{eff}}}{E} = 1 + \frac{4k^s}{aE}, \tag{157}$$

where k^s is the surface elastic constant proposed by Gurtin-Murdoch (1975, 1978) and a is the side of square cross section.

Employing orthogonal least squares method, the coefficients k^s is determined by fitting the atomistic simulation data to the theoretical model (157). Moreover, surface stress τ_0 can be determined from the preliminary relaxation of the beam under absence of external strain. Clearly,

$$4h\tau^0 + EA\varepsilon^* = 0, \tag{158}$$

where ε^* is the amount of compressive strain after initial relaxation and A is the cross section area of the beam. For wire with flat surface, the coefficients are obtained as: τ^0= 0.023096 eV/Å^2, k^s= -0.184628 eV/Å^2. Shenoy (2005) also computed the elastic constants k^s for the $[100]$ surface orientations and found the constants to be negative for Silver. For the wire with rough surfaces these constants change to: $\left(\tau^0\right)^{\mathrm{eff}}$=0.01895, and $\left(k^s\right)^{\mathrm{eff}}$ = -0.622491 eV/Å^2.

4.2 Discussion of the Theoretical and Computational Results

4.2.1 Discussion on Theoretical Predictions

We can use the simple expressions we have derived to make some assessments on the effect of roughness on the surface properties. Our theoretical expression predicts that

$$\left(\tau^0\right)^{eff} = \tau^o\left(1-\frac{3}{4}\delta^2\right) \quad \& \quad \left(k^s\right)^{\text{eff}} = k^s - \delta^2\frac{E}{k\left(1-\nu^2\right)}\frac{\left(9-8\nu\right)}{8\left(1-\nu\right)}, \tag{159}$$

where k is the wave number, $\delta = ak$, a is the wave amplitude and ν is the Poisson's ratio.

Taking Copper as an example, with Young's modulus E of 115 GPa, Poisson's ratio ν of 0.34, surface stress $\tau^o \approx 1.04$ N/m and surface elastic constant $k^s \approx -3.16$ N/m for the (001) crystal face (Shenoy, 2005). If we consider a sinusoidal roughness with $ak = 0.2$ and wave length λ equal to at least 10 nm, k will be of the order of $\frac{2\pi}{\lambda} = \frac{2\pi}{10^{-8}} = 6.28\times10^8$ m^{-1} and by (159) the effective surface stress can be calculated to be

$$\left(\tau^0\right)^{eff} = 0.97\tau^o. \tag{160}$$

So $\left(\tau^0\right)^{eff}$ for this rough surface is barely 3 percent less than the pristine value, τ^o.

Likewise by (159), $\left(k^s\right)^{eff}$ is obtained as

$$\left(k^s\right)^{eff} = k^s - \delta^2\frac{E}{k\left(1-\nu^2\right)}\left(\frac{9-8\nu}{8(1-\nu)}\right) \cong -13.01. \tag{161}$$

A dramatic change from the flat surface value of -3.16 N/m! Therefore, we can conclude that while residual surface stress is hardly affected by the roughness, the surface elastic parameters undergo a dramatic shift. It should be noted here that surface roughness can cause even change of sign in surface elastic depending on the extent of the roughness. Finally, as evident from the expressions for the both the periodic and random roughness case, even if the bare surface possesses zero surface elasticity i.e., $k^s \approx 0$ roughness will "create" surface elasticity i.e. effective value of k^s will be non-zero.

4.2.2 Comparison of Theoretical and Computational Results

As is well-evident from the simulation results, surface corrugation decreases the surface elastic constant k^s by almost three times. Comparatively, there is only a modest change in the residual surface stress τ^0. This is in complete consistency with the theoretical results presented earlier. It should be mentioned here that these homogenized properties are obtained with the key assumption of $\delta = ak << 1$. In other words, Equation (159) is only approximately applicable to our case, nevertheless it is useful for making qualitative comparisons. Using a typical surface roughness of $ak = 0.2$, wave length of 10 nm and considering ν = 0.37, E = 50 GPa, τ^0=0.023096 eV/Å^2 and k^s = -0.184628 eV/Å2 = -2.69 N/m, we obtain the theoretical value of $\left(\tau^0\right)^{eff}$ = 0.02240 eV/Å^2 , $\left(k^s\right)^{eff}$ = - 0.7055 eV/Å2 = -11.300027 N/m. So the value of surface stress decreases by three percent. Also, the value of surface elastic constant decreases by more than four times in the presence of surface roughness---qualitatively consistent with the dramatic decrease observed in our simulations.

4.2.3 Comparison with Weissmuller and Duan's (2008) Results

Weissmuller and Duan (2008) showed that the response of the curvature of cantilevers to changes in their surface stress in the presence of the surface roughness is different from nominally planar surfaces. Considering surface residual stress for cantilevers, they concluded that deliberate structuring of the surface allows the magnitude and even its sign to be tuned. They have concluded that bending of the substrate is controlled by changes in in-plane component of the surface-induced stress, T only. Their calculation shows that T for the isotropic solid with a nearly planar surface $\theta^2 \ll 1$ (assuming isotropy) is equal to

$$T = \frac{\langle f \rangle_s}{h^l}\left(1 - \frac{\nu^l}{1-\nu^l}\langle \theta^2 \rangle\right), \tag{162}$$

where f is surface residual stress and ν^l is the Poisson's ratio. Through their calculations, they assumed that f depends on the surface orientation but this assumption does not have any contribution in creating $\left(1 - \frac{\nu^l}{1-\nu^l}\langle \theta^2 \rangle\right)$ term that shows the apparent action of f will be reduced by a geometric effect that scales with the root-mean-square of θ.

To compare our results with theirs we assume that the roughness profile is co-sinusoidal. Then the average of square of inclination angle can be expressed as

$$\theta = \frac{dh}{dx}$$

$$\left\langle \theta^2 \right\rangle = \left\langle \left(\frac{dh}{dx} \right)^2 \right\rangle = \left\langle a^2 k^2 \sin^2 kx \right\rangle = \frac{1}{\lambda} \int_0^\lambda a^2 k^2 \left(\sin^2 kx \right) dx = \frac{1}{\lambda} \int_0^\lambda a^2 k^2 \left(\frac{1 - \cos 2kx}{2} \right) dx = \quad (163)$$

$$= \frac{a^2 k^2}{2} = \frac{\delta^2}{2}.$$

In order to calculate the maximum reduction in $\left(1 - \frac{\nu^l}{1 - \nu^l} \left\langle \theta^2 \right\rangle \right)$, we select the value of 0.2 for δ and 0.44 for ν for Gold and then obtain

$$1 - \frac{\nu^l}{1 - \nu^l} \left\langle \theta^2 \right\rangle = 1 - 0.016. \quad (164)$$

So based on the assumed range of δ our model suggests that the reduction of the effective surface stress because of the roughness is 1.6 % while Weissmuller and Duan's work shows 10 % reduction with assumption of $\left\langle \theta^2 \right\rangle = 0.33$. The somewhat larger shifts in the surface stress calculated by Weissmuller and Duan (2008) can only be obtained for extremely large roughness. Since both works (ours and Duan et. al.) assume "small roughness", it is not clear whether our models are applicable for the large range of roughness that lead to the dramatic shifts in surface stress observed by them.

4.2.4 Resonance Frequency of Nano-cantilevers

Nanofabricated cantilever structures have been demonstrated to be extremely versatile sensors and have potential applications in physical, chemical, and biological sciences. Adsorption on surface of such a sensor may induce mass, damping, and stress changes of the cantilever response. One cantilever sensor technique is to monitor changes in the cantilever resonance frequency. The effect of surface stress on the resonance frequency of a cantilever have been modeled analytically by Lu et al. (2005) by incorporating strain-dependant surface stress terms into the equations of motion.

Consider a cantilever used as a sensor. The experimental quantity measured is the surface stress difference, $\Delta\sigma^s = \sigma_u^s - \sigma_l^s$, where σ_u^s and σ_l^s are the surface stresses on the upper and the lower surfaces, respectively. In the isotropic case, the surface stresses may be written as

$$\sigma_u^s = \tau^o{}_u + k^s{}_u \left(\varepsilon_{ss}\right)_u \quad \text{and} \quad \sigma_l^s = \tau^o{}_l + k^s{}_l \left(\varepsilon_{ss}\right)_l, \tag{165}$$

where τ^o is the strain-independent surface stress, k^s is a constant associated with the surface strain, ε_{ss} is the surface strain measured from the pre-stressed configuration, and the subscripts u and l always refer to the upper and lower surface, respectively. The surface stress difference can be written as

$$\Delta\sigma^s = \Delta\sigma^o + \Delta\sigma^1, \tag{166}$$

with $\Delta\sigma^o = \tau^o{}_u - \tau^o{}_l$ and $\Delta\sigma^1 = k^s{}_u \left(\varepsilon_{ss}\right)_u - k^s{}_l \left(\varepsilon_{ss}\right)_l$. While the strain-independent part of the surface stress, $\Delta\sigma^o$ can have an impact on the resonance frequency (in a nonlinear setting), it is expected to be small. The strain-dependent part (i.e. surface elasticity) definitely will change the resonance frequency and can be expressed as

$$\frac{(\omega_s)^2-(\omega_0)^2}{(\omega_0)^2}=3\frac{k^s{}_u+k^s{}_l}{Eh}, \tag{167}$$

where ω_0 is the fundamental resonance frequency without considering surface elasticity, ω_s is the resonance frequency with surface stresses acting, h is the thickness and E is Young's modulus. Liu and Rajapakse (2010) as well came up with the same expression for resonance frequency shift considering surface energy.

To compare the change in resonance frequency of cantilevers with rough surfaces, we consider a beam that has a sinusoidal rough surface on top and flat surface on the bottom. We have

$$k^s{}_u=\left(k^s\right)^{eff}=k^s-\delta^2\frac{E}{k\left(1-\nu^2\right)}\left(\frac{9-8\nu}{8(1-\nu)}\right). \tag{168}$$

for top surface and $k^s{}_l=k^s$ for the lower surface. Then the change in resonance frequency can be obtained as

$$\frac{(\omega_{rough})^2-(\omega_0)^2}{(\omega_0)^2}=\frac{3}{Eh}\left(2k^s-\delta^2\frac{E}{k\left(1-\nu^2\right)}\left(\frac{9-8\nu}{8(1-\nu)}\right)\right). \tag{169}$$

Compared to a cantilever with upper and lower flat surface with resonance frequency

$$\frac{(\omega_s)^2-(\omega_0)^2}{(\omega_0)^2}=\frac{3}{Eh}\left(2k^s\right). \tag{170}$$

Evidently, frequency shift will decrease significantly or even in some cases, may change sign. For instance for copper considering the (001) crystal face (Shenoy, 2005) if we consider a sinusoidal roughness with $ak = 0.2$ and wave length of 10 nm on top surface of cantilever, the change of resonance frequency would be expressed as

$$\frac{\left(\omega_{rough}\right)^2-\left(\omega_0\right)^2}{\left(\omega_0\right)^2}=\frac{3}{Eh}\left(-16.17\right), \tag{171}$$

from its value of

$$\frac{\left(\omega_s\right)^2-\left(\omega_0\right)^2}{\left(\omega_0\right)^2}=\frac{3}{Eh}\left(-6.32\right). \tag{172}$$

So quantitatively, the square of resonance frequency is shifted by 2.55 times.

As another example, we consider aluminum with Young's modulus E of 70 GPa, Poisson's ratio ν of 0.35, $\tau^o \approx 0.91$ N/m and $k^s \approx 4.53$ N/m for the (111) crystal face (Shenoy, 2005). Then the resonance frequency of the cantilever with top rough surface is calculated as

$$\frac{\left(\omega_{rough}\right)^2-\left(\omega_0\right)^2}{\left(\omega_0\right)^2}=\frac{3}{Eh}\left(3\right), \tag{173}$$

while in case of considering flat surfaces for cantilever it would be

$$\frac{\left(\omega_s\right)^2-\left(\omega_0\right)^2}{\left(\omega_0\right)^2}=\frac{3}{Eh}\left(9.06\right). \tag{174}$$

In this case, the square resonance frequency is decreased by three times.

In summary, we have presented simple expressions for homogenized surface stress and surface elasticity for both randomly and periodically rough surfaces. Residual surface stress does not appear to be significantly affected by the presences of roughness----this appears to be in contrast to the conclusions of Weismuller and Duan (2008) although we do notice a dramatic change in the surface elastic modulus. The latter for example, as we demonstrated through simple illustrative quantitative examples, should have significant impact on the way sensing data based on surface effects is interpreted. Our simulation results also validate the theoretical predictions.

Chapter 5: Atomistic Elucidation of the Effect of Surface Roughness on Curvature-dependent Surface Energy, Surface Stress and Elasticity

5.1 Introduction

Surface effects, represented phenomenologically through “surface energy”, dramatically affect the physical properties and behavior of nanostructures. Surface energy effects are usually accounted through the theoretical framework proposed by Gurtin and Murdoch (1975, 1978). In their theory, surface is a zero-thickness deformable entity that is attached to the bulk and possesses a residual stress (the so-called “surface stress”) and surface elasticity (which is distinct from macroscopic bulk elasticity). In the original Gurtin-Murdoch theory, surface energy, as shown below, depends only on the surface strains. Let e_n be the outward unit normal to the surface then

$$\mathrm{I}_s = \mathrm{PIP} \quad \& \quad \mathrm{P} = \mathrm{I} - e_n \otimes e_n . \tag{175}$$

P is the projection operator to the subspace orthogonal to e_n, and I_s is the identity mapped to the tangential surface. So the Gurtin-Murdoch surface energy function is expressed as

$$\gamma = \gamma_0 + \tau_0 \mathrm{I}_s \mathbf{E}_\mathrm{S} + \frac{1}{2}\mathrm{C}_0 \mathbf{E}_\mathrm{S}^2 . \tag{176}$$

Here γ_o is a constant unimportant to the objectives of the present work, $\mathbf{E}_S = \mathrm{P}\mathbf{E}\mathrm{P}$ is the surface strain, τ_0 is the residual surface stress, and C_0 is the surface elastic constant. It is worthwhile to note that a fair amount of literature (in some cases, justifiably) ignore surface elasticity (i.e. $\mathrm{C}_0 = 0$). More recently, we have discussed a modified surface energy that, in addition to strain, also penalizes changes in curvature. This theory (based on the work of Steigmann-Ogden, 1997, 1999) successfully explained the observation that the effective elastic modulus of nanostructures under bending is significantly different than under stretching. This discrepancy between the elastic response under bending vs stretching was a source of puzzlement since the conventional Gurtin-Murdoch theory predicts only a small difference between the two deformation modes. A simplified version of the curvature dependent surface energy can be written as:

$$\gamma = \gamma_0 + \tau_0 \mathrm{I}_s \mathbf{E}_S + \frac{1}{2}\mathrm{C}_0 \mathbf{E}_S^2 + \frac{1}{2}\mathrm{C}_1 \boldsymbol{\kappa}^2, \tag{177}$$

where C_1 is the Steigmann-Ogden material constant that reflects the penalty in surface energy upon changes in curvature. The details of the theory can be found in Steigmann-Ogden (1997, 1999), and Chhapadia et al. (2011). The constant C_1 can be also interpreted as Tolman's (1949) length for crystalline solids or alternatively can be used to assign a thickness for a surface

($t = \sqrt{\dfrac{C_1}{C_0}}$ can be argued to be related to the "definition" of surface thickness---see Chhapadia et. al., 2011).

In the beginning of the present chapter, we derive a continuum model that predicts the deviation of elastic property of a nanobar, E_{eff}, from that of conventional continuum mechanics, E, for bending of a cantilever beam. In the second part of this chapter, we address a simple question: what is the effect of roughness on the surface energy–related properties e.g. τ_0, C_0 and C_1? Surfaces of real materials even for the most thoroughly polished ones will typically exhibit roughness. Alternatively, one may even consider intentionally nanostructuring the surface to design a tailored response. Here, we carry out atomistic simulations of nano-cantilever beams of both flat and rough surfaces and assess the change in the Steigmann-Ogden material constant C_1.

5.2. Predictions for a Thin Cantilever Beam

Consider a thin cantilever beam loaded with a uniform lateral load $q(x)$ on top. The beam has longitudinal axis in x direction and vertical deflection in y direction (--we assume a square-cross section with side a without loss of any generality of our final qualitative results). Let $w(x)$ denote the deflection of the beam as a function of position x from the fixed end. Using the variational method, we will re-derive the equations governing beam bending theory considering surface free energy (177).

The axial and vertical displacements of the beam are approximated by

$$u_x = -y\frac{dw(x)}{dx}, \qquad u_y = w(x). \tag{178}$$

For thin beams, we ignore the shear deformation of the beam. Therefore the bulk strains are

$$\varepsilon_{xx} = -y\frac{d^2w(x)}{dx^2}, \qquad \varepsilon_{xy} = \varepsilon_{yy} = 0. \tag{179}$$

Liu and Rajapakse (2010) have shown that the effect of vertical stress σ_{yy} on beam deformation is very small and can be neglected. So, the relevant bulk stresses are

$$\sigma_{xx} = -Ey\frac{d^2w(x)}{dx^2}, \qquad \sigma_{xy} = \sigma_{yy} = 0, \tag{180}$$

where E is the bulk Young's modulus. Also, the elastic surface with outward unit normal n_y has surface free energy represented by Eq. (177). We proceed by computing the total energy $U(w)$ of the cantilever beam by noting tangential surface strain as ε_{xx} and curvature as $\frac{d^2w(x)}{dx^2}$,

$$U_{Bulk}(w) = \int_0^l \int_A \frac{1}{2}\mathrm{E}\left(y\frac{d^2w(x)}{dx^2}\right)^2 \mathrm{dA}\, dx, \tag{181}$$

where A is the cross section area and l is length of the beam. Also, the surface energy is

$$U_{Surface}(w)=\int_0^l\int_S\left[-\tau_0 y\frac{d^2w(x)}{dx^2}+\frac{1}{2}\mathrm{C}_0y^2\left(\frac{d^2w(x)}{dx^2}\right)^2+\frac{1}{2}\mathrm{C}_1\left(\frac{d^2w(x)}{dx^2}\right)^2\right]\mathrm{dS}\,dx, \tag{182}$$

where C_0, C_1 are surface elastic modulus and Steigmann-Ogden constant respectively, and S is the perimeter of the cross section. The potential energy of the external force is

$$U_q(w)=-\int_0^l q(x)w(x)dx. \tag{183}$$

Standard variational arguments require

$$\int_0^l\left[\left(\mathrm{EI}+\mathrm{C}_0\mathrm{I}^*+\mathrm{C}_1S^*\right)\left(\frac{d^2w(x)}{dx^2}\frac{d^2\delta w(x)}{dx^2}\right)-q(x)\delta w(x)\right]dx=0 \tag{184}$$

where $\mathrm{I}=\int_A y^2dA$ is the moment of inertia of the beam cross section, $\mathrm{I}^*=\int_S y^2dS$ is the perimeter moment of inertia, and $\mathrm{S}^*=\int_S {n_y}^2dS$.

Using integration by part, the governing equation for bending of thin cantilever beam is obtained as

$$\left(\mathrm{EI}+\mathrm{C}_0\mathrm{I}^*+\mathrm{C}_1S^*\right)\frac{d^4w(x)}{dx^2}-q(x)=0. \tag{185}$$

Upon comparison with the classical Euler-Bernoulli beam equation with an "effective" elastic modulus, i.e.,

$$\mathrm{E}_{\mathrm{eff}}\mathrm{I}\frac{d^4w(x)}{dx^2}-q(x)=0. \tag{186}$$

We find the following:

$$\frac{\mathrm{E}_{\mathrm{eff}}}{\mathrm{E}}=\frac{\mathrm{EI}+\mathrm{C}_0\mathrm{I}^*+\mathrm{C}_1S^*}{\mathrm{EI}}. \tag{187}$$

In the case of a beam with square cross section of side a ,

$$\mathrm{I}=\frac{a^4}{12}, \qquad \mathrm{I}^*=\frac{2a^3}{3}, \qquad \mathrm{S}^*=2a\ . \tag{188}$$

the effective elastic modulus is obtained as

$$\frac{\mathrm{E}_{\mathrm{eff}}}{\mathrm{E}}=1+\frac{8C_0}{a\mathrm{E}}+\frac{24C_1}{\underbrace{a^3\mathrm{E}}}. \tag{189}$$

It is worth pointing out that the asymmetrical term in the surface constitutive law and the dependence of elastic modulus on the residual stress should not be ignored in general (Mogilevskaya et al., 2008) and (Wang et al., 2010) however it is justified in the present case for two reasons: (i) inclusion of that term makes not qualitative difference to our conclusions and (ii) while residual surface stress can be important for the stress state, its impact on renormalized elastic modulus has been found to be small in recent works see for example (Liu et al., 2011).

5.3. Molecular Static Simulation on Bending of the Ag nanowire

In this section, using LAMMPS molecular dynamics software, molecular static simulations are performed on the nanowire and effective Young's elastic moduli of the nanowires are computed under bending. As our model system, we have chosen the same configuration, geometry and interatomic potential for the Ag nanowire as we have used in the previous simulation (see section 4.1.1).

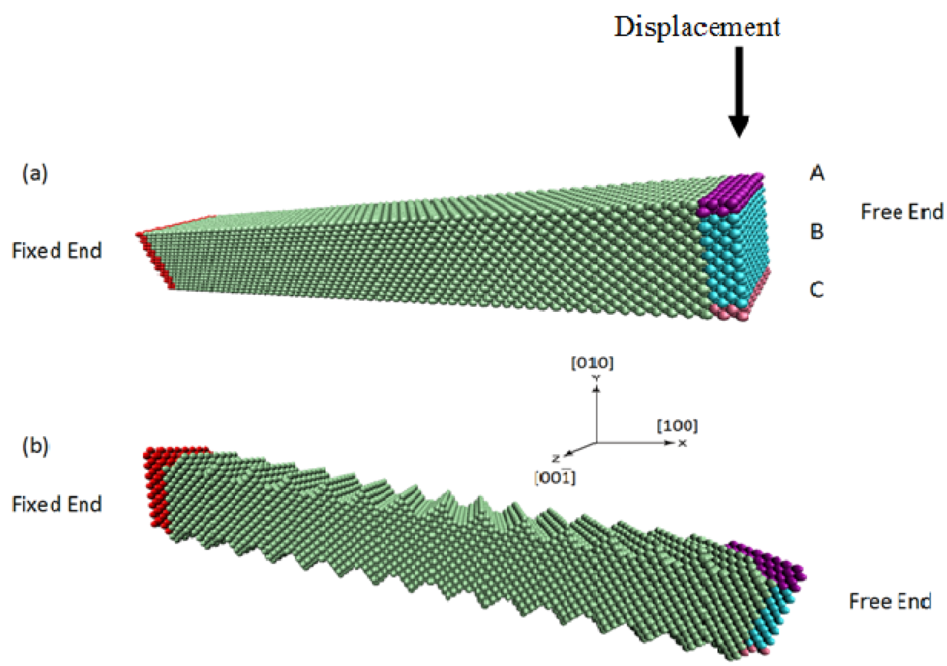

Figure 5-1: Schematic representation of the two nanowire configuration.

The nanowires are initially created based on the silver atom configuration corresponding to a perfect fcc bulk crystal and in order to consider the contribution of free surfaces, the boundary conditions in all directions are chosen to be non-periodic. The nanowire geometry is then relaxed to a local minimum energy state at zero K temperature using the conjugate gradient method. The atoms on or close to the surface change their equilibrium position during this process.

Cantilever bending simulation method proposed by McDowell et al. (2008), is performed on both nanowires with flat and rough surfaces. In our simulations, we consider a sufficiently long nanowire ($l/t > 8$) and keep the same aspect ratio with increasing nanowire thickness. Therefore, it is reasonable to ignore the shear forces created as a result of lateral deflection and only consider the bending moment effect. After initial relaxation, one end of the nanowire is held fixed and the free end is given an incremental downward displacement of 0.1 nm. The free end atoms are divided to three regions ‘A’, ‘B’, and ‘C’ (fig. 1). In each displacement increment, first, all the atoms in free end are displaced downward. Then atoms in region ‘A’ are held fixed and the nanowire is underwent energy minimization using conjugate gradient method. Finally the atoms in region ‘C’ are held fixed and the nanowire is relaxed to the minimum energy state. This entire displacement–double relaxation cycle is repeated for a desired number of increments.

In continuum beam theory, for small deflections, the change in strain energy of a cantilever beam is obtained as (McDowell et al., 2008),

$$\Delta U = \int_0^l \frac{EI}{2}\left(\frac{\partial^2 v}{\partial x^2}\right)^2 dx, \tag{190}$$

where E is the Young's modulus, I is the moment of inertia, v is the deflection as a function of x and l is the length of the beam. In our simulation, for each bending increment, the deflection profile of the mid-plane that is a cubic polynomial of x is determined. Then change in strain energy and curvature data which is the second derivative of deflection with respect to x are fitting into equation (190), and the effective Young's modulus E_{eff} is determined. The final Young's modulus is obtained as average of the values for the last three bending increments.

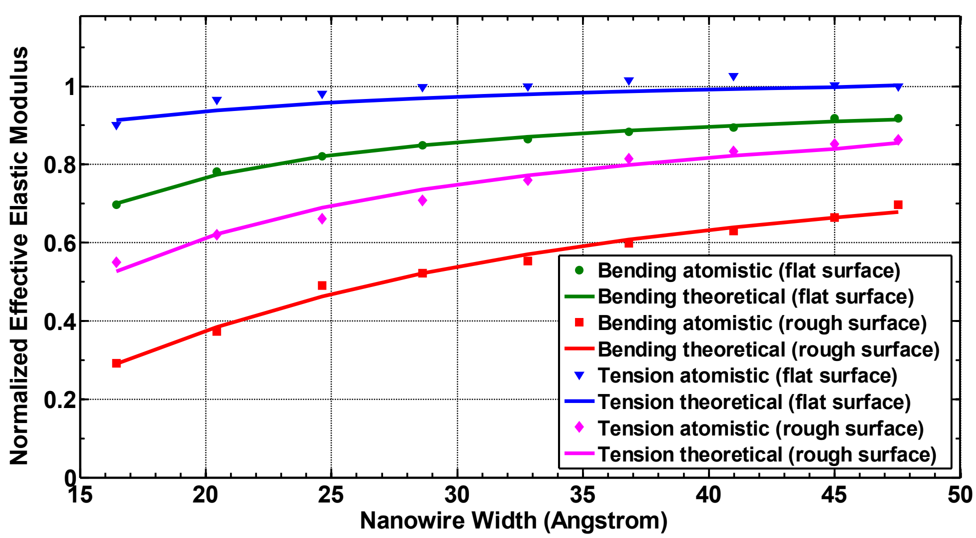

Figure 5-2: Normalized effective elastic modulus of nanowires with flat surface and rough surface.

Figure 5-2 presents our results for bending. The tension simulation results obtained in previous chapter is also displayed in the figure. As already explained by Chhapadia et al. (2011), the elastic modulus in case of bending is less than (in absolute value) under tension. We observe that the wire with rough surface has a lower Young's modulus compared to the wire with flat surface. Therefore our simulation results prove that surface corrugation causes softening in the wire.

In case of bending, we use the continuum model (189) that predicts the deviation of elastic property of a nanobar, E_{eff}, from that of conventional continuum mechanics, E. Employing orthogonal least squares method, the coefficients C_0 and C_1 are determined by fitting the atomistic simulation data to the theoretical model (15). Moreover, surface stress τ_0 can be determined with exact procedure as before (see section 4.1.1). For wire with flat surface, the coefficients are obtained as: τ^0=0.023096 eV/Å^2 , C_0 = -0.168157 eV/Å^2 and C_1 = -3.181146 eV. For the wire with rough surfaces these constants change to: $\left(\tau^0\right)^{\mathrm{eff}}$=0.01895, $\left(C_0\right)^{\mathrm{eff}}$ = -0.506521 eV/Å^2 and $\left(C_1\right)^{\mathrm{eff}}$=6.853007 eV. As is well-evident from the results, surface corrugation decreases the surface elastic constant C_0 by almost three times. This is in complete consistency with the theoretical results presented in our previous work. The theoretical expression predicts that

$$\left(\tau^0\right)^{eff} = \tau^o\left(1-\frac{3}{4}\delta^2\right) \quad \& \quad \left(C_0\right)^{\mathrm{eff}} = C_0 - \delta^2\frac{E}{k\left(1-\nu^2\right)}\frac{\left(9-8\nu\right)}{8\left(1-\nu\right)}, \tag{191}$$

where k is the wave number, $\delta = ak$, a is the wave amplitude and ν is the Poisson's ratio. This theoretical expression is obtained with the key assumption of $\delta = ak << 1$. In other words, Equation (191) is only approximately applicable to our case, nevertheless it is useful for making qualitative comparisons. Using a typical surface roughness of $ak = 0.2$, wave length of 10 nm and considering ν = 0.37, E = 50 GPa, τ^0= 0.023096 eV/Å^2 and C_0 = - 0.168157 eV/Å2 = - 2.69 N/m, we obtain the theoretical value of $\left(\tau^0\right)^{eff}$ = 0.02240 eV/Å^2, $\left(C_0\right)^{\mathrm{eff}}$ = - 0.72177 eV/Å2 = - 11.5628 N/m. So the value of surface stress decreases by three percent. Also, the value of surface elastic constant decreases by more than four times in the presence of surface roughness---qualitatively consistent with the dramatic decrease observed in our simulations. In addition it is observed that the roughness causes a large shift in the value of C_1 as well as a change in the sign.

Micro and nano-fabricated cantilevers are frequently used as chemical, biological and mechanical sensors. One of the sensing mechanisms is to detect a shift in the resonant frequency subject to a stimuli. Lu et al. (2005) have derived that the change in fundamental resonance frequency due to surface stress $\Delta\omega_{stress}$ in general can be expressed as

$$\frac{\omega_{stress}^2 - \omega_0^2}{\omega_0^2} = \frac{E_{\text{eff}} - E}{E}, \tag{192}$$

where ω_0 is the fundamental resonance frequency in absence of surface stress and ω_{stress} is the new resonance frequency with surface stress.

Since surface roughness affects the effective elastic modulus of nanostructures (as we have already seen), we therefore expect a shift in the resonance frequency also. Chhapadia et al. (2011) for a 2 nm thick $\langle 100 \rangle$ axially oriented cantilever with flat lateral surfaces predicated that term in Equation (192) is -0.22. Considering a similar beam but with roughned surfaces identical to what we modeled in our atomistic simulations the term in Equation (192) becomes: -0.61. This simple example clearly indicates the enormous role roughness can play in the interpretation of sensing data.

Chapter 6: Flexoelectric Membranes and their Effective Properties

6.1 Introduction

Piezoelectricity is perhaps the most widely known and exploited forms of electromechanical coupling. In a piezoelectric material, a uniform mechanical strain induces an electric field and vice-versa. Piezoelectricity is preferentially used where precise control of mechanical motion is required e.g. in scanning probe microscopes and have now found wide applications: next-generation energy harvesters (Wang et al., 2010), artificial muscles (Madden et al., 2004), sensors and actuators (Gautschi, 2002) among others. Crystallographic considerations restrict this technologically important property to non-centrosymmetric crystal systems (Nye, 1985) and indeed the latter is a necessary condition for a material to display piezoelectricity. However a non-uniform strain field or presence of strain gradients can locally break inversion symmetry and induce polarization even in centrosymmetric crystals. This phenomenon is termed flexoelectrictiy (Maskevich and Tolpygo, 1957; Bursian et al., 1974; Tagantsev, 1986, 1991), inspired by a similar effect in liquid crystals (Meyer, 1969; Schmidt et al., 1972; Indenbom et al., 1981). The reader is encouraged to refer to some recent review articles on flexoelectricity by Cross (2006), Sharma et al. (2007), and Tagantsev et al. (2009).

Recently, flexoelectricity has attracted a fair amount of attention from both fundamental and applications points of view leading to intensive experimental

(Ma and Cross, 2001, 2002, 2003, 2006; Catalan et al., 2004; Cross, 2006; Zubko et al. 2007, Fu et al., 2006, 2007) and theoretical (Sharma et al., 2007; Eliseev et al. 2009, 2011; Maranganti and Sharma, 2009; Majdoub et al., 2008, 2009; Sharma et al., 2010; Gharbi et al., 2011; Kalinin and Meunier, 2008; Eliseev and Morozovska, 2009; Dumitrica et al., 2002) activity in this topic. Lack of symmetry at surfaces and the capability to support large strain gradient in nanoscale structures enable unusual forms of piezoelectricity and flexoelectricity; for example, creating piezoelectric meta-material from a non-piezoelectric material has been investigated experimentally and computationally (Cross and co-workers, 1999, 2006a-c; Sharma et al*.* 2010, Baskaran et al., 2010). In fact, Chandratre and Sharma (2012) recently showed that predicated on the phenomenon of flexoelectricity, Graphene can be "coaxed" to behave like a piezoelectric material merely by creating holes of certain symmetry. The artificial piezoelectricity thus produces was found to be almost as strong as that of well-known piezoelectric substances such as quartz.

Several other works have appeared on elucidating flexoelectricity in two-dimensional structures (Naumov et al., 2009). Dumitrica et al. (2002) and Kalinin and Meunier (2008) showed that low dimensional systems such as graphene tend to exhibit electronic flexoelectricity, e.g., bending of non-polar quantum systems leading to emergence of net dipole moments. Upon bending, redistribution of the electron gas in the normal direction results in the formation of a net dipole moment, and hence flexoelectric coupling. For large radii of curvatures and in the extreme case of closed seamless cylinder, the dipoles (formed) cancel out each other and the net polarization vanishes—which is why non-chiral (dielectric) carbon nanotubes have no dipole moment.

It is worthwhile to mention that investigating flexoelectricity effect in curved structures is also common in soft condensed materials such as liquid crystals and cellular membranes (Petrov et al., 1996, 1998, 2011; Kuczynski and Hoffmann, 2005; Spector, et al., 2006; Harden et al., 2010; Jewell, 2011) pioneered by Meyer (1969). Synthetic and biological flexoelectric membranes are actuators that bend under the action of external electric fields, a phenomenon of interest to the development of emerging adaptive materials as well as biological mechano-transduction. Several works have explored biological implications of membrane flexoelectricity e.g., mechanosensitivity, electromotility and hearing systems (Petrov, 1975, 2002, 2006, 2007; Raphael et al., 2000; Brownell et al., 2001, 2003; Breneman and Rabbitt, 2009).

Flexoelectricity in membranes is fundamentally different from three-dimensional materials (crystalline or otherwise). In this paper, we consider an important emerging problem that is unaddressed so far: what is the renormalized or effective flexoelectric, response of a heterogeneous 2-dimensional structure? How do the elastic and dielectric responses alter due to flexoelectricity? The answer to these questions may help interpret the behavior of complex biological membranes, in tailoring membranes such as graphene and boron-nitride sheets for various technological applications, energy harvesting for stretchable electronics among others. In section 2, we present a simplified and linear theory of flexoelectricity of 2-dimensional deformable solid membranes. The homogenization problem is quite difficult even in the linear setting and hence we defer to future work, the more complex case of non-linear elastic membranes (see Steigmann, 2009). In section 3, we present our homogenization approach and specialize our results to a fluid membrane in section 4 (--this case corresponds to the much-studied lipid membranes or the Helfrich Hamiltonian). In section 5, we present some simple illustrative examples of our work using graphene as an example material.

6.2 A theory of flexoelectric solid membranes

Let $\Omega \subset \mathbb{R}^2$ be a domain in xy-plane. Consider a thin dielectric membrane occupying $\Omega \times \left(-h/2, h/2\right) \subset \mathbb{R}^3$, where h is the thickness of the membrane. If the thickness $h \ll 1$, the thin membrane may be idealized as a two-dimensional body; the thermodynamic state is described by the out-of-plane displacement $w : \Omega \to \mathbb{R}$ and the out-of-plane polarization $P : \Omega \to \mathbb{R}$. The curvature of the membrane is defined as

$$\kappa_{\alpha\beta} = -\nabla_\alpha \nabla_\beta w. \tag{193}$$

If $L_{\alpha\beta\xi\eta}$ be the elastic stiffness tensor of the membrane, for an isotropic case,

$$L_{\alpha\beta\xi\eta} = \frac{D\left(1-\nu\right)}{2}\left(\delta_{\alpha\xi}\delta_{\beta\eta} + \delta_{\alpha\eta}\delta_{\beta\xi}\right) + D\nu\delta_{\alpha\beta}\delta_{\xi\eta}. \tag{194}$$

The elastic energy part of the total energy density can be written as (Reddy, 2007)

$$\Pi(\kappa) = \frac{1}{2} L_{\alpha\beta\xi\eta} \kappa_{\alpha\beta} \kappa_{\xi\eta} = \frac{1}{2}\left[k_b^1 \left(\kappa_{\alpha\beta}\right)^2 + k_b^2 \left(\kappa_{\alpha\alpha}\right)^2 \right]. \tag{195}$$

where $k_b^1 = D(1-\nu)$, $k_b^2 = D\nu$ and $D = \dfrac{Eh^3}{12\left(1-\nu^2\right)}$ is the bending rigidity (stiffness), ν is the Poisson's ratio, E is the Young's modulus and h is the thickness of the membrane.

To model the flexoelectric effect, we postulate that the total internal energy of the isotropic membrane is given by

$$U[w, P] = \int_\Omega W\left(\nabla\nabla w, \Delta w, P\right) d\Omega, \tag{196}$$

where $W : \mathbb{R}^2 \to \mathbb{R}$ is the total internal energy density function and is given by a quadratic function

$$\begin{aligned} W\left(\nabla\nabla w, \Delta w, P\right) &= \Pi\left(\kappa\right) + f\,\Delta w P + \frac{1}{2} a P^2 \\ &= \frac{1}{2} k_b^1 \left|\nabla\nabla w\right|^2 + \frac{1}{2} k_b^2 \left(\Delta w\right)^2 + f\,\Delta w P + \frac{1}{2} a P^2. \end{aligned} \tag{197}$$

In the above equation, coefficients k_b^1, k_b^2, f and a are material properties and can in general depend on in-plane positions. In particular, a is the reciprocal dielectric susceptibility and f is the flexoelectric coefficient of the material. Under the application of an external electric field $E_z^0 : \Omega \to \mathbb{R}$ and a mechanical body force $b_z : \Omega \to \mathbb{R}$, the total free energy of the membrane is given by

$$F\left[w,P\right]=\int_{\Omega}\left(\frac{1}{2}k_b^1\left|\nabla\nabla w\right|^2+\frac{1}{2}k_b^2\left(\Delta w\right)^2+f\,\Delta wP+\frac{1}{2}aP^2\right)d\Omega-\int_{\Omega}\left(PE_z^0+wb_z\right)d\Omega. \tag{198}$$

The first integral is the internal energy of the flexoelectric membrane, and the second one is the potential energy arising from the interaction between the membrane and the external electric field and mechanical loading device. We remark that the external field $E_z^0:\Omega\to\mathbb{R}$, arising from a fixed distribution of charges, is independent of the polarization state of the membrane.

Clearly, the stability of trivial state $\left(\nabla\nabla w,P\right)=\left(0,0\right)$ in the absence of external electric fields E_z^0 and mechanical load b_z requires that

$$\begin{gathered}\frac{1}{2}k_b^1\left|\alpha_3\right|^2+\frac{1}{2}k_b^2\left(tr\alpha_3\right)^2+f\left(tr\alpha_3\right)\alpha_2+\frac{1}{2}a\left(\alpha_2\right)^2\geq 0,\\ \text{for}\quad\forall\alpha_3\in\mathbb{R}^{2\times2}_{SYM},\ \alpha_1\in\mathbb{R}\end{gathered} \tag{199}$$

which requires

$$A=\begin{bmatrix}k_b^1+k_b^2 & 0 & k_b^2 & f\\ 0 & 2k_b^1 & 0 & 0\\ k_b^2 & 0 & k_b^1+k_b^2 & f\\ f & 0 & f & a\end{bmatrix}\ \text{is positive-definite,}$$

i.e., $k_b^1>0$, $k_b^1+k_b^2>0$, $a>0$ & $\det A>0$ or $\dfrac{1}{2}k_b^1+k_b^2>\dfrac{f^2}{a}$.

Let Γ_1 and Γ_2 be a disjoint subdivision of the boundary $\partial\Omega$. As for the classic Kirchhoff-Love plate theory, typical homogeneous boundary conditions include (for detail of derivation see section IV.I.I):

1. Clamped boundary conditions:

$$w = 0, \quad \nabla w = 0 \qquad \text{on } \Gamma_1 \tag{200}$$

2. Natural boundary conditions:

$$\left(\left(k_b^2 - \frac{f^2}{a}\right)\Delta w I + k_b^1 \nabla\nabla w\right).n = 0, \quad \left(\left(k_b^2 - \frac{f^2}{a}\right)\nabla\Delta w + k_b^1 \nabla.\nabla\nabla w\right).n = 0 \qquad \text{on } \Gamma_2 \tag{201}$$

More general and inhomogeneous boundary conditions are also allowed.

We remark that the postulated internal energy density (196) may be validated from a well-grounded three-dimensional theory of flexoelectricity. Alternatively, we may regard the postulated form of internal energy (196) for membranes as the linearized version of some more complete theory of flexoelectric membranes, containing only the leading order terms. Such a postulation or equivalently a constitutive law is necessary for completing a continuum theory. Here we do not attempt to rigorously justify either of the above viewpoints and merely take postulate (196) as our starting point.

In the equilibrium state, the pair of (w, P) shall minimize the total free energy (197):

$$\min_{(w,P)\in A} F[w, P] \tag{202}$$

where the admissible space for (w, P) is given by

$$A := \left\{ \left(w, P \right) : w \in W^{2,2}\left(\Omega \right), P \in L^2\left(\Omega \right), w, \nabla w\big|_{\Gamma_1} = 0 \right\}. \tag{203}$$

Standard first variation calculations

$$\begin{cases} \dfrac{d}{d\varepsilon} F\left[w + \varepsilon \upsilon, P \right]\Big|_{\varepsilon=0} = 0, \\ \dfrac{d}{d\varepsilon} F\left[w, P + \varepsilon \eta \right]\Big|_{\varepsilon=0} = 0, \end{cases} \tag{204}$$

gives

$$\begin{cases} \int_\Omega \left[k_b^1 \left(\nabla\nabla w \cdot \nabla\nabla \upsilon \right) + k_b^2 \left(\Delta w \Delta \upsilon \right) + fP\Delta \upsilon \right] - \int_\Omega \upsilon b_z = 0, \\ \int_\Omega \left[f\eta\Delta w + aP\eta \right] - \int_\Omega \eta E_z^0 = 0. \end{cases} \tag{205}$$

and finally we can show that the Euler-Lagrange equations associated with the above variational principle are given by

$$\begin{cases} \nabla\nabla \cdot \left(k_b^1 \nabla\nabla w \right) + \Delta\left(k_b^2 \Delta w \right) + \Delta\left(fP \right) - b_z = 0 \quad \text{on } \Omega, \\ f\Delta w + aP - E_z^0 = 0 \quad \text{on } \Omega. \end{cases} \tag{206}$$

Operating the second of (205) by $-\Delta\left(\dfrac{f}{a}(\ ) \right)$ and adding the result to the first of (205), we obtain

$$\nabla\nabla \cdot \left(k_b^1 \nabla\nabla w \right) + \Delta\left[\left(k_b^2 - \frac{f^2}{a} \right) \Delta w \right] + \Delta\left(\frac{f}{a} E_z^0 \right) - b_z = 0 \quad \text{on } \Omega. \tag{207}$$

We remark that the partial differential equation (206), together with the boundary conditions (199) and (200), forms a well-posed boundary value problem whose existence, uniqueness and stability has been thoroughly investigated, see e.g. Evans (1997).

Here it is important to have an explanation about the material constants appear in the above-mentioned formulae. Kalinin and Meunier (2008) showed that the net macroscopic electromechanical polarization developed in a bent structure is linearly proportional to its curvature and accordingly expressed the constitutive relation for direct flexoelectric effect as

$$P = f^k \left(c_1 + c_2\right), \tag{208}$$

where c_1 and c_2 are the principle curvatures, P is the polarization [C/m], and f^k is the flexoelectric constant [C] which is quantitatively different with flexoelectric coefficient in our expressions. If we consider a homogenous material, in the absence of external electric field, (205-2) gives the following relation between the average of polarization and average of curvature in the bent structure,

$$P = -\frac{f}{a}\Delta w. \tag{209}$$

This implies that

$$f = -af^k, \tag{210}$$

where $a = \dfrac{1}{\varepsilon_0 \chi_e h}$ is the reciprocal dielectric susceptibility, ε_0 is the electric permittivity of the free space, χ_e is the electric susceptibility and h is the thickness of the material. Therefore our definition of flexoelectric constant is $f = -\frac{f^k}{\varepsilon_0 \chi_e h}$ [N.m/C].

6.3 Homogenization of heterogeneous flexoelectric membranes

We now consider a heterogeneous flexoelectric membrane whose coefficients are given by

$$k_b^{1(\varepsilon)}(x) = k_p^1\left(\frac{x}{\varepsilon}\right), \quad k_b^{2(\varepsilon)}(x) = k_p^2\left(\frac{x}{\varepsilon}\right), \quad f^{(\varepsilon)}(x) = f_p\left(\frac{x}{\varepsilon}\right), \quad a^{(\varepsilon)}(x) = a_p\left(\frac{x}{\varepsilon}\right), \tag{211}$$

where $\varepsilon \ll 1$ characterizes the length scale of the microscopic variations of the material properties, and without loss of generality, we assume k_p^1, k_p^2, f_p, and $a_p : \mathbb{R}^2 \to \mathbb{R}$ are periodic functions with unit cell $Y = (0,1)^2$. For the above highly oscillating material coefficients, we anticipate the solutions to (205) or (206), denoted by $\left(w^{(\varepsilon)}, P^{(\varepsilon)}\right)$, are highly oscillating as well. Nevertheless we are only interested in the macroscopic behavior of $\left(w^{(\varepsilon)}, P^{(\varepsilon)}\right)$ whose governing equations can be found by a formal two-scale expansion:

$$\left(w^{(\varepsilon)}, P^{(\varepsilon)}\right) = \sum_{k=0}^{\infty} \varepsilon^k \left(w_k(x,y), P_k(x,y)\right), \tag{212}$$

where $y = x/\varepsilon$ is the ``fast'' variable for capturing the microscopic oscillations, $\left(w_k(x,y), P_k(x,y)\right)$ are y-periodic functions of period Y, and

$$\frac{1}{|Y|}\int_Y \left(w_k(x,y), P_k(x,y)\right) = \left(0,0\right) \qquad \forall k \geq 1. \tag{213}$$

Direct calculations show that

$$\begin{aligned}
\Delta w_k\left(x,y\right) &= \frac{1}{\varepsilon^2}\Delta_y w_k\left(x,y\right) + \frac{2}{\varepsilon}\nabla_y \cdot \nabla_x w_k\left(x,y\right) + \Delta_x w_k\left(x,y\right), \\
\nabla\nabla w_k\left(x,y\right) &= \frac{1}{\varepsilon^2}\nabla_y\nabla_y w_k\left(x,y\right) + \frac{2}{\varepsilon}\nabla_y\nabla_x w_k\left(x,y\right) + \nabla_x\nabla_x w_k\left(x,y\right).
\end{aligned} \tag{214}$$

where subscript x or y indicates that the derivatives are taken with respect to the first or the second variables of w_k. Then, $\Delta w^{(\varepsilon)}\left(x\right)$ and $\nabla\nabla w^{(\varepsilon)}\left(x\right)$ can be written as

$$\begin{aligned}
\Delta w^{(\varepsilon)}\left(x\right) &= \Delta_x w_0\left(x,y\right) + \frac{2}{\varepsilon}\nabla_y \cdot \nabla_x w_0\left(x,y\right) + \frac{1}{\varepsilon^2}\Delta_y w_0\left(x,y\right) + \varepsilon\Delta_x w_1\left(x,y\right) + \\
&\quad + 2\nabla_y \cdot \nabla_x w_1\left(x,y\right) + \frac{1}{\varepsilon}\Delta_y w_1\left(x,y\right) + \varepsilon^2\Delta_x w_2\left(x,y\right) + 2\varepsilon\nabla_y . \nabla_x w_2\left(x,y\right) + \Delta_y w_2\left(x,y\right), \\
\nabla\nabla w^{(\varepsilon)}\left(x\right) &= \nabla_x\nabla_x w_0\left(x,y\right) + \frac{2}{\varepsilon}\nabla_y\nabla_x w_0\left(x,y\right) + \frac{1}{\varepsilon^2}\nabla_y\nabla_y w_0\left(x,y\right) + \varepsilon\nabla_x\nabla_x w_1\left(x,y\right) + \\
&\quad +2\nabla_y\nabla_x w_1\left(x,y\right) + \frac{1}{\varepsilon}\nabla_y\nabla_y w_1\left(x,y\right) + \varepsilon^2\nabla_x\nabla_x w_2\left(x,y\right) + 2\varepsilon\nabla_y\nabla_x w_2\left(x,y\right) + \\
&\quad +\nabla_y\nabla_y w_2\left(x,y\right).
\end{aligned} \tag{215}$$

For simplicity in representing our calculations we assume that $\tilde{k}^{(\varepsilon)}\left(x\right) = k_b^{2(\varepsilon)}\left(x\right) - \frac{\left(f^{(\varepsilon)}\left(x\right)\right)^2}{a^{(\varepsilon)}\left(x\right)}$ and $\tilde{k}^{(\varepsilon)}\left(x\right) = \tilde{k}_p\left(\frac{x}{\varepsilon}\right)$. Then, equation (206) can be rewritten as

$$\Delta\left[\tilde{k}_p(y)\Delta w^{(\varepsilon)}(x,y)\right]+\nabla\nabla\cdot\left(k_p^1(y)\nabla\nabla w^{(\varepsilon)}(x,y)\right)+\Delta\left(\frac{f(y)}{a(y)}E_z^0\right)-b_z=0. \qquad (216)$$

Inserting (211) into (215) provides that (215) becomes a series in ε. Identifying each coefficient of ε as an individual equation yields a cascade of equations (a series of the variable ε is zero for all value of ε if each coefficient is zero). The ε^{-4} equation is

$$\varepsilon^{-4}: \qquad \Delta_y\left[\tilde{k}_p(y)\Delta_y w_0(x,y)\right]+\nabla_y\nabla_y\cdot\left[k_p^1(y)\nabla_y\nabla_y w_0(x,y)\right]=0. \qquad (217)$$

which is nothing but the equation in unit cell Y with periodic boundary conditions. In this equation, y is the variable, and x behaves as a parameter. There exists a unique solution of this equation up to a constant (with respect to y). This implies that w_0 is a function which does not depend on y and

$$w_0 \equiv w_0(x). \qquad (218)$$

With $\Delta_y w_0(x)=\nabla_y w_0(x)=0$. Also ε^{-3} is obtained as

$$\Delta_y\left[\tilde{k}_p(y)\Delta_y w_1(x,y)\right]+\nabla_y\nabla_y\cdot\left[k_p^1(y)\nabla_y\nabla_y w_1(x,y)\right]=0, \qquad (219)$$

which similarly yields

$$w_1 \equiv w_1(x). \qquad (220)$$

Since $\frac{1}{|Y|}\int_Y w_1(x,y)dy=0$ in unit cell Y, it is concluded that

$$w_1 = w_1(x) = 0\,. \tag{221}$$

That is, the zeroth-order term in the two-scale expansion of $w^{(\varepsilon)}$ is independent of the fast variables y whereas the first-order term vanishes everywhere. Also, ε^{-2}, ε^{-1}, and ε^{0} terms can be expressed as

$$\begin{aligned}\varepsilon^{-2}: \quad & \Delta_y\left[\tilde{k}_p(y)\left(\Delta_x w_0(x) + \Delta_y w_2(x,y)\right) + \frac{f(y)}{a(y)}E_z^0\right] + \\ & + \nabla_y\nabla_y\cdot\left[k_p^1(y)\left(\nabla_x\nabla_x w_0(x) + \nabla_y\nabla_y w_2(x,y)\right)\right] = 0,\end{aligned} \tag{222}$$

$$\begin{aligned}\varepsilon^{-1}: \quad & \nabla_y\cdot\nabla_x\left[\tilde{k}_p(y)\Delta_x w_0(x,y)\right] + \Delta_y\left[\tilde{k}_p(y)\nabla_y\cdot\nabla_x w_2(x,y)\right] + \\ & + \nabla_y\cdot\nabla_x\left[\tilde{k}_p(y)\Delta_y w_2(x,y)\right] + \nabla_y\nabla_x\cdot\left[k_p^1(y)\nabla_x\nabla_x w_0(x,y)\right] + \\ & + \nabla_y\nabla_y\cdot\left[k_p^1(y)\nabla_x\nabla_y w_2(x,y)\right] + \nabla_y\nabla_x\cdot\left[k_p^1(y)\nabla_y\nabla_y w_2(x,y)\right] = 0,\end{aligned} \tag{223}$$

$$\begin{aligned}\varepsilon^{0}: \quad & \Delta_x\left[\tilde{k}_p(y)\Delta_x w_0(x,y)\right] + \Delta_y\left[\tilde{k}_p(y)\Delta_x w_2(x,y)\right] + \Delta_x\left[\tilde{k}_p(y)\Delta_y w_2(x,y)\right] \\ & + 4\nabla_y\cdot\nabla_x\left[\tilde{k}_p(y)\nabla_y.\nabla_x w_2(x,y)\right] + \nabla_x\nabla_x\cdot\left[k_p^1(y)\nabla_x\nabla_x w_0(x,y)\right] + \\ & + \nabla_y\nabla_y\cdot\left[k_p^1(y)\nabla_x\nabla_x w_2(x,y)\right] + 4\nabla_y\nabla_x\cdot\left[k_p^1(y)\nabla_y\nabla_x w_2(x,y)\right] + \\ & + \nabla_x\nabla_x\cdot\left[k_p^1(y)\nabla_y\nabla_y w_2(x,y)\right] = b_z.\end{aligned} \tag{224}$$

Inserting (211) into (197) and recalling the identity that for small enough ε,

$$\int_\Omega f(x, x/\varepsilon)\,dx = \frac{1}{|Y|}\int_\Omega\int_Y f(x,y)dydx + O(\varepsilon), \tag{225}$$

we find that in terms of w_0, w_2 and P_0, the total free energy is given by

$$F\left[w^{(\varepsilon)},P^{(\varepsilon)}\right]=F^{2S}\left[w_0,w_2,P_0\right]+O(\varepsilon) \tag{226}$$

where the leading order free energy functional in terms of two-scale states is given by

$$\begin{aligned}
&F^{2S}\left[w_0,w_2,P_0\right]=\\
&=\frac{1}{|Y|}\int_\Omega\int_Y\left(\begin{aligned}&\frac{1}{2}k_p^1(y)\left|\nabla_x\nabla_x w_0(x)+\nabla_y\nabla_y w_2(x,y)\right|^2+\frac{1}{2}k_p^2(y)\left(\Delta_x w_0(x)+\Delta_y w_2(x,y)\right)^2\\&+f_p(y)P_0(x,y)\left(\Delta_x w_0(x)+\Delta_y w_2(x,y)\right)+\frac{1}{2}a_p(y)\left(P_0(x,y)\right)^2\end{aligned}\right)dydx\\
&\quad-\frac{1}{|Y|}\int_\Omega\int_Y\left(P_0(x,y)E_z^0(x)+w_0(x)b_z(x)\right)dydx
\end{aligned} \tag{227}$$

Neglecting the higher order terms in (225), from the variational principle (201) we infer that the two-scale variational problem

$$\min_{w_0,w_2,P_0} F^{2S}\left[w_0,w_2,P_0\right], \tag{228}$$

determines the macroscopic behavior and microscopic states of the heterogeneous flexoelectric membrane. Let $\overline{P}_0(x)=\frac{1}{|Y|}\int_Y P_0(x,y)dy$, and for $\Delta w_0=\alpha_1$, $\overline{P}_0=\alpha_2$ and $\nabla\nabla w_0=\alpha_3$. We define the effective energy density and the coefficients $\left(k_b^1\right)^e$, $\left(k_b^2\right)^e$, f^e, a^e, A^1 and A^2 as such that for any $(\alpha_1,\alpha_2)\in\mathbb{R}^2$ and $\alpha_3\in\mathbb{R}^{2\times 2}$

$$\begin{aligned}
W^e(\alpha_1,\alpha_2,\alpha_3)&=\frac{1}{2}\left(k_b^2\right)^e\alpha_1^{\,2}+f^e\alpha_1\alpha_2+A^1\cdot\alpha_1\alpha_3+\frac{1}{2}a^e\alpha_2^{\,2}+A^2\cdot\alpha_2\alpha_3+\frac{1}{2}\left(k_b^1\right)^e|\alpha_3|^2\\
&=\min_{(w_2',P_0')\in A_p}\left\{\frac{1}{|Y|}\int_Y\left(\begin{aligned}&\frac{1}{2}k_p^2\left(\alpha_1+\Delta_y w_2'\right)^2+f_p\left(\alpha_2+P_0'\right)\left(\alpha_1+\Delta_y w_2'\right)+\frac{1}{2}a_p\left(\alpha_2+P_0'\right)^2+\\&+\frac{1}{2}k_p^1\left(\alpha_3+\nabla_y\nabla_y w_2'\right)\cdot\left(\alpha_3+\nabla_y\nabla_y w_2'\right)\end{aligned}\right)\right\}.
\end{aligned} \tag{229}$$

Where the admissible space for (w_2', P_0') is given by

$$A_p := \left\{ (w_2', P_0') : w \in W_{per}^{2,2}(Y), P \in L_{per}^2(Y) : \frac{1}{|Y|}\int_Y (w_2', P_0')\, dy = (0,0) \right\}. \tag{230}$$

Then direct calculations show that the two-scale variational problem (227) can be written as

$$\min_{w_0, w_2, P_0} F^{2S}[w_0, w_2, P_0] = \min_{(w_0, \bar{P}_0) \in A} \left\{ \int_\Omega W^e\left(\Delta w_0, \nabla\nabla w_0, \bar{P}_0\right) - \int_\Omega \left(w_0 b_z + \bar{P}_0 E_z^0\right) \right\}. \tag{231}$$

Comparing the variational problem on the right hand side of (230) with the original variational problem (201), we henceforth justify our definition of effective energy density and associated effective coefficients (or material properties) as (228).

We remark that (228) is reminiscence of classic variational definitions of the effective properties and it completely determines the effective coefficients $\left(k_b^1\right)^e$, $\left(k_b^2\right)^e$, f^e and a^e. If P_0' is the minimizer of the right hand side of (228), then any perturbation from P_0' will increase the energy. Considering perturbation $P_0' + \delta P_0''$, yields

$$\left\{\frac{1}{|Y|}\int_Y\left(\begin{array}{l}\frac{1}{2}k_p^2\left(\alpha_1+\Delta_y w_2'\right)^2+f_p\left(\alpha_2+P_0'+\delta P_0''\right)\left(\alpha_1+\Delta_y w_2'\right)+\\+\frac{1}{2}a_p\left(\alpha_2+P_0'+\delta P_0''\right)^2+\frac{1}{2}k_p^1\left(\alpha_3+\nabla_y\nabla_y w_2'\right)\cdot\left(\alpha_3+\nabla_y\nabla_y w_2'\right)\end{array}\right)-\lambda_2\frac{1}{|Y|}\int_Y\left(P_0'+\delta P_0''\right)\right\}\geq$$

$$\left\{\frac{1}{|Y|}\int_Y\left(\begin{array}{l}\frac{1}{2}k_p^2\left(\alpha_1+\Delta_y w_2'\right)^2+f_p\left(\alpha_2+P_0'\right)\left(\alpha_1+\Delta_y w_2'\right)+\\+\frac{1}{2}a_p\left(\alpha_2+P_0'\right)^2+\frac{1}{2}k_p^1\left(\alpha_3+\nabla_y\nabla_y w_2'\right)\cdot\left(\alpha_3+\nabla_y\nabla_y w_2'\right)\end{array}\right)-\lambda_2\frac{1}{|Y|}\int_Y\left(P_0'\right)\right\}. \tag{232}$$

This can be simplified to

$$\delta\frac{1}{|Y|}\int_Y\left[f_p\left(P_0''\right)\left(\alpha_1+\Delta_y w_2'\right)+a_p P_0''\left(\alpha_2+P_0'\right)-\lambda_2 P_0''\right]+\delta^2\frac{1}{|Y|}\int_Y\frac{a_p}{2}\left(P_0''\right)^2\geq 0. \tag{233}$$

Ignoring δ^2 and considering the fact that δ can be positive or negative we conclude

$$\frac{1}{|Y|}\int_Y\left[f_p\left(\alpha_1+\Delta_y w_2'\right)+a_p\left(\alpha_2+P_0'\right)-\lambda_2\right]\left(P_0''\right)=0 \tag{234}$$

Similarly, if w_2' is the minimizer of the right hand side of (228), then perturbation $w_2'+\delta w_2''$ yields

$$\frac{1}{|Y|}\int_Y\left(\begin{array}{l}\frac{1}{2}k_p^2\left(\alpha_1+\Delta_y\left(w_2'+\delta w_2''\right)\right)^2+f_p\left(\alpha_2+P_0'\right)\left(\alpha_1+\Delta_y\left(w_2'+\delta w_2''\right)\right)+\\+\frac{1}{2}a_p\left(\alpha_2+P_0'\right)^2+\frac{1}{2}k_p^1\left(\alpha_3+\nabla_y\nabla_y\left(w_2'+\delta w_2''\right)\right)\cdot\left(\alpha_3+\nabla_y\nabla_y\left(w_2'+\delta w_2''\right)\right)\end{array}\right)-$$

$$-\lambda_3\frac{1}{|Y|}\int_Y\left(w_2'+\delta w_2''\right)\geq \tag{235}$$

$$\left\{\frac{1}{|Y|}\int_Y\left(\begin{array}{l}\frac{1}{2}k_p^2\left(\alpha_1+\Delta_y w_2'\right)^2+f_p\left(\alpha_2+P_0'\right)\left(\alpha_1+\Delta_y w_2'\right)+\\+\frac{1}{2}a_p\left(\alpha_2+P_0'\right)^2+\frac{1}{2}k_p^1\left(\alpha_3+\nabla_y\nabla_y w_2'\right)\cdot\left(\alpha_3+\nabla_y\nabla_y w_2'\right)\end{array}\right)-\lambda_3\frac{1}{|Y|}\int_Y\left(w_2'\right)\right\}$$

and consequently

$$\frac{1}{|Y|}\int_Y\left(\left[k_p^2\left(\alpha_1+\Delta_y w_2'\right)+f_p\left(\alpha_2+P_0'\right)\right]\Delta_y w_2''+k_p^1\left(\alpha_3+\nabla_y\nabla_y w_2'\right).\nabla_y\nabla_y w_2''\right)-\lambda_3\frac{1}{|Y|}\int_Y w_2''=0. \tag{236}$$

Using integration by parts (44) is converted to

$$\begin{aligned}&\frac{1}{|Y|}\int_Y\nabla_y\cdot\left[\left[k_p^2\left(\alpha_1+\Delta_y w_2'\right)+f_p\left(\alpha_2+P_0'\right)\right]\nabla_y w_2''\right]-\frac{1}{|Y|}\int_Y\nabla_y\cdot\left[\nabla_y\left(k_p^2\left(\alpha_1+\Delta_y w_2'\right)+f_p\left(\alpha_2+P_0'\right)\right)w_2''\right]\\&\quad+\frac{1}{|Y|}\int_Y\Delta_y\left[k_p^2\left(\alpha_1+\Delta_y w_2'\right)+f_p\left(\alpha_2+P_0'\right)\right]w_2''+\frac{1}{|Y|}\int_Y\nabla_y\cdot\left[k_p^1\left(\alpha_3+\nabla_y\nabla_y w_2'\right)\cdot\nabla_y w_2''\right]-\\&\quad-\frac{1}{|Y|}\int_Y\nabla_y\left[\nabla_y\cdot\left[k_p^1\left(\alpha_3+\nabla_y\nabla_y w_2'\right)\right]w_2''\right]+\frac{1}{|Y|}\int_Y\nabla_y\nabla_y\cdot\left[k_p^1\left(\alpha_3+\nabla_y\nabla_y w_2'\right)\right]w_2''-\lambda_3\int_Y w_2''=0.\end{aligned} \tag{237}$$

By divergence theorem, the first, second, fourth and fifth integrals in this expression are reduced to boundary integrals and because of periodicity of the integrands, they must be set to zero. So

$$\frac{1}{|Y|}\int_Y\left\{\Delta_y\left[k_p^2\left(\alpha_1+\Delta_y w_2'\right)+f_p\left(\alpha_2+P_0'\right)\right]+\nabla_y\nabla_y\cdot\left[k_p^1\left(\alpha_3+\nabla_y\nabla_y w_2'\right)\right]-\lambda_3\right\}w_2''=0. \tag{238}$$

To this end, we notice that for every value of P_0'' and w_2'', equations (233) and (237) respectively provide the Euler-Lagrange equations associated with the variational problem (228) and are given by

$$\begin{cases}\Delta_y\left[k_p^2\left(\alpha_1+\Delta_y w_2'\right)+f_p\left(\alpha_2+P_0'\right)\right]+\nabla_y\nabla_y\cdot\left[k_p^1\left(\alpha_3+\nabla_y\nabla_y w_2'\right)\right]=\lambda_3 & \text{on Y,}\\ f_p\left(\alpha_1+\Delta_y w_2'\right)+a_p\left(\alpha_2+P_0'\right)=\lambda_2 & \text{on Y,}\end{cases} \tag{239}$$

where the constants or Lagrangian mulitipliers $\lambda_2\in\mathbb{R}$ and $\lambda_3\in\mathbb{R}$ arise from the constraint $\frac{1}{|Y|}\int_Y P_0'dy=0$ and $\frac{1}{|Y|}\int_Y w_2'dy=0$, respectively. By the second of (238) we have

$$\left(\alpha_2 + P_0'\right) = \frac{\lambda_2}{a_p} - \frac{f_p}{a_p}\left(\alpha_1 + \Delta_y w_2'\right), \tag{240}$$

and hence

$$\lambda_2 \frac{1}{|Y|}\int_Y \frac{1}{a_p} = \alpha_2 + \alpha_1 \frac{1}{|Y|}\int_Y \frac{f_p}{a_p} + \frac{1}{|Y|}\int_Y \frac{f_p}{a_p}\Delta_y w_2' . \tag{241}$$

By (238-b) we eliminate $f_p\left(\alpha_2 + P_0'\right)$ in (238-a) and obtain

$$\Delta_y\left[\tilde{k}_p\left(\alpha_1 + \Delta_y w_2'\right) + \frac{f_p}{a_p}\lambda_2\right] + \nabla_y\nabla_y \cdot \left[k_p^1\left(\alpha_3 + \nabla_y\nabla_y w_2'\right)\right] = \lambda_3 \qquad \text{on Y}, \tag{242}$$

where

$$\tilde{k}_p = k_p^2 - \frac{{f_p}^2}{a_p} . \tag{243}$$

Periodicity of the two terms in (241) results that λ_3 is zero. As a conclusion we mention that in order to find the effective material properties we need to solve

$$\Delta_y\left[\tilde{k}_p\left(\alpha_1 + \Delta_y w_2'\right) + \frac{f_p}{a_p}\lambda_2\right] + \nabla_y\nabla_y \cdot \left[k_p^1\left(\alpha_3 + \nabla_y\nabla_y w_2'\right)\right] = 0 \qquad \text{on Y}, \tag{244}$$

which is dependent on the shape and size of the inhomogeneity.

6.4 Homogenization of heterogeneous fluid membranes

For the particular case of fluid membranes that can be used to approximate biological membranes, k_b^1 approaches zero. Therefore, the effective energy density can be defined as

$$
\begin{aligned}
W^e(\alpha_1,\alpha_2) &= \frac{1}{2}\left(k_b^2\right)^e \alpha_1{}^2 + f^e\alpha_1\alpha_2 + \frac{1}{2}a^e\alpha_2{}^2 \\
&= \min_{(w_2',P_0')\in A_p}\left\{\frac{1}{|Y|}\int_Y\left(\frac{1}{2}k_p^2\left(\alpha_1+\Delta_y w_2'\right)^2 + f_p\left(\alpha_2+P_0'\right)\left(\alpha_1+\Delta_y w_2'\right)+\frac{1}{2}a_p\left(\alpha_2+P_0'\right)^2\right)\right\},
\end{aligned}
\tag{245}
$$

and consequently the Euler-Lagrange equations in the unit cell can be written as

$$
\begin{cases}
\Delta_y\left[k_p^2\left(\alpha_1+\Delta_y w_2'\right)+f_p\left(\alpha_2+P_0'\right)\right]=\lambda_3 & \text{on Y,} \\
f_p\left(\alpha_1+\Delta_y w_2'\right)+a_p\left(\alpha_2+P_0'\right)=\lambda_2 & \text{on Y,}
\end{cases}
\tag{246}
$$

where the constants or Lagrangian mulitipliers $\lambda_2 \in \mathbb{R}$ and $\lambda_3 \in \mathbb{R}$ arise from the constraint $\frac{1}{|Y|}\int_Y P_0' dy = 0$ and $\frac{1}{|Y|}\int_Y w_2' dy = 0$, respectively. By the second of (245) we have

$$
\left(\alpha_2+P_0'\right)=\frac{\lambda_2}{a_p}-\frac{f_p}{a_p}\left(\alpha_1+\Delta_y w_2'\right),
\tag{247}
$$

and hence

$$
\lambda_2\frac{1}{|Y|}\int_Y\frac{1}{a_p}=\alpha_2+\alpha_1\frac{1}{|Y|}\int_Y\frac{f_p}{a_p}+\frac{1}{|Y|}\int_Y\frac{f_p}{a_p}\Delta_y w_2'.
\tag{248}
$$

By (245-b) we eliminate $f_p\left(\alpha_2+P_0'\right)$ in (245-a) and obtain

$$
\Delta_y\left[\tilde{k}_p\left(\alpha_1+\Delta_y w_2'\right)+\frac{f_p}{a_p}\lambda_2\right]=\lambda_3 \qquad \text{on Y,}
\tag{249}
$$

with

$$\tilde{k}_p = k_p^2 - \frac{f_p{}^2}{a_p}. \tag{250}$$

A solution to the above problem is given by

$$\tilde{k}_p\left(\alpha_1 + \Delta_y w_2'\right) + \frac{f_p}{a_p}\lambda_2 = \lambda_1 \qquad \text{on Y,} \tag{251}$$

where $\lambda_1 \in \mathbb{R}$ is a constant. Since $\frac{1}{|Y|}\int_Y \Delta_y w_2' = 0$, (250) gives

$$\alpha_1 = \lambda_1 \frac{1}{|Y|}\int_Y \frac{1}{\tilde{k}_p} - \lambda_2 \frac{1}{|Y|}\int_Y \frac{f_p}{\tilde{k}_p a_p} \tag{252}$$

and

$$\left(\alpha_1 + \Delta_y w_2'\right) = \frac{\lambda_1}{\tilde{k}_p} - \frac{f_p}{\tilde{k}_p a_p}\lambda_2. \tag{253}$$

Inserting (252) into (246) we obtain

$$\lambda_2 \frac{1}{|Y|}\int_Y \frac{1}{a_p} = \alpha_2 + \lambda_1 \frac{1}{|Y|}\int_Y \frac{f_p}{\tilde{k}_p a_p} - \lambda_2 \frac{1}{|Y|}\int_Y \frac{f_p{}^2}{\tilde{k}_p a_p{}^2}. \tag{254}$$

It will be convenient to define a symmetric 2x2 matrix

$$S = \begin{bmatrix} s_{11} & s_{12} \\ s_{21} & s_{22} \end{bmatrix},$$
$$s_{11} = \frac{1}{|Y|}\int_Y \frac{1}{\tilde{k}_p}, \qquad s_{12} = -\frac{1}{|Y|}\int_Y \frac{f_p}{\tilde{k}_p a_p}, \qquad s_{22} = \frac{1}{|Y|}\int_Y \left(\frac{1}{a_p} + \frac{f_p{}^2}{\tilde{k}_p a_p{}^2}\right). \tag{255}$$

Then equations (231) and (233) can be rewritten as

$$S\lambda = \alpha, \quad \lambda = \begin{bmatrix} \lambda_1 \\ \lambda_2 \end{bmatrix}, \quad \alpha = \begin{bmatrix} \alpha_1 \\ \alpha_2 \end{bmatrix}. \tag{256}$$

Further, inserting (246) and then (252) into the right hand side of (244) we arrive at

$$W^e(\alpha_1, \alpha_2) = \frac{1}{2}\alpha . S^{-1}\alpha, \tag{257}$$

with

$$S^{-1} = \begin{bmatrix} \left(k_b^2\right)^e & f^e \\ f^e & a^e \end{bmatrix}. \tag{258}$$

To our knowledge, Equation (257) represents one of the few exact results in homogenization theory.

For the particular case of fluid membranes, the effective properties depend solely on the volume fractions and are independent of the specific microstructure.

6.5 Applications

Below we calculate the effective properties of two-phase flexoelectric membranes with microstructures of circular inclusions (Fig. 6-a) and simple laminates (Fig. 6-b). These solutions give useful guides on designing flexoelectric membranes for variety of applications.

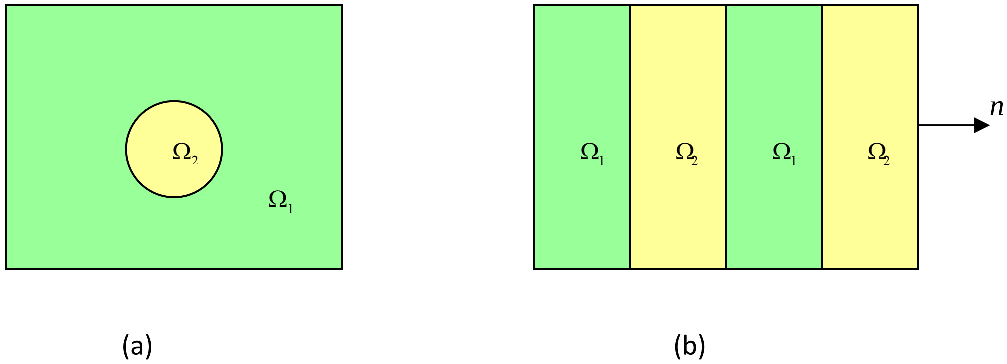

Figure 6.1: A representative volume element with two phases (a) macroscopically isotropic membrane (circular inhomogeneity) and (b) laminate membrane.

6.5.1 Circular inhomogeneity in flexoelecric membranes

Consider a flexoelectric membrane with a dilute concentration of inhomogeneities. We model this membrane by a single inclusion in a matrix and the unit cell problem is given by

$$\begin{cases} \Delta_y\left[\tilde{k}_p\left(\alpha_1+\Delta_y w_2'\right)+\dfrac{f_p}{a_p}\lambda_2\right]+\nabla_y\nabla_y\cdot\left[k_p^1\left(\alpha_3+\nabla_y\nabla_y w_2'\right)\right]=0 & \text{on Y} \\ \text{Periodic B.C.} \quad \text{in } \partial\text{Y} \end{cases} \tag{259}$$

In the dilute limit, the interactions between inhomogeneities are negligible and we replace the unit cell Y by $\mathbb{R}^2$ and periodic boundary condition by decay condition

$$\left|\Delta w_2'(x)\right| \to 0 \quad \text{as} \quad x \to +\infty. \tag{260}$$

To solve (259) explicitly, we now derive the interfacial conditions on $\partial\Omega$.

6.5.1.1 Interfacial conditions

1. Continuity of deflection at the interface yields

$$w_2'\big|_{\partial\Omega^-} = w_2'\big|_{\partial\Omega^+} . \tag{261}$$

2. $\nabla w_2'$ must be continuous as well across the interface, otherwise $\nabla\nabla w_2'$ would be in the form of δ function which results the energy being rendered infinite,

$$\nabla w_2'\big|_{\partial\Omega^-} = \nabla w_2'\big|_{\partial\Omega^+} \tag{262}$$

3. In deriving interface jump conditions, we do the standard first variation on the variational form of the total energy in one unit cell (229),

$$\begin{aligned} W^e(\alpha_1,\alpha_2,\alpha_3) &= \min_{w\in A_p}\left\{\frac{1}{|Y|}\int_Y \left(\begin{array}{l} \frac{1}{2}k_p^2\left(\alpha_1+\Delta_y w_2'\right)^2 + f_p\left(\alpha_2+P_0'\right)\left(\alpha_1+\Delta_y w_2'\right)+\frac{1}{2}a_p\left(\alpha_2+P_0'\right)^2 + \\ +\frac{1}{2}k_p^1\left|\alpha_3+\nabla\nabla w_2'\right|^2 \end{array}\right)\right\} = \\ &\min_{w\in A_p}\left\{\begin{array}{l} \int_{\Omega_1}\left(\frac{1}{2}k_M^2\left(\alpha_1+\Delta_y w_2'\right)^2 + f_M\left(\alpha_2+P_0'\right)\left(\alpha_1+\Delta_y w_2'\right)+\frac{1}{2}a_M\left(\alpha_2+P_0'\right)^2+\frac{1}{2}k_M^1\left|\alpha_3+\nabla_y\nabla_y w_2'\right|^2\right) \\ +\int_{\Omega_2}\left(\frac{1}{2}k_I^2\left(\alpha_1+\Delta_y w_2'\right)^2 + f_I\left(\alpha_2+P_0'\right)\left(\alpha_1+\Delta_y w_2'\right)+\frac{1}{2}a_I\left(\alpha_2+P_0'\right)^2+\frac{1}{2}k_I^1\left|\alpha_3+\nabla_y\nabla_y w_2'\right|^2\right) \end{array}\right\}, \end{aligned} \tag{263}$$

where subscripts M and I are denoting the material properties associated with Ω_1 and Ω_2, respectively. Also for simplicity ∇_y is representing by ∇ in later calculations. After doing first variation in w_2' we have

$$\int_{\Omega_1}\Big(k_M^2\left[\left(\alpha_1+\Delta w_2'\right)\Delta\nu\right]+f_M\left(\alpha_2+P_0'\right)\Delta\nu+k_M^1\left[\left(\alpha_3+\nabla\nabla w_2'\right)\cdot\nabla\nabla\nu\right]\Big)+$$
$$+\int_{\Omega_2}\Big(k_I^2\left[\left(\alpha_1+\Delta w_2'\right)\Delta\nu\right]+f_I\left(\alpha_2+P_0'\right)\Delta\nu+k_I^1\left[\left(\alpha_3+\nabla\nabla w_2'\right)\cdot\nabla\nabla\nu\right]\Big)=0, \quad (264)$$

or in index form

$$\int_{\Omega_1}\Big(k_M^2\left[\left(\alpha_1+w'_{2,ii}\right)\nu_{,jj}\right]+\left[f_M\left(\alpha_2+P_0'\right)\nu_{,jj}\right]+k_M^1\left[\left(\alpha_{3ij}+w'_{2,ij}\right)\nu_{,ij}\right]\Big)+$$
$$+\int_{\Omega_2}\Big(k_I^2\left[\left(\alpha_1+w'_{2,ii}\right)\nu_{,jj}\right]+\left[f_I\left(\alpha_2+P_0'\right)\nu_{,jj}\right]+k_I^1\left[\left(\alpha_{3ij}+w'_{2,ij}\right)\nu_{,ij}\right]\Big)=0. \quad (265)$$

Applying integration by part gives us

$$\int_{\Omega_1}k_M^2\left[\left(\left(\alpha_1+w'_{2,kk}\right)\nu_{,j}\right)_{,j}-\left(\left(\alpha_1+w'_{2,kk}\right)_{,j}\nu_{,j}\right)\right]+\int_M f_M\left[\left(\left(\alpha_2+P_0'\right)\nu_{,j}\right)_{,j}-\left(\left(\alpha_2+P_0'\right)_{,j}\nu_{,j}\right)\right]$$
$$+\int_{\Omega_1}k_M^1\left[\left(\left(\alpha_{3ij}+w'_{2,ij}\right)\nu_{,i}\right)_{,j}-\left(\left(\alpha_{3ij}+w'_{2,ij}\right)_{,j}\nu_{,i}\right)\right]=$$
$$\int_{\Omega_2}k_I^2\left[\left(\left(\alpha_1+w'_{2,kk}\right)\nu_{,j}\right)_{,j}-\left(\left(\alpha_1+w'_{2,kk}\right)_{,j}\nu_{,j}\right)\right]+\int_I f_I\left[\left(\left(\alpha_2+P_0'\right)\nu_{,j}\right)_{,j}-\left(\left(\alpha_2+P_0'\right)_{,j}\nu_{,j}\right)\right]+ \quad (266)$$
$$\int_{\Omega_2}k_I^1\left[\left(\left(\alpha_{3ij}+w'_{2,ij}\right)\nu_{,i}\right)_{,j}-\left(\left(\alpha_{3ij}+w'_{2,ij}\right)_{,j}\nu_{,i}\right)\right]$$

and using divergence theorem leads to

$$\int_{\delta\Omega_1}k_M^2\left[\left(\left(\alpha_1+w'_{2,kk}\right)\nu_{,j}\right)n_j\right]-\int_{\delta\Omega_1}k_M^2\left[\left(\alpha_1+w'_{2,kk}\right)_{,j}\nu n_j\right]+\int_{\Omega_1}k_M^2\left[\left(\alpha_1+w'_{2,kk}\right)_{,jj}\nu\right]+$$
$$\int_{\delta\Omega_1}f_M\left[\left(\left(\alpha_2+P_0'\right)\nu_{,j}\right)n_j\right]-\int_{\delta\Omega_1}f_M\left[\left(\alpha_2+P_0'\right)_{,j}\nu n_j\right]+\int_{\Omega_1}f_M\left[\left(\alpha_2+P_0'\right)_{,jj}\nu\right]+$$
$$+\int_{\delta\Omega_1}k_M^1\left[\left(\alpha_{3ij}+w'_{2,ij}\right)\nu_{,i}n_j\right]-\int_{\delta\Omega_1}k_M^1\left[\left(\alpha_{3ij}+w'_{2,ij}\right)_{,j}\nu n_i\right]+\int_{\Omega_1}k_M^1\left[\left(\alpha_{3ij}+w'_{2,ij}\right)_{,ij}\nu\right]=$$
$$=\int_{\delta\Omega_2}k_I^2\left[\left(\left(\alpha_1+w'_{2,kk}\right)\nu_{,j}\right)n_j\right]-\int_{\delta\Omega_2}k_I^2\left[\left(\alpha_1+w'_{2,kk}\right)_{,j}\nu n_j\right]+\int_{\Omega_2}k_I^2\left[\left(\alpha_1+w'_{2,kk}\right)_{,jj}\nu\right]+ \quad (267)$$
$$\int_{\delta\Omega_2}f_I\left[\left(\left(\alpha_2+P_0'\right)\nu_{,j}\right)n_j\right]-\int_{\delta\Omega_2}f_I\left[\left(\alpha_2+P_0'\right)_{,j}\nu n_j\right]+\int_{\Omega_2}f_I\left[\left(\alpha_2+P_0'\right)_{,jj}\nu\right]+$$
$$+\int_{\delta\Omega_2}k_I^1\left[\left(\alpha_{3ij}+w'_{2,ij}\right)\nu_{,i}n_j\right]-\int_{\delta\Omega_2}k_I^1\left[\left(\alpha_{3ij}+w'_{2,ij}\right)_{,j}\nu n_i\right]+\int_{\Omega_2}k_I^1\left[\left(\alpha_{3ij}+w'_{2,ij}\right)_{,ij}\nu\right].$$

Therefore at the common interface denoted by $\delta\Omega=\delta\Omega_1=\delta\Omega_2$

$$\int_{\partial\Omega} k_M^2\left[\left(\left(\alpha_1\delta_{ij}+w'_{2,kk}\delta_{ij}\right)\nu_{,i}\right)n_j\right]+\int_{\partial\Omega} f_M\left[\left(\left(\alpha_2\delta_{ij}+P'_0\delta_{ij}\right)\nu_{,i}\right)n_j\right]+\int_{\partial\Omega} k_M^1\left[\left(\alpha_{3ij}+w'_{2,ij}\right)\nu_{,i}n_j\right]=$$
$$\int_{\partial\Omega} k_I^2\left[\left(\left(\alpha_1\delta_{ij}+w'_{2,kk}\delta_{ij}\right)\nu_{,i}\right)n_j\right]+\int_{\partial\Omega} f_I\left[\left(\left(\alpha_2\delta_{ij}+P'_0\delta_{ij}\right)\nu_{,i}\right)n_j\right]+\int_{\partial\Omega} k_I^1\left[\left(\alpha_{3ij}+w'_{2,ij}\right)\nu_{,i}n_j\right] \quad (268)$$

and

$$\int_{\partial\Omega} k_M^2\left[\left(\alpha_1+w'_{2,kk}\right)_{,i}\nu n_i\right]+\int_{\partial\Omega} f_M\left[\left(\alpha_2+P'_0\right)_{,i}\nu n_i\right]+\int_{\partial\Omega} k_M^1\left[\left(\alpha_{3ij}+w'_{2,ij}\right)_{,j}\nu n_i\right]=$$
$$\int_{\partial\Omega} k_I^2\left[\left(\alpha_1+w'_{2,kk}\right)_{,i}\nu n_i\right]+\int_{\partial\Omega} f_I\left[\left(\alpha_2+P'_0\right)_{,i}\nu n_i\right]+\int_{\partial\Omega} k_I^1\left[\left(\alpha_{3ij}+w'_{2,ij}\right)_{,j}\nu n_i\right]. \quad (269)$$

Since this should be valid for any $\nu_{,i}$ and ν, we conclude that at the interface

$$\left[\left(k_M^2\left(\alpha_1+\Delta w'_2\right)I+f_M\left(\alpha_2+P'_0\right)I+k_M^1\left(\alpha_3+\nabla\nabla w'_2\right)\right)n\right]_{\partial\Omega^-}=$$
$$\left[\left(k_I^2\left(\alpha_1+\Delta w'_2\right)I+f_I\left(\alpha_2+P'_0\right)I+k_I^1\left(\alpha_3+\nabla\nabla w'_2\right)\right)n\right]_{\partial\Omega^+}, \quad (270)$$

and

$$\left[\left(\left(k_M^2+k_M^1\right)\nabla\Delta w'_2+f_M\nabla P'_0\right)\cdot n\right]_{\partial\Omega^-}=\left[\left(\left(k_I^2+k_I^1\right)\nabla\Delta w'_2+f_I\nabla P'_0\right)\cdot n\right]_{\partial\Omega^+}. \quad (271)$$

Now we use

$$\left(\alpha_2+P'_0\right)=\frac{\lambda_2}{a_p}-\frac{f_p}{a_p}\left(\alpha_1+\Delta_y w'_2\right), \quad (272)$$

then (270) and (271) will be converted to

$$\left[\left(\tilde{k}_M\left(\alpha_1+\Delta w'_2\right)I+\left(\frac{f_M\lambda_2}{a_M}\right)I+k_M^1\left(\alpha_3+\nabla\nabla w'_2\right)\right)n\right]_{\partial\Omega^-}=$$
$$\left[\left(\tilde{k}_I\left(\alpha_1+\Delta w'_2\right)I+\left(\frac{f_I\lambda_2}{a_I}\right)I+k_I^1\left(\alpha_3+\nabla\nabla w'_2\right)\right)n\right]_{\partial\Omega^+}, \quad (273)$$

and

$$\left[\left(\left(\tilde{k}_M + k_M^1 \right) \nabla \Delta w_2' \right) \cdot n \right]_{\partial\Omega^-} = \left[\left(\left(\tilde{k}_I + k_I^1 \right) \nabla \Delta w_2' \right) \cdot n \right]_{\partial\Omega^+} . \tag{274}$$

6.5.1.2 Unit Cell Problem and Solution

Now we consider the problem to be axisymmetric. Then unit cell PDE (259) can be converted to the following ODE in polar coordinate.

$$\begin{gathered} \left(\tilde{k}_p + k_p^1 \right) r^3 \frac{d^4 w_2'}{dr^4} + 2\left(\tilde{k}_p + k_p^1 \right) r^2 \frac{d^3 w_2'}{dr^3} - \left(\tilde{k}_p + k_p^1 \right) r \frac{d^2 w_2'}{dr^2} + \left(\tilde{k}_p + k_p^1 \right) \frac{dw_2'}{dr} = 0 \\ r \in \left(0, R_0\right) \cup \left(R_0, \infty\right) \end{gathered} . \tag{275}$$

Here we assume that the material is macroscopically isotropic and we choose $\alpha_1 = tr\left(\alpha_3\right)$ and $\alpha_3 = \frac{\alpha_1}{2} I$. Thus, the general solution can be obtained as

$$\begin{aligned} w_2'\left(r\right) &= C_1 \ln r + C_2 r^2 + C_3 r^2 \ln r + C_4 \quad \text{for} \quad \mathrm{r} < R_0, \\ &= D_1 \ln r + D_2 r^2 + D_3 r^2 \ln r + D_4 \quad \text{for} \quad \mathrm{r} > R_0, \end{aligned} \tag{276}$$

where $C_1, C_2, C_3, C_4, D_1, D_2, D_3, D_4$ are constants to be determined from the boundary conditions.

To avoid singularity for w_2' and $\nabla w_2'$ at $r = 0$, we set $C_1 = C_3 = 0$. In the total energy expression (229) for this particular problem, the integration is over a unit cell with infinite boundary ($\mathrm{r} \to \infty$). So the second derivative of w_2' cannot be a constant. Therefore, D_2 and D_3 must be zero. So (275) can be rewritten as

$$\begin{aligned} w_2'\left(r\right) &= C_2 r^2 + C_4 \quad \text{for} \quad \mathrm{r} < R_0 \\ &= D_1 \ln r + D_4 \quad \text{for} \quad \mathrm{r} > R_0. \end{aligned} \tag{277}$$

The rest of the constants can be obtained by the boundary conditions (260), (261), (271) and (273). These boundary conditions in polar coordinates are expressed as

$$w_2'^{-}\Big|_{r=R_0} = w_2'^{+}\Big|_{r=R_0}, \tag{278}$$

$$\nabla w_2'^{-}\Big|_{r=R_0} = \nabla w_2'^{+}\Big|_{r=R_0}, \tag{279}$$

$$\begin{aligned}&\left[\left(\tilde{k}_M + k_M^1\right)\left(\frac{\alpha_1}{2} + \frac{\partial^2 w_2'}{\partial r^2}\right) + \tilde{k}_M\left(\frac{\alpha_1}{2} + \frac{1}{r}\frac{\partial w_2'}{\partial r}\right) + \left(\frac{f_M\lambda_2}{a_M}\right)\right]_{r=R_0}^{-} = \\ &= \left[\left(\tilde{k}_I + k_I^1\right)\left(\frac{\alpha_1}{2} + \frac{\partial^2 w_2'}{\partial r^2}\right) + \tilde{k}_I\left(\frac{\alpha_1}{2} + \frac{1}{r}\frac{\partial w_2'}{\partial r}\right) + \left(\frac{f_I\lambda_2}{a_I}\right)\right]_{r=R_0}^{+},\end{aligned} \tag{280}$$

and

$$\left[\left(\tilde{k}_M + k_M^1\right)\left(\frac{\partial^3 w_2'}{\partial r^3} + \frac{1}{r}\frac{\partial^2 w_2'}{\partial r^2} - \frac{1}{r^2}\frac{\partial w_2'}{\partial r}\right)\right]_{r=R_0}^{-} = \left[\left(\tilde{k}_I + k_I^1\right)\left(\frac{\partial^3 w_2'}{\partial r^3} + \frac{1}{r}\frac{\partial^2 w_2'}{\partial r^2} - \frac{1}{r^2}\frac{\partial w_2'}{\partial r}\right)\right]_{r=R_0}^{+}. \tag{281}$$

From these boundary conditions, we have

$$\begin{aligned}C_2 &= -\frac{\alpha_1\left(a_I a_M k_I^1 - a_I a_M k_M^1 + 2a_I a_M \tilde{k}_I - 2a_I a_M \tilde{k}_M\right) + 2a_M f_I\lambda_2 - 2a_I f_M\lambda_2}{4a_I a_M\left(k_I^1 + k_M^1 + 2\tilde{k}_I\right)}, \\ D_1 &= -\frac{\left[\alpha_1\left(a_I a_M k_I^1 - a_I a_M k_M^1 + 2a_I a_M \tilde{k}_I - 2a_I a_M \tilde{k}_M\right) + 2a_M f_I\lambda_2 - 2a_I f_M\lambda_2\right]R_0^{\,2}}{2a_I a_M\left(k_I^1 + k_M^1 + 2\tilde{k}_I\right)}, \\ D_4 &= C_4 - \frac{\left[\alpha_1\begin{pmatrix}a_I a_M k_I^1 - a_I a_M k_M^1 + \\ 2a_I a_M \tilde{k}_I - 2a_I a_M \tilde{k}_M\end{pmatrix} + 2a_M f_I\lambda_2 - 2a_I f_M\lambda_2\right]\left(R_0^{\,2} - 2R_0^{\,2}\ln R_0\right)}{4a_I a_M\left(k_I^1 + k_M^1 + 2\tilde{k}_I\right)}.\end{aligned} \tag{282}$$

and the value of D_4 is unimportant in calculating the energy. The polarization can also be calculated by (240). Therefore we have

$$\left(\alpha_2+P_0'\right)=\frac{\lambda_2}{a_p}-\frac{f_p}{a_p}\left(\alpha_1+\left(w_2'\right)''+\frac{1}{r}\left(w_2'\right)'\right)=$$
$$=\begin{cases}\dfrac{\lambda_2}{a_I}-\dfrac{f_I}{a_I}\left(\alpha_1+4C_2\right) & \text{for } \mathrm{r}<R_0\\ \dfrac{\lambda_2}{a_M}-\dfrac{f_M}{a_M}\left(\alpha_1\right) & \text{for } \mathrm{r}>R_0.\end{cases} \tag{283}$$

Now the constant λ_2 can be calculated by setting $\frac{1}{|Y|}\int_Y P_0'dy=0$. So

$$\begin{aligned}\frac{1}{|Y|}\int_Y P_0'dy&=-\alpha_2+(1-\theta)\left(\frac{\lambda_2}{a_M}-\frac{f_M}{a_M}\alpha_1\right)+\theta\frac{\lambda_2}{a_I}-\theta\frac{f_I}{a_I}\alpha_1-\theta\left(\frac{f_I}{a_I}\right)4C_2\\&=\lambda_2\left[\frac{(1-\theta)}{a_M}+\frac{\theta}{a_I}\right]-\alpha_2-\left[\frac{(1-\theta)\,f_M}{a_M}+\frac{\theta f_I}{a_I}\right]\alpha_1-4\theta\left(\frac{f_I}{a_I}\right)C_2=0\end{aligned} \tag{284}$$

And therefore

$$\lambda_2=\left(\frac{1-\theta}{a_M}+\frac{\theta}{a_I}\right)^{-1}\left[\alpha_2+\left(\frac{(1-\theta)\,f_M}{a_M}+\frac{\theta f_I}{a_I}\right)\alpha_1+4\theta\left(\frac{f_I}{a_I}\right)C_2\right]. \tag{285}$$

As mentioned earlier, the effective energy density can be obtained as

$$\begin{aligned}W^e\left(\alpha_1,\alpha_2,\alpha_3\right)&=\frac{1}{2}\left(k_b^2\right)^e\alpha_1{}^2+f^e\alpha_1\alpha_2+A^1\cdot\alpha_1\alpha_3+\frac{1}{2}a^e\alpha_2{}^2+A^2\cdot\alpha_2\alpha_3+\frac{1}{2}k_b^{1e}\left|\alpha_3\right|^2\\&=\left\{\frac{1}{|Y|}\int_Y\left(\begin{array}{l}\frac{1}{2}k_p^2\left(\alpha_1+\Delta w_2'\right)^2+f_p\left(\alpha_2+P_0'\right)\left(\alpha_1+\Delta w_2'\right)+\frac{1}{2}a_p\left(\alpha_2+P_0'\right)^2\\+\frac{1}{2}k_p^1\left(\alpha_3+\nabla\nabla w_2'\right).\left(\alpha_3+\nabla\nabla w_2'\right)\end{array}\right)\right\}.\end{aligned} \tag{286}$$

By assuming $\alpha_3=\frac{\alpha_1}{2}I$ and $A^1=A^2=0$, we have

$$W^e(\alpha_1,\alpha_2)=\left\{\frac{1}{|Y|}\int_Y\left(\begin{array}{l}\frac{1}{2}k_p^2(\alpha_1+\Delta w_2')^2+f_p(\alpha_2+P_0')(\alpha_1+\Delta w_2')+\frac{1}{2}a_p(\alpha_2+P_0')^2\\+\frac{1}{2}k_p^1\left(\frac{\alpha_1}{2}I+\nabla\nabla w_2'\right)\cdot\left(\frac{\alpha_1}{2}I+\nabla\nabla w_2'\right)\end{array}\right)\right\}=$$

$$=\left\{\begin{array}{l}\frac{1}{2}\left((1-\theta)k_M^2+\theta k_I^2+\frac{1}{2}\left((1-\theta)k_M^1+\theta k_I^1\right)\right)(\alpha_1)^2+\left((1-\theta)f_M+\theta f_I\right)\alpha_1\alpha_2+\\ \frac{1}{2}\left((1-\theta)a_M+\theta a_I\right)(\alpha_2)^2+\frac{1}{2}(\alpha_1)\left(k_I^2-k_M^2\right)\theta\frac{1}{|\Omega|}\int_\Omega(\Delta w_2')+\left(-\theta f_M P_I'+\theta f_I P_I'\right)\alpha_1\\ +\left((f_I)P_I'\right)\theta\frac{1}{|\Omega|}\int_\Omega\Delta w_2'+(f_I-f_M)\theta\alpha_2\frac{1}{|\Omega|}\int_\Omega\Delta w_2'+\left(-a_M P_I'+a_I P_I'\right)\theta\alpha_2+\\ \frac{1}{2}\theta(a_I)(P')^2+\frac{1}{2}\left(\frac{\alpha_1}{2}\right)\left(k_I^1-k_M^1\right)\theta\frac{1}{|\Omega|}\int_\Omega(I.\nabla\nabla w_2')\end{array}\right\}, \tag{287}$$

Finally, the effective properties are obtained as

$$a^e=\frac{1}{\left(-2a_M f_I^2\theta+a_I\left(2f_I f_M\theta+\left(k_M^1+k_I^1+2\tilde{k}_I\right)\left(a_I(-1+\theta)-a_M\theta\right)\right)\right)^2}\times$$
$$\times a_I\left(\begin{array}{l}-4a_M^2 f_I^4\theta+2a_I a_M f_I^2\left(4f_I f_M+a_M\left(k_I^1+2k_I^2\right)\right)\theta+\\ +a_I^2\left(-4f_I^2 f_M^2-4a_M f_I f_M\left(k_I^1+2k_I^2\right)+a_M^2\left(k_M^1+k_I^1+2\tilde{k}_I\right)^2\right)\theta+\\ +a_I^3\left(-a_M\left(k_M^1+k_I^1+2\tilde{k}_I\right)^2(-1+\theta)+2f_M^2\left(k_I^1+2k_I^2\right)\theta\right)+2a_I\left(a_M f_I-a_I f_M\right)^2 k_M^1\theta^2\end{array}\right), \tag{288}$$

$$\left(k_b^2\right)^e+\frac{1}{2}\left(k_b^1\right)^e=$$
$$=\frac{A+(B+C)^2}{\left(2a_M^2\left(-2a_M f_I^2\theta+a_I\left(2f_I f_M\theta+\left(k_M^1+k_I^1+2\tilde{k}_I\right)\left(a_I(-1+\theta)-a_M\theta\right)\right)\right)^2\right)}, \tag{289}$$

$$
f^{e}=\frac{1}{\left(a_M\left(-2a_M f_I^{\,2}\theta+a_I\left(2f_I f_M\theta+\left(k_M^1+k_I^1+2\tilde{k}_I\right)\left(a_I\left(-1+\theta\right)-a_M\theta\right)\right)\right)^2\right)}\times
$$

$$
\times a_I\begin{pmatrix}
4a_M^{\,2}f_I^{\,3}\theta\left(f_I f_M\left(-1+\theta\right)+a_M\left(k_M^1+\tilde{k}_M\right)\theta\right)- \\
a_I^{\,3}f_M\left(-1+\theta\right)\begin{pmatrix}2f_M^{\,2}\left(k_I^1+2k_I^2\right)\theta+ \\ a_M\left(\left(k_M^1+k_I^1+2\tilde{k}_I\right)^2-\begin{pmatrix}\left(k_I^1\right)^2+k_M^1\left(k_M^1-4k_I^2\right)+4\tilde{k}_I\left(k_M^1+\tilde{k}_I\right)+ \\ k_I^1\left(4\tilde{k}_I-2\tilde{k}_M\right)-4k_I^2\tilde{k}_M\end{pmatrix}\theta\right)\end{pmatrix}+ \\
+a_I^{\,2}\theta\begin{pmatrix}4f_I^{\,2}f_M\left(f_M^{\,2}+a_M\left(k_M^1+\tilde{k}_M\right)\right)\left(-1+\theta\right)- \\ -2a_M f_I\left(-2f_M^{\,2}\left(k_I^1+2k_I^2\right)+a_M\left(k_M^1-2k_I^2+2\tilde{k}_I\right)\left(k_M^1+\tilde{k}_M\right)\right)\left(-1+\theta\right)+ \\ a_M^{\,2}f_M\left(\left(k_M^1+k_I^1+2\tilde{k}_I\right)^2-\begin{pmatrix}\left(k_I^1\right)^2+k_M^1\left(k_M^1-4k_I^2\right)+4\tilde{k}_I\left(k_M^1+\tilde{k}_I\right)+ \\ k_I^1\left(4\tilde{k}_I-2\tilde{k}_M\right)-4k_I^2\tilde{k}_M\end{pmatrix}\theta\right)\end{pmatrix}+ \\
+2a_I a_M f_I\theta\begin{pmatrix}-2f_I^{\,2}\left(2f_M^{\,2}+a_M\left(k_M^1+\tilde{k}_M\right)\right)\left(-1+\theta\right)+a_M^{\,2}\left(k_M^1-2k_I^2+2\tilde{k}_I\right)\left(k_M^1+\tilde{k}_M\right)\theta+ \\ a_M f_I f_M\left(k_I^1+2k_I^2-\left(k_I^1+2\left(k_M^1+k_I^2+\tilde{k}_M\right)\right)\theta\right)\end{pmatrix}+ \\
\left(a_M f_I-a_I f_M\right)k_M^1\theta\begin{pmatrix}a_I^{\,2}\left(2f_M^{\,2}+a_M\left(-k_I^1+k_M^1-2\tilde{k}_I+2\tilde{k}_M\right)\right)\left(-1+\theta\right)+2a_M^{\,2}f_I^{\,2}\theta+ \\ a_I a_M\left(f_I f_M\left(2-4\theta\right)-a_M\left(-k_I^1+k_M^1-2\tilde{k}_I+2\tilde{k}_M\right)\theta\right)\end{pmatrix}^2
\end{pmatrix}, \qquad (290)
$$

where

$$
A=\left\{\begin{matrix}-4a_M^{\,3}f_I^{\,4}\left(-2f_M^{\,2}+a_M\left(k_M^1+2k_M^2\right)\right)\left(-1+\theta\right)\theta^2- \\
-4a_I a_M^{\,2}f_I^{\,2}\left(-1+\theta\right)\theta\begin{pmatrix}2f_I^{\,2}f_M^{\,2}\left(-1+\theta\right)+ \\ a_M\begin{pmatrix}-2f_M^{\,2}+ \\ a_M\left(k_M^1+2k_M^2\right)\end{pmatrix}\left(k_M^1+k_I^1+2\tilde{k}_I\right)\theta \\ +2f_I f_M\left(2f_M^{\,2}+a_M\left(k_M^1-2k_M^2+2\tilde{k}_M\right)\right)\theta\end{pmatrix}\end{matrix}\right\}, \qquad (291)
$$

$$
C=\left\{\begin{array}{l}
a_I{}^2 a_M \theta \left(\begin{array}{l}
16 f_I{}^3 f_M \left(f_M{}^2 + a_M \left(k_M^1 + \tilde{k}_M\right)\right)\left(-1+\theta\right)^2 + \\
+4 a_M f_I f_M \left(\begin{array}{l}
-2 f_M{}^2 \left(k_I^1 + k_M^1 + 2\tilde{k}_I\right) + \\
a_M \left(\begin{array}{l}
-\left(k_M^1\right)^2 + 4\left(k_I^2 k_M^1 + 2k_M^1 k_M^2 + k_I^1\left(k_M^1 + 2k_M^2\right)\right) - \\
-2k_M^1 \tilde{k}_I + 4k_M^2 \tilde{k}_I - 2\left(-2k_I^2 + k_M^1 + 2\tilde{k}_I\right)\tilde{k}_M
\end{array}\right)
\end{array}\right)\left(-1+\theta\right)\theta + \\
+a_M{}^2\theta \left(\begin{array}{l}
\left(-2 f_M{}^2 + a_M\left(k_M^1 + 2k_M^2\right)\right)\left(k_I^1 + k_M^1 + 2\tilde{k}_I\right)^2 + \\
\left(\begin{array}{l}
2 f_M{}^2 \left(k_I^1 + k_M^1 + 2\tilde{k}_I\right)^2 + \\
a_M \left(\begin{array}{l}
k_M^1\left(-\left(k_I^1 - k_M^1\right)^2 + 8k_M^1 k_I^2\right) - 2\left(k_I^1 + k_M^1\right)^2 k_M^2 - \\
-4\left(k_I^1 + k_M^1\right)\left(k_M^1 + 2k_M^2\right)\tilde{k}_I - 4\left(k_M^1 + 2k_M^2\right)\left(\tilde{k}_I\right)^2 \\
+8k_M^1\left(k_I^1 + 2k_I^2\right)\tilde{k}_M + 4\left(k_I^1 + 2k_I^2\right)\left(\tilde{k}_M\right)^2
\end{array}\right)
\end{array}\right)\theta
\end{array}\right) + \\
4 f_I{}^2\left(-1+\theta\right)\left(\begin{array}{l}
2 f_M{}^4\theta + a_M f_M{}^2 \left(\begin{array}{l}
k_I^1 + 2k_M^1 - 2k_I^2 + 4\tilde{k}_I + \\
\left(-k_I^1 + k_M^1 + 2k_I^2 - 2k_M^2 - 4\tilde{k}_I + 4\tilde{k}_M\right)\theta
\end{array}\right) + \\
a_M{}^2 \left(\begin{array}{l}
-\left(k_M^1 + 2k_M^2\right)\left(k_I^1 + k_M^1 + 2\tilde{k}_I\right) + \\
\left(\begin{array}{l}
3\left(k_M^1\right)^2 + k_I^1\left(k_M^1 + 2k_M^2\right) + \\
+2k_M^1\left(k_M^2 + \tilde{k}_I + 2\tilde{k}_M\right) + 2\left(2k_M^2\tilde{k}_I + \left(\tilde{k}_M\right)^2\right)
\end{array}\right)\theta
\end{array}\right)
\end{array}\right)
\end{array}\right) + \\
+k_M^1\theta\left(\begin{array}{l}
a_I{}^2\left(2 f_M{}^2 + a_M\left(-k_I^1 + k_M^1 - 2\tilde{k}_I + 2\tilde{k}_M\right)\right)\left(-1+\theta\right) + 2a_M{}^2 f_I{}^2\theta + a_I a_M\left(f_I f_M\right)\left(2-4\theta\right) + \\
a_M\left(k_I^1 - k_M^1 + 2\tilde{k}_I - 2\tilde{k}_M\right)\theta
\end{array}\right)
\end{array}\right\}, \quad (292)
$$

$$
B=\left\{\begin{array}{l}
-a_I{}^4\left(-1+\theta\right)^2\left(\begin{array}{l}
-4f_M{}^4\left(k_I^1+2k_I^2\right)\theta-8a_M f_M{}^2\left(k_I^1+2k_I^2\right)\left(k_M^1+\tilde{k}_M\right)\theta+\\
-a_M{}^2\left(k_M^1+2k_M^2\right)\left(k_M^1+k_I^1+2\tilde{k}_I\right)^2+a_M{}^2\left(\begin{array}{l}
\left(k_M^1\right)^3+\left(k_I^1\right)^2\left(k_M^1+2k_M^2\right)+\\
8k_M^2\left(\tilde{k}_I\right)^2+2\left(k_M^1\right)^2\left(\begin{array}{l} k_M^2-\\ -4k_I^2+2\tilde{k}_I\end{array}\right)\\
-8k_I^2\left(\tilde{k}_M\right)^2+4k_M^1\left(\begin{array}{l} 2k_M^2\tilde{k}_I+\tilde{k}_I{}^2\\ -4k_I^2\tilde{k}_M\end{array}\right)\\
-2k_I^1\left(\begin{array}{l}
\left(k_M^1\right)^2-4k_M^2\tilde{k}_I\\
-2k_M^1\left(k_M^2+\tilde{k}_I-2\tilde{k}_M\right)\\
+2\left(\tilde{k}_M\right)^2
\end{array}\right)
\end{array}\right)\theta
\end{array}\right)\\
-2a_I{}^3\left(-1+\theta\right)\theta\left(\begin{array}{l}
4f_I{}^2\left(\begin{array}{l} f_M{}^2+\\ a_M\left(k_M^1+\tilde{k}_M\right)\end{array}\right)^2\left(-1+\theta\right)-2a_M f_I f_M\left(\begin{array}{l}
2f_M{}^2\left(k_M^1-2k_I^2+2\tilde{k}_I\right)+\\
a_M\left(\begin{array}{l}
\left(k_M^1\right)^2-k_I^1\left(k_M^1+2k_M^2\right)\\
+2k_M^1\left(\begin{array}{l} -2k_I^2-k_M^2+\\ \tilde{k}_I+\tilde{k}_M\end{array}\right)-\\
-4\left(\begin{array}{l} k_M^2\tilde{k}_I-\tilde{k}_I\tilde{k}_M+\\ k_I^2\tilde{k}_M\end{array}\right)
\end{array}\right)
\end{array}\right)\left(-1+\theta\right)\\
+a_M{}^2\left(\begin{array}{l}
\left(-f_M{}^2+a_M\left(k_M^1+2k_M^2\right)\right)\left(k_M^1+k_I^1+2\tilde{k}_I\right)^2+\\
\left(\begin{array}{l}
a_M\left(\begin{array}{l}
k_M^1\left(-\left(k_I^1-k_M^1\right)^2+8k_M^1k_I^2\right)-2\left(k_I^1+k_M^1\right)^2k_M^2-\\
-4\left(k_I^1+k_M^1\right)\left(k_M^1+2k_M^2\right)\tilde{k}_I-4\left(k_M^1+2k_M^2\right)\left(\tilde{k}_I\right)^2\\
+8k_M^1\left(k_I^1+2k_I^2\right)\tilde{k}_M+4\left(k_I^1+2k_I^2\right)\left(\tilde{k}_M\right)^2
\end{array}\right)+\\
+f_M{}^2\left(\begin{array}{l}
\left(k_I^1\right)^2+\left(k_M^1\right)^2+8k_M^1k_I^2+4k_M^1\tilde{k}_I+4\left(\tilde{k}_I\right)^2+\\
8k_I^2\tilde{k}_M+k_I^1\left(6k_M^1+4\left(\tilde{k}_I+\tilde{k}_M\right)\right)
\end{array}\right)
\end{array}\right)\theta
\end{array}\right)
\end{array}\right)
\end{array}\right\}, \quad (293)
$$

We can use these expressions to make an assessment of the effect of inhomogeneitie on the effective flexoelectric coefficient. Consider a graphene sheet with circular holes. Graphene is a semi-metal however depending on its edge termination or the presence of porosity, it can behave like a dielectric. We assume that the graphene sheet with holes behaves like a deielectric. If subscript M and I are respectively attributed to graphene and vacuum, then the material properties (Kalinin and Meunier, 2008; Lu et al., 2009; Li 2007; Lemme et al., 2007) can be written as

$$\begin{cases} f_M \to 1.29\times 10^{-9} & \dfrac{\text{N.m}}{\text{C}} \\ k_M^1 \to 0.9849\times 10^{-18} & \text{N.m} \\ k_M^2 \to 0.225\times 10^{-18} & \text{N.m} \\ a_M \to 8.067\times 10^{10} & \dfrac{\text{N.m}}{\text{C}^2} \end{cases} \quad \& \quad \begin{cases} f_I \to 0 \\ k_I^1 \to 0 \\ k_I^2 \to 0 \\ a_I \to \infty \end{cases}. \tag{294}$$

Then the effective flexoelectric constant can written is a very simple form:

$$f^e = f_M + \frac{f_M\left(2 f_M{}^2 + a_M\left(k_M^1 + 2\tilde{k}_M\right)\right)\theta}{a_M k_M^1\left(1-\theta\right)}. \tag{295}$$

In figure 6-3, the flexoelectric coefficient normalized with respect to graphene flexoelectric constant is plotted with respect to the volume fraction of holes. As can be seen, the flexoelectric response of graphene sheet with increase leading to a 26% increase for a 15% volume fraction.

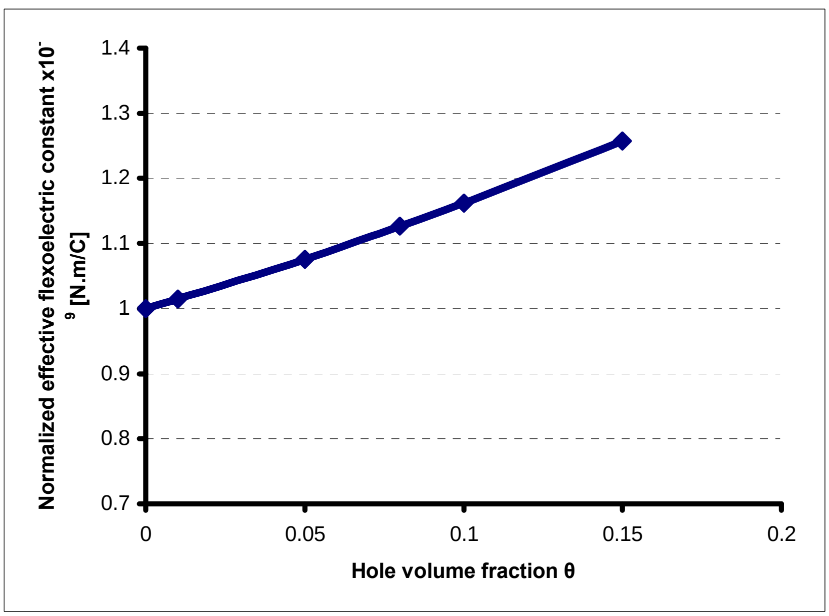

Figure 6.2: Normalized effective flexoelectric constant of graphene sheet with holes

6.5.2 Laminate flexoelectric membranes

In this case the material is macroscopically anisotropic. As illustrated in Fig. (6-b), we now consider a two-phase in-plane laminate with material property $\tilde{k}_r$, k_r^1 , k_r^2 , f_r and a_r , volume fraction θ_r $(r=1,2)$, and interfacial normal n . Let w_2' be a solution to the cell problem

$$\begin{cases} \Delta_y\left[\tilde{k}_p\left(\alpha_1+\Delta_y w_2'\right)+\dfrac{f_p}{a_p}\lambda_2\right]+\nabla_y\nabla_y\cdot\left[k_p^1\left(\alpha_3+\nabla_y\nabla_y w_2'\right)\right]=0 \qquad \text{on Y.} \\ \text{Periodic B.C.} \qquad \text{in } \partial\text{Y} \end{cases} \tag{296}$$

Since this is an elliptical partial differential equation, a unique solution is ensured. We assume that $\nabla\nabla w_2'$ and $\tilde{k}\ (\alpha_1+\Delta w_2')I+\dfrac{f}{a}\lambda_2 I+k^1\left(\alpha_3+\nabla\nabla w_2'\right)$ are constant in each laminate, and are denoted by $E_r=\nabla\nabla\left(w_2'\right)_r$ and

$$J_r=\tilde{k}_r\left(\alpha_1+\left(\Delta w_2'\right)_r\right)I+\frac{f_r}{a_r}\lambda_2 I+k_r^1\left(\alpha_3+\left(\nabla\nabla w_2'\right)_r\right)=\tilde{k}_r\left(\alpha_1+trE_r\right)I+\frac{f_r}{a_r}\lambda_2 I+k_r^1\left(\alpha_3+E_r\right)$$

on Ω_r $(r=1,2)$, respectively. Continuity of w_2' and $\nabla w_2'$ across the interface implies that $E_1-E_2=dn\otimes n$ for some scalar $a\in\mathbb{R}$. Also, we have $\theta_1 E_1+\theta_2 E_2=\dfrac{1}{|Y|}\int_Y\nabla\nabla w_2'=0$, and henceforth,

$$E_1=\theta_2 dn\otimes n, \qquad E_2=-\theta_1 dn\otimes n\,. \tag{297}$$

Further, balance of (273) implies that

$$\left(J_1 - J_2\right)n = \begin{bmatrix} \tilde{k}_1\left(\alpha_1 + trE_1\right)I + \left(\dfrac{f_1\lambda_2}{a_1}\right)I + k_1^1\left(\alpha_3 + E_1\right) - \tilde{k}_2\left(\alpha_1 + trE_2\right)I \\ -\left(\dfrac{f_2\lambda_2}{a_2}\right)I - k_2^1\left(\alpha_3 + E_2\right) \end{bmatrix} n = 0\,. \tag{298}$$

Inserting (297) in (298) we obtain

$$\begin{bmatrix} \tilde{k}_1\left(\alpha_1 + \theta_2 d\ \ tr\left(n\otimes n\right)\right)I + \left(\dfrac{f_1\lambda_2}{a_1}\right)I + k_1^1\left(\alpha_3 + \theta_2 dn\otimes n\right) - \\ -\tilde{k}_2\left(\alpha_1 - \theta_1 d\ \ tr\left(n\otimes n\right)\right)I - -\left(\dfrac{f_2\lambda_2}{a_2}\right)I - k_2^1\left(\alpha_3 - \theta_1 dn\otimes n\right) \end{bmatrix} n = 0\,\cdot \tag{299}$$

This results

$$\begin{bmatrix} \left(\tilde{k}_1 - \tilde{k}_2\right)\alpha_1 I + d\left(\theta_2\tilde{k}_1 + \theta_1\tilde{k}_2\right)I + \left(k_1^1 - k_2^1\right)\alpha_3 + d\left(\theta_2 k_1^1 + \theta_1 k_2^1\right)n\otimes n + \\ +\lambda_2\left(\dfrac{f_1}{a_1} - \dfrac{f_2}{a_2}\right)I \end{bmatrix} n = 0. \tag{300}$$

To solve this equation for d, we assume that $\alpha_3 = \alpha I$. Then

$$d = -\frac{\left(k_1^1 - k_2^1\right)\alpha + \left(\tilde{k}_1 - \tilde{k}_2\right)\alpha_1 + \lambda_2\left(\dfrac{f_1}{a_1} - \dfrac{f_2}{a_2}\right)}{\left[\left(\theta_2\tilde{k}_1 + \theta_1\tilde{k}_2\right) + \left(\theta_2 k_1^1 + \theta_1 k_2^1\right)\right]}. \tag{301}$$

For future convenience, we introduce notations:

$$A = \left(\theta_1\tilde{k}_2 + \theta_2\tilde{k}_1\right);\ \ B = \left(k_2^1\theta_1 + k_1^1\theta_2\right);\ \ C = \left(k_1^1 - k_2^1\right);\ \ D = \left(\tilde{k}_1 - \tilde{k}_2\right);\ \ \mathrm{F} = \left(\frac{f_1}{a_1} - \frac{f_2}{a_2}\right). \tag{302}$$

Therefore, inserting (302) in (297) gives

$$E_1 = -\frac{\theta_2 \left(C\alpha + D\alpha_1 + F\lambda_2 \right)}{A+B} n \otimes n, \quad E_2 = \frac{\theta_1 \left(C\alpha + D\alpha_1 + F\lambda_2 \right)}{A+B} n \otimes n \,. \tag{303}$$

And consequently polarization is calculated as

$$\begin{aligned}
P_1 &= -\alpha_2 + \frac{\lambda_2}{a_1} - \frac{f_1}{a_1}\left(\alpha_1 + trE_1\right) = -\alpha_2 + \frac{\lambda_2}{a_1} - \frac{f_1}{a_1}\left(\alpha_1 - \frac{\theta_2 \left(C\alpha + D\alpha_1 + F\lambda_2 \right)}{A+B} \right) = \\
&= -\alpha_2 + \lambda_2 \left(\frac{1}{a_1} + \frac{\theta_2 f_1 F}{a_1 \left(A+B \right)} \right) - \frac{f_1}{a_1}\left(\alpha_1 - \frac{\theta_2 \left(C\alpha + D\alpha_1 \right)}{A+B} \right), \\
P_2 &= -\alpha_2 + \frac{\lambda_2}{a_2} - \frac{f_2}{a_2}\left(\alpha_1 + trE_2\right) = -\alpha_2 + \frac{\lambda_2}{a_2} - \frac{f_2}{a_2}\left(\alpha_1 + \frac{\theta_1 \left(C\alpha + D\alpha_1 + F\lambda_2 \right)}{A+B} \right) = \\
&= -\alpha_2 + \lambda_2 \left(\frac{1}{a_2} - \frac{\theta_1 f_2 F}{a_2 \left(A+B \right)} \right) - \frac{f_2}{a_2}\left(\alpha_1 + \frac{\theta_1 \left(C\alpha + D\alpha_1 \right)}{A+B} \right).
\end{aligned} \tag{304}$$

Now the constant λ_2 can be calculated by setting $\frac{1}{|Y|}\int_Y P dy = 0$. So

$$\lambda_2 = \left(\frac{\theta_1}{a_1} + \frac{\theta_2}{a_2} + \frac{\theta_1 \theta_2 F^2}{\left(A+B \right)} \right)^{-1} \left(\alpha_2 + \left(\frac{\theta_1 f_1}{a_1} + \frac{\theta_2 f_2}{a_2} \right) \alpha_1 - F \left(\frac{\theta_1 \theta_2 \left(C\alpha + D\alpha_1 \right)}{A+B} \right) \right). \tag{305}$$

We use

$$\begin{aligned}
W^e \left(\alpha_1, \alpha_2, \alpha \right) &= \frac{1}{2}\left(k_b^2 \right)^e {\alpha_1}^2 + f^e \alpha_1 \alpha_2 + A^1 \cdot \alpha_1 \alpha + \frac{1}{2} a^e {\alpha_2}^2 + A^2 \cdot \alpha_2 \alpha + \frac{1}{2}\left(k_b^1 \right)^e |\alpha|^2 \\
&= \min_{\left(w_2', P_0' \right) \in A_p} \left\{ \frac{1}{|Y|} \int_Y \left(\begin{array}{l} \frac{1}{2} k_p^2 \left(\alpha_1 + \Delta_y w_2' \right)^2 + f_p \left(\alpha_2 + P_0' \right)\left(\alpha_1 + \Delta_y w_2' \right) + \frac{1}{2} a_p \left(\alpha_2 + P_0' \right)^2 + \\ + \frac{1}{2} k_p^1 \left(\alpha + \nabla_y \nabla_y w_2' \right) \cdot \left(\alpha + \nabla_y \nabla_y w_2' \right) \end{array} \right) \right\},
\end{aligned} \tag{306}$$

to find the effective properties and assume that A^1 and A^2 are zero. The expressions for effective coefficients are very long and we just present the result for the effective dielectric response. Interested readers can obtain the others directly from Equation (306).

$$
f^{e}=\frac{1}{\left(A+B\right)\left(a_1F^2\theta_1\theta_2+\left(A+B\right)\left(a_2\theta_1+a_1\theta_2\right)\right)^2}\times
$$

$$
\times\left(\begin{array}{l}
a_2{}^2\left(A+B\right)^2\theta_1\left(\left(A+B\right)f_1\theta_1-a_1DF\theta_1\theta_2\right)+\\
\left(\begin{array}{l}
A^3a_1a_2\left(f_1+f_2\right)\theta_1+a_2{}^2B^2Ff_1{}^2\theta_1^2-\\
-a_1{}^2F\left(\begin{array}{l}
a_2B^2D+BF\left(Ff_2{}^2+a_2\left(4Df_2+Fk_2^1-Fk_2^2\right)\right)\theta_1+\\
DF^2\left(\left(1+3a_2\right)f_2{}^2+\left(-1+a_2\right)a_2\left(k_1^2+k_2^2\right)\right)\theta_1^2
\end{array}\right)\theta_1\theta_2+\\
+a_2A^2\left(\theta_1\left(3a_1B\left(f_1+f_2\right)+F\left(a_1\left(4f_1-f_2\right)f_2+a_2\left(f_1{}^2-a_1k_2^1+a_1k_2^2\right)\right)\theta_1\right)-a_1{}^2DF\theta_1\theta_2\right)+\\
a_1a_2B\theta_1\left(\begin{array}{l}
B^2\left(f_1+f_2\right)+BF\left(4f_1f_2-f_2{}^2-a_2k_2^1+a_2k_2^2\right)\theta_1+\\
F\left(D\left(-f_2{}^2+a_2k_1^2+a_2k_2^2\right)+Ff_1\left(3f_2{}^2+a_2\left(k_1^2+k_2^2\right)\right)\right)\theta_1^2+F^3f_1{}^2\theta_1\theta_2
\end{array}\right)+\\
+A\left(\begin{array}{l}
2a_2{}^2BFf_1^2\theta_1^2-a_1{}^2F\left(2a_2BD+F\left(Ff_2{}^2+a_2\left(4Df_2+F\left(k_2^1-k_2^2\right)\right)\right)\theta_1\right)\theta_1\theta_2+\\
+a_1a_2\theta_1\left(\begin{array}{l}
3B^2\left(f_1+f_2\right)+2BF\left(\left(4f_1-f_2\right)f_2-a_2\left(k_2^1-k_2^2\right)\right)\theta_1+\\
F\left(D\left(-f_2{}^2+a_2k_1^2+a_2k_2^2\right)+Ff_1\left(3f_2{}^2+a_2\left(k_1^2+k_2^2\right)\right)\right)\theta_1^2+F^3f_1{}^2\theta_1\theta_2
\end{array}\right)
\end{array}\right)
\end{array}\right)\theta_2+\\
+\left(\begin{array}{l}
A^3a_1{}^2f_2-a_2{}^2BFf_1^2\left(D+Ff_1\right)\theta_1^2+A^2a_1\left(3a_1Bf_2+F\left(3a_1f_2{}^2+a_2\left(f_1{}^2-a_1\left(k_2^1-k_2^2\right)\right)\right)\theta_1\right)+\\
+A\left(\begin{array}{l}
3a_1{}^2B^2f_2+2a_1BF\left(3a_1f_2{}^2+a_2\left(f_1{}^2-a_1\left(k_2^1-k_2^2\right)\right)\right)\theta_1+\\
F\left(\begin{array}{l}
a_1^2f_2^2\left(-D+3Ff_2\right)-a_2{}^2\left(D+Ff_1\right)\left(f_1{}^2-a_1\left(k_1^1+k_2^1\right)\right)+\\
a_1^2a_2\left(D+Ff_2\right)\left(k_1^2+k_2^2\right)
\end{array}\right)\theta_1^2
\end{array}\right)+\\
+a_1a_2F\theta_1\left(B^2f_1{}^2+a_2B\left(D+Ff_1\right)\left(k_1^1+k_2^1\right)\theta_1+\left(-1+a_2\right)DF^2f_1{}^2\theta_1\theta_2\right)+\\
a_1{}^2\left(\begin{array}{l}
B\left(\begin{array}{l}
B^2f_2+BF\left(3f_2{}^2-a_2\left(k_2^1-k_2^2\right)\right)\theta_1+\\
F\left(D\left(-f_2{}^2+a_2k_1^2+a_2k_2^2\right)+Ff_2\left(3f_2{}^2+a_2\left(k_1^2+k_2^2\right)\right)\right)\theta_1^2
\end{array}\right)-\\
\left(-1+a_2\right)a_2DF^3\theta_1^2\theta_2\left(k_1^1+k_2^1\right)
\end{array}\right)
\end{array}\right)\theta_2{}^2+\\
+a_1a_2\left(A+B\right)F\left(D+Ff_2\right)\left(-f_1{}^2+a_1\left(k_1^1+k_2^1\right)\right)\theta_1\theta_2{}^3
\end{array}\right),\qquad(307)
$$

$$a^e = \frac{a_1 a_2 \begin{pmatrix} a_2 (A+B)^2 \theta_1 + a_1 \left((A+B)^2 + 4(A+B) F f_2 \theta_1 + F^2 \left(3 f_2{}^2 + a_2 \left(k_1^2 + k_2^2 \right) \right) \theta_1{}^2 \right) \theta_2 \\ + a_2 F^2 \left(- f_1{}^2 + a_1 \left(k_2^1 + k_1^1 \right) \right) \theta_1 \theta_2{}^2 \end{pmatrix}}{2 \left(a_1 F^2 \theta_1 \theta_2 + (A+B)(a_2 \theta_1 + a_1 \theta_2) \right)^2}. \tag{308}$$

6.5.3 Discussion

We have developed a general framework to estimate the effective elastic, dielectric and flexoelectric properties of heterogeneous membranes. Our results are analytical due to the approximations made (dilute limit) and the simplified microstructures considered (circular inhomogeneities and laminate). However, the presented framework can be solved numerically to consider more complex microstructures and to “design” flexoelectricity. There is strong evidence of the importance of flexoelectricity in 2-dimensional structures such as graphene and soft-lipid bilayers and the presented work can serve as the starting point for further explorations. Even a moderate fraction of holes in graphene leads to a fairly large change in its flexoelectric response. Given this outcome, specifically introducing inhomogeneities that are polar may provide avenues to significantly enhance flexoelectric response for graphene.

Several challenges remain. We have stayed strictly within the linearized regime. For solid membranes, out of plane deformation modes are coupled to the in-plane behavior. Homogenization of non-linear membranes is non-trivial and presents both a challenging problem and opportunity for future work.

Chapter 7: Pyroelectric Graphene

7.1 Introduction

Graphene, a perfect two-dimensional single layer of sp^2-hybridized carbon atoms, has recently attracted a fair amount of attention. Graphene is nature's thinnest elastic material, and due to its outstanding elastic, mechanical, thermal and electronic properties (Katsnelson, 2007; Geim et al., 2007, 2009; Tombros et al., 2007; Scarpa et al., 2009), it holds enormous potential in a variety of applications, including nanoelectronic devices, transparent electrodes, gas separation membranes, supercapacitors and ultracapacitors, sensors, and composites (Stoller et al., 2008; Schedin et al., 2007; Kim et el., 2009).

In a pyroelectric material, a temperature change induces polarization. Similar to the well-known phenomenon of piezoelectricity (strain-polarization coupling), pyroelectricity has found broad applications including solar energy conversion, refrigeration, infra-red detectors and nuclear fusion (Lang, 1976; Whatmore, 1986; Muralt, 2001; Hadni, 1981; Naranjo et al., 2005).

7.2 The Central Concept

Formally, pyroelectric coefficient of a material, p (c/ k.m^3), under constant stress σ and electric field E is defined by the expression (Bhalla and Newnham, 1980),

$$p = \left(\frac{\partial P_s}{\partial T}\right)_{E,\sigma}, \tag{309}$$

where P_s (c/m^3) is the spontaneous polarization and T (k) is the temperature. Equation (309) may be rewritten in the following form:

$$\left(\frac{\partial P_s}{\partial T}\right)_{E,\sigma} = \left(\frac{\partial P_s}{\partial T}\right)_{E,\varepsilon} + \left(\frac{\partial P_s}{\partial \varepsilon}\right)_{E,T} \left(\frac{\partial \varepsilon}{\partial T}\right)_{E,\sigma}, \tag{310}$$

Here ε is the strain. The pyroelectric coefficient in Equation (310) is decomposed into two contributions. In the first term on the right, strain is held fixed. This is known as the primary pyroelectric effect. The second term is the so-called secondary pyroelectricity and is caused by thermal expansion of the material due to the temperature change. Denoting piezoelectric coefficient and thermal expansion coefficient by d and α respectively, we can rewrite (310) as:

$$p = p_{primary} + p_{secondary} = \left(\frac{\partial P_s}{\partial T}\right)_{E,\varepsilon} + \alpha d. \tag{311}$$

The primary pyroelectric effect is restricted to only certain crystals---ones that are non-centrosymmetric and have polar directions. Some materials that exhibit primary pyroelectricity are: tourmaline, lithium sulfate monohydrate, and ferroelectric barium titanate.

Due to the semi-metallic nature of pristine graphene (Geim and Novoselov, 2007; Novoselov et al., 2005) piezoelectricity and pyroelectricity are hardly properties associated with it. Graphene can however exhibit dielectric behavior depending on deformation, defects and (if in ribbon form) surface termination (Geim and Novoselov, 2007; Du et al., 2010; Son et al., 2006; Baskin and Kral, 2011). Chandratre and Sharma (2012) showed that merely by creating holes of the right symmetry will "coax" graphene to act as a piezoelectric.

Is it then also possible for graphene to behave like a pyroelectric? Can graphene be "coaxed" to act as a pyroelectric? We believe that flexoelectricity allows a route to achieve this. The central concept is as follows: A *non-uniform strain* or the presence of *strain gradients* may potentially break the inversion symmetry and induce polarization even in *centrosymmetric* crystals. This is tantamount to extending relation the conventional piezoelectric relation to include strain gradients:

$$P_i = \underbrace{d_{ijk}\varepsilon_{jk}}_{=0,\ for\ non-piezo\ materials} + f_{ijkl}\frac{\partial \varepsilon_{jk}}{\partial x_l}. \qquad (312)$$

Here f_{ijkl} are the so-called flexoelectric coefficients. While the piezoelectric property is non-zero only for select materials, the strain gradient-polarization coupling (i.e. flexoelectric coefficients) *is in principle non-zero for all dielectric materials*. This implies that under a non-uniform strain, all dielectric materials are capable of producing a polarization. This is indeed true for graphene nanoribbons as well.

Consider now a material consisting of two or more different non-piezoelectric dielectric materials—one example is simply a (dielectric) graphene sheet with holes in which case air serves as the 2nd dielectric. Even under the application of uniform stress, differences in material properties at the interfaces will result in the presence of strain gradients. Those gradients will induce polarization due to the flexoelectric effect. As long as certain symmetry rules are followed, the net average polarization will be nonzero. Thus, the nanostructure will exhibit an overall electromechanical coupling under uniform stress behaving like a piezoelectric material. The length scales must be nanoscale since this concept requires very large strain gradients and those for a given strain are generated easily only at the nanoscale. Regarding symmetry: Topologies of only certain symmetries can realize the central concept discussed in this work. For example, circular holes distributed in a material will not yield apparently piezoelectric behavior even though the flexoelectric effect will cause local polarization fields. Due to circular symmetry, the overall average polarization is zero. A similar material but containing triangular shaped holes (or inclusions) for example, and aligned in the same direction, will exhibit the required apparent piezoelectricity.

7.3 Atomistic Simulation

We conduct a three-step simulation process to verify our hypothesis: (i) DFT based calculations to first ensure that the defective graphene sheet is dielectric. This is the primary requirement for pyroelectricity or piezoelectricity. The defective graphene sheet is relaxed and its electronic structure is calculated to verify that a finite band gap exists. (ii) Empirical molecular dynamics at finite temperature of interest. Since pyroelectricity is based on polarization response to a small temperature change, purely quantum mechanical methods cannot be used (DFT is at zero degrees Kelvin), (iii) the geometry obtained from finite temperature MD is “frozen” and transferred back to DFT and the net polarization is calculated.

Quantum Mechanical Calculations: The electronic polarization is obtained using the Berry-phase approach through the quantum package “Espresso” (Giannozi et al., 2009). The electronic ground state wavefunctions are collected using the grid of 1x6x6 k-points. The Berry-phase approach is then applied to the obtained ground state configuration with dense mesh of k points in the desired direction for observation of polarization. All geometries were optimized to energy minimum state by ensuring that maximum force per atom is constrained to 0.05 eV/Å.

Molecular Dynamic Simulations: The configuration of the graphene in our simulation is shown in Figure 7-1. We consider a 25.75 A° x 24.61 A° graphene supercell with a triangular hole in the center (222 atoms). Periodic boundary conditions (PBC) are imposed in all three dimensions and the dangling bonds at the edges of the hole are passivated using hydrogen atoms. The MS and MD simulations are performed in Lammps (Plimpton, 1995) using Adaptive Intermolecular Reactive Empirical Bond Order (AIREBO) (Stuart et al., 2000). Size of the simulation box in out of plane direction is selected large enough (20 nm in our simulation) compared to the cut-off radius considered for C-C bonds in the interatomic potential to ensure that defects in different cells don’t interact. The geometry is initially relaxed at zero temperature using the conjugate gradient method.

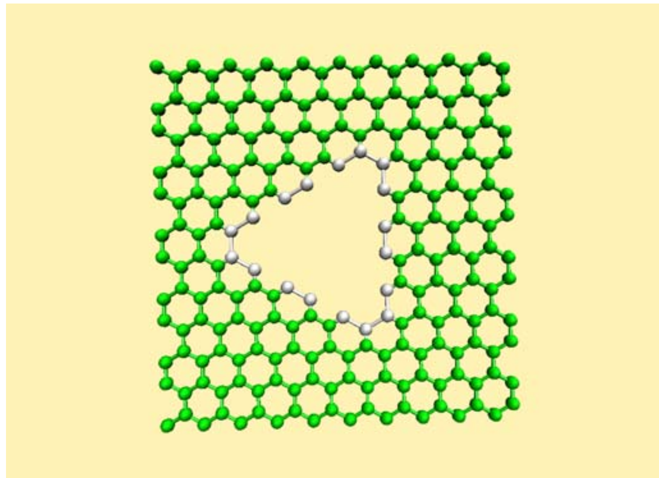

Figure 7-1: Geometry considered in our simulation for graphene sheet. The white colored atoms refer to H atoms.

After initial relaxation, the molecular dynamic simulation is performed to bring the configuration to the state of thermal equilibrium at the desired finite temperature using the Nose-Hoover thermostat (Hoover, 1985) within the isothermal-isobaric (NPT) ensemble. The initial velocities of carbon atoms at finite temperature are generated through a random Gaussian distribution with variables deduced from Maxwell-Boltzmann distribution. The Velocity-Verlet integration algorithm is used with 0.1 fs time steps. The simulation time is selected to be large enough to ensure that the system reaches steady-state. 7.5×10^5 MD simulation steps are used for thermal equilibration and an additional 12.5×10^5 MD steps are applied to calculate the time-averaged quantities (Jiang et al., 2009). The graphene sheet contracts with increasing temperature and the negative thermal expansion for graphene at room temperature has been reported by other works also (Steward, 1960; Yoon et al., 2011). We also observed, in the course of our simulations, that the hydrogen atoms move out of plane and some corrugation appear as shown in Figure 7-2. Thereafter, the simulation box size is deformed to the time-averaged box size obtained from the previous part and by using canonical (NVT) ensemble the system is brought to thermal equilibration at constant volume. Finally, the atom coordinates at the expected temperature are obtained and can be used as the input configuration for quantum calculation. The procedure is repeated for different temperatures around room temperature (T=300 K).

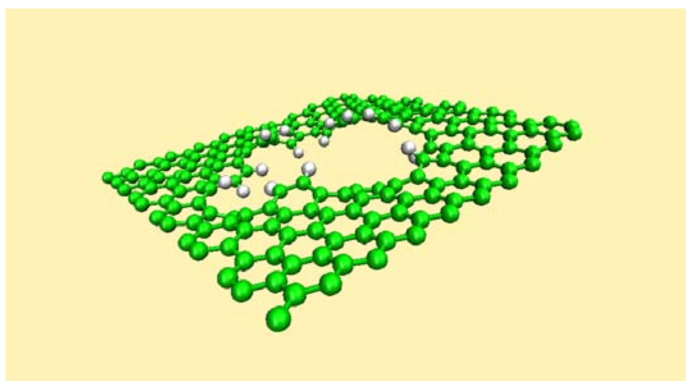

Figure 7-2: Configuration of graphene sheet at room temprature.

The atomic configurations obtained from MD simulation at each temperature are used as the input file for quantum calculation to determine net polarization.

7.4 Results and Discussion

Then pyroelectric constant at each temperature is calculated based on equation (1). The values are normalized with respect to the Lithium Sulphate pyroelectric coefficient at room temperature (~ 6.88x10-5 C/(m2K)) (Zheludev,

1975) and are shown in Figures (7-3) and (7-4). As can be observed from the graphs, the pyroelectric constant in the temperature range of 275 to 300 is similar in magnitude to Lithium Sulphate but dramatically increases at 325. Considering the first 3 data points, the average pyroelectric coefficient can be considered to be 6.88x10-5 C/(m2K).

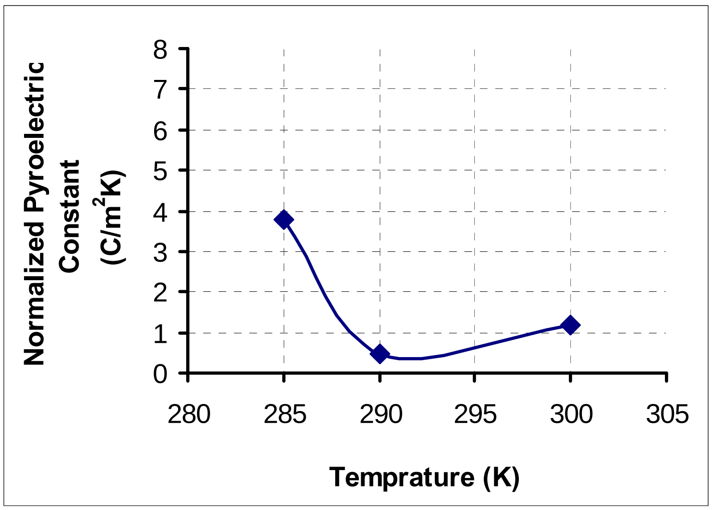

Figure 7-3: Graph showing normalized pyroelectric constant of graphene with respect to Lithium Sulphate at different temperatures (T=275-300).

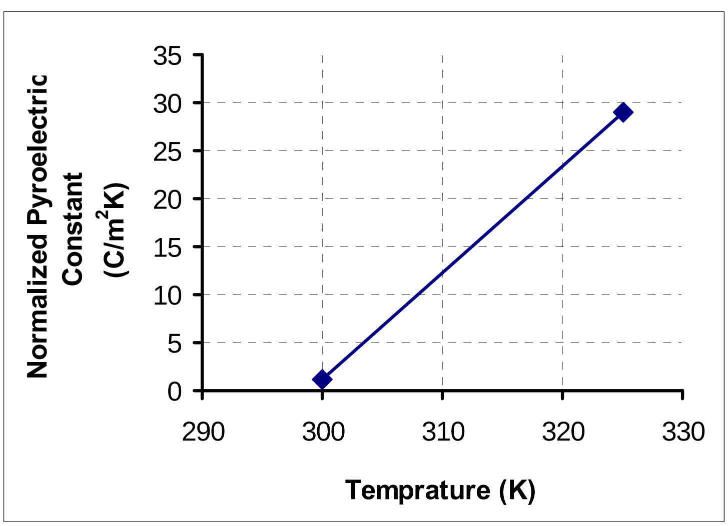

Figure 7-4: Graph showing normalized Pyroelectric constant of graphene with respect to Lithium Sulphate at different temperatures (T=300-325).

We are unable to explain the non-intuitive temperature dependence of pyroelectric response of graphene and its resolution is deferred for future. Possible reasons could be unusual changes in electronic structure with temperature, thermal expansion anomalies and nonlinear effects.

Chapter 8. Summary and Future Work

In this dissertation, we have provided insights into the effect of surface structure on several technologically important physical properties and developed the homogenized constitutive response for heterogeneous surfaces. The main conclusions of this work can be summarized as below:

1. For three dimensional entities, the effect of surface roughness on the surface stress and surface elastic behavior has been relatively understudied. We have presented theoretical derivations that relate both periodic and random roughness to the effective surface elastic behavior. We have found that the residual surface stress is hardly affected by roughness while the superficial elasticity properties are dramatically altered and, importantly, may also result in a change in its sign----this has ramifications in the interpretation of sensing based on frequency measurement changes due to surface elasticity. We have shown that the resonance frequency of a cantilever beam with rough surface decreases as much as 3 times of its value for flat surface.
2. In parallel to the theoretical calculations, we have conducted atomistic simulations to further elucidate the interplay between surface energy and roughness. In particular, we have also highlighted on the effect of roughness on the term that represents the curvature dependence of surface energy (crystalline Tolman's length). We have found, consistent with our theoretical predictions and in sharp contrast to a few others, that the surface stress is negligibly impacted by roughness. However, even moderate

roughness is seen to dramatically alter the surface elasticity modulus as well as the crystalline Tolman's length.

3. In the context of independent deformable surfaces, our focus has been on flexoelectricity. We have considered a heterogenous flexoelectric membrane, and derived the homogenized flexoelectric, dielectric and elastic response. In particular for purely fluid (lipid type) membranes, we have obtained exact results. Our work allows design of microstructure to tailor flexoelectric response and a simple application has been illustrated for graphene sheets.
4. We have used a combination of insights from theory and detailed quantum calculations and have shown that graphene be designed to be pyroelectric thus providing an avenue for the thinnest possible thermo-electro-mechanical material.

References

Asaro, R., Lubarda, V., A., Mechanics of solids and materials, Cambridge, 2006.

Bar On, B., Altus, E., Tadmor, E.B., "Surface Effects in Non-uniform Nanobeams: Continuum vs. Atomistic Modeling," *International Journal of Solids and Structures* 47, 9, 1243-1252, 2010.

Baskaran, S., Thiruvannamalai, S., Heo, H., Lee, H.J., Francis, S. M., Ramachandran, N , Fu, J.Y., "Converse Piezoelectric Responses in Nonpiezoelectric Materials Implemented via Asymmetric Configurations of Electrodes," *Journal of Applied Physics* 108 6, 064116, 2010.

Baskin, A., and Kral, P., "Electronic Structures of Porous Nanocarbons," *Scientific Reports* 1, 1-7, 2011.

Bhalla, A. S., Newnham, R. E., "Primary and Secondary Pyroelectricity," *Phys. Stat. Sol. (a)* 58, 1980.

Brenemann, K. D., Rabbitt, R.D., "Piezo- and Flexoelectric Membrane Materials Underlie Fast Biological Motors in the Ear," *Mater Res Soc Symp* Proc. 2009 Spring;1186E. pii: 1186-JJ06-04, 2009.

Brownell W.E., Farrell B., Rapheal R.M., "Membrane Electromechanics at Hair-cell Synapses," *Biophysics of the Cochlea: from Molecules to Models*, 169-176, 2003.

Brownell W.E., Spector A.A., Raphael R.M., Popel, A.S., “Micro- and Nanomechanics of the Cochlear Outer Hair Cell,” *Annual Review of Biomedical Engineering* 3, P 169-194, 2001.

Bursian, E. V., Trunov, N. N., “Nonlocal piezoelectric effect,” *Sov. Physics Solid State,* 16 (4) 760-762, 1974.

Cahn, J.W., “Interfacial Free-energy and Interfacial Stress – The case of an Internal Interface in a Solid,” *Acta Metallurgica* 37, 3, 773-776, 1989.

Cammarata, R.C., “Surface and Interface Stress Effects in Thin Films,” *Progress in Surface Science* 46, 1, 1-38, 1994.

Cammarata, R.C., “Generalized Thermodynamics of Surfaces with Applications to Small Solid Systems,” *Solid State Physics* 61, 1-75, 2009.

Cammarata, R.C., “Surface and Interface Stress Effects in Thin films,” *Progress in Surface Science* 46, 1, 1-38, 2009.

Catalan, G., Sinnamon, L.J. and Gregg, J.M., “The Effect of flexoelectricity on the Dielectric Properties of Inhomogeneously Strained Ferroelectric Thin Films,” *Journal of Physics: Condensed Matter*, 16(13), 2253-2264, 2004.

Chandratre, S., Sharma, P., “Coaxing Graphene to be Piezolectric,” *Applied Physics Letters*, 100, 023114-1-023114-3, 2012.

Chhapadia, P., Mohammadi, P., Sharma, P., “Curvature-dependent Surface Energy and Implications for Nanostructures,” *Journal of the Mechanics and Physics of Solids* 59, 2103-2115, 2011.

Cohen, H., DeSilva, C.N., "Nonlinear Theory of Elastic Surfaces," *Journal of Mathematical Physics* 7, 246, 1966.

Cross, L. E., "Flexoelectric Effects: Charge Separation in Insulating Solids Subjected to Elastic Strain Gradients," *J. Mater. Sci.* 41, 53–63, 2006.

Dai, S., Gharbi, M., Sharma, P. and Park, H.S. "Surface Piezoelectricity, Size-effects in Nanostructures and Emergent Piezoelectricity in Non-piezoelectric Materials," *Journal of Applied Physics* 110, 104305, 2011.

Diao, J., Gall, K. and Dunn, M.L, "Surface-stress-induced Phase Transformation in Metal Nanowires," *Nature Materials* 2, 656-60, 2003.

Diao, J., Gall, K., Dunn and M.L., "Atomistic Simulation of the Structure and Elastic properties of Gold Nanowires," *Journal of the Mechanics and Physics of Solids* 52, 1935-62, 2004.

Diao, J., Gall, K., Dunn, M.L. and Zimmerman, J.A., "Atomistic Simulations of the Yielding of Gold Nanowires," *Acta Materialia* 54, 643-53, 2006.

Dingreville, R., Qu, J., Cherkauoi, M., "Surface Free Energy and its Effect on the Elastic Behavior of Nano-sized Particles, Wires and Films," *J. Mech. Phys. Solids* 53,1827-1854, 2005.

Du, A., Zhu, Z., and Smith S. C., "Multifunctional Porous Graphene for Nanoelectronics and Hydrogen Storage: New Properties Revealed by First Principle Calculations," *J. Am. Chem. Soc.* 132 (9), 2876–2877, 2010.

Duan, H. L., Wang, J., Huang, Z. P., Karihaloo, B. L., "Eshelby Formalism for Nano-inhomogeneities," *Proceeding of the Royal Society A* 4612062, 335-3353, 2005.

Duan, H. L., Wang, J., Huang, Z. P., Karihaloo, B. L., "Size-dependent Effective Elastic Constants of Solids Containing Nano-inhomogeneities with Interface Stress," *J. Mech. Phys. Solids* 53,1574-1596, 2005.

Duan, H. L., Xue, Y., Yi, X., "Vibration of Cantelevers with Rough Surfaces," *Acta Mechanica Solida Sinica* 22, No.6, 550-554, 2009.

Dumitrica, T., Landis, C. M., Yakobson, B. I., "Curvature Induced Polarization in Carbon Nanoshells," *Chemical Physics Letters*, 360 (1-2), 182-188, 2002.

Eguiluz, A.G., Maradudin, A.A., "Effective Boundary Conditions for a Semi-infinite Elastic Mediu Bounded by a Rough Planar Stress-free Surface," *Phys. Rev. B* 28 713-727, 1983.

Eguiluz, A.G., Maradudin, A.A., "Frequency Shift and Attenuation Length of Reyleigh Wave due to Surface Roughness," *Phys. Rev. B* 28 728-747,1983.

Eliseev E.A., Morozovska, A.N., Glinchuk, M.D. and Blinc, R. "Spontaneous Flexoelectric/flexomagnetic Effect in Nanoferroics," *Physical Review B*, 79, 165433, 2009.

Eliseev E.A. and Morozovska A.N. "General Approach for the Description of Size Effects in Ferroelectric Nanosystems," *Journal of Materials Science*, 44, 19, 5149, 2009.

Eliseev, E.A., Glinchuk, M.D., Khist, V., Skorokhod, V.V., Blinc, R., Morozovska, A.N., "Linear Magnetoelectric Coupling and Ferroelectricity Induced by the Flexomagnetic Effect in Ferroics," *Physical Review B* 84, I 17, 174112, 2011.

Fousek, J., Cross, L.E. and Litvin, D.B. "Possible Piezoelectric Composites Based on the Flexoelectric Effect," *Materials Letters*, 39, 287, 1999.

Fu, J.Y., Zhu, W., Li, N. and Cross, L.E. "Experimental Studies of the Converse Flexoelectric Effect Induced by Inhomogeneous Electric Field in a Barium Strontium Titanate Composition," *Journal of Applied Physics*, 100, 024112, 2006.

Fu, John Y., Zhu, Wenyi, Li, Nan, Smith, Nadine B., Eric Cross, L., "Gradient Scaling Phenomenon in Microsize Flexoelectric Piezoelectric Composites," *Applied Physics Letters* 91, 182910, 2007.

Gautschi, G., "Piezoelectric Sensorics: Force, Strain, Pressure, Acceleration and Acoustic Emission Sensors, Materials and Amplifiers," 2002.

Gere, J.M., Goodno, B.J., Mechanics of materials. Cengage Learning, 2004.

Geim, A. K., and Novoselov, K. S., "The Rise of Graphene," *Nature Materials*, 6(3), 183-191, 2007.

Geim, A.K., “Graphene: Status and Prospects,” *Science*, 324 5934, 1530, 2009.

Gharbi, M., Sun, Z.H., White, K., El-Borgi, S., and Sharma, P. , “Flexoelectric Properties of Ferroelectrics and the Nanoindentation Size-effect,” *International Journal of Solids and Structures*, 48, 249-256, 2011.

Giannozzi, P., Baroni, S., Bonini, N., Calandra, M., Car, R., Cavazzoni, C., Ceresoli, D., Chiarotti, G,L., Cococcioni, M., Dabo, I., Corso, A. D., Gironcoli, S., Fabris, S., Fratesi, G., Gebauer, R., Gerstmann, U., Gougoussis, C., Kokalj, A., Lazzeri, M., Martin-Samos, L., Marzari, N., Mauri, F., Mazzarello, R., Paolini, S., Pasquarello, A., Paulatto, L., Sbraccia, C., Scandolo, S., Sclauzero, G., Seitsonen, A. P., Smogunov, A., Umari, P., Wentzcovitch, R. M., “Quantum Espresso: a Modular and Open-source Project for Quantum Simulation of Materials,” *Journ. of Phys: Condensed Matter*, 21 (39), 2009.

Goudeau, P., Renault, P. O., Villain, P., Coupeau, C., Pelosin, V., Boubeker, B., Badawi, K. F., Thiaudiere, D., and Gailhanou, M., “Characterization of Thin Film Elastic Properties Using X-ray Diffraction and Mechanical Methods: Application to Polycrystalline Stainless Steel,” *Thin Solid Films* 398, 496-500, 2001.

Gurtin, M. E., Murdoch, A., “A Continuum Theory of Elastic Material Surfaces,” *Arch. Ration. Mech. Anal.* 57, 291-323, 1975.

Gurtin, M.E. and Murdoch, A.I., “Surface Stress in Solids,” *International Journal of Solids and Structures* 14, 431-40, 1978.

Gurtin, M. E., Weissmuller, J., and Larche, F., “The General Theory of Curved Deformable Interfaces in Solids at Equilibrium,” *Philosophical Magazine A*, 78, 1093–1109, 1998.

Hadni, A., “Applications of the pyroelectric effect**,**” *J. Phy. E: Sci. Instrum*., 14, 1233, 1981.

Harden, J., Chambers, M., Verduzco, R., Luchette, P., Gleeson, J. T., Sprunt, S., Jákli, A., “Giant Flexoelectricity in Bent-core Nematic Liquid Crystal Elastomers,” *Applied Physics Letters* 96, 10, 102907, 2010.

He, L.H., Li, Z.R., “Impact of Surface Stress on Stress Concentration,” *Intenational Journal of Solids and Structures* 43, 20, 6208-6219, 2006.

Hoover, W. G., ”Canonical dynamics: Equilibrium phase-space distributions,” Phys. Rev. A. 31 (3), 1695-1697 (1985).

Huang, Z.P. and Sun, L., “Size-dependent Effective Properties of a Heterogeneous Material with Interface Energy Effect: from Finite Deformation Theory to Infinitesimal Strain Analysis,” *Acta Mechanica*, 190, 151-163, 2007.

Hui, T., Chen, Y. H., “Surface Effect and Size Dependence on the Energy Release due to a Nano InAs inclusion Expansion in a GaAs Matrix Material,” *Adv. Studies Theor. Phys.* 4, no. 8, 369 – 381, 2010.

Hurley, C., Tewary, V. K., Richards, A. J., “Thin-film Elastic-property Measurements with Laser-ultrasonic SAW Spectrometry,” *Thin Solid Films* 398, 326-330, 2001.

Indenbom, V. L., Loginov, V. B., Osipov, M. A., “Flexoelectric Effect and Structure of Crystals,” *Kristallografiya* 28, 1157, 1981.

Jiang, J. W., Wang, J. S., Li, B., “Young’s Modulus of Graphene: A Molecular Dynamic Study,” *Phys. Rev. A.* 80 113405 (2009).

Jing, G.Y., Duan, H.L., Sun, X.M., Zhang, Z.S., Xu, J., Li, Y.D., Wang, J.X. and Yu, D.P., “Surface Effects on Elastic Properties of Silver Nanowires: Contact Atomic-force Microscopy,” *Physical Review B*, 73, 235409, 2006.

Johnson, K. L., <u>Contact Mechanics</u>, 1985.

Johnson, W.C., “Superficial Stress and Strain at Coherent Interfaces,” *Acta Materialia* 48, 2, 433-444, 2000.

Jewell, S. A., “Living Systems and Liquid Crystals,” *Liquid Crystals* 38 11-12, 1699-1714, 2011.

Kalinin, S. V., Meunier, V. “Electronic Flexoelectricity in Low-dimensional Systems,” *Physical Review B*, 77 (3), 033403-1-4, 2008.

Katsnelson, M.I, “Graphene: Carbon in Two Dimensions,” *Mater Today*, 10 1–2, 20, 2007.

Kim, K.S., Zhao, Y., Jang, H., Lee, S.Y., Kim, J.M., Kim, K.S. et al. “Large-scale pattern growth of graphene films for stretchable transparent electrodes,” *Nature,* 457 7230, 706, 2009.

Kuczynski W., Hoffmann J., “Determination of Piezoelectric and Flexoelectric Polarization in Ferroelectric Liquid Crystals,” *Physical Review E* 72, I 4, 041701, 2005.

Lim, C. W., He, L. H., “Size-dependent Nonlinear Response of Thin Elastic Films with Nano-scale Thickness,” *Int. J. Mech. Sci.* 46, 1715–1726, 2004.

Lim, C. W., Li, Z. R., He, L. H., “Size Dependent, Non-uniform Elastic Field Inside a Nano-scale Spherical Inclusion due to Interface Stress,” *International Journal of Solids and Structures* 43 5055–5065, 2005.

Liang, H.Y., Upmanyu, M., Huang, H.C., “Size-dependent Elasticity of Nanowires: Nonlinear Effects,” *Phys. Rev. B* 71, 241403, 2005.

Liu, C., Rajapakse, R. K. N. D., “Continuum Models Incorporating Surface Energy for Static and Dynamic Response of Nanoscale Beams,” *IEEE Transactions on Nanotechnology* 9, NO. 4, 422-431, 2010.

Liu, C., Rajapakse, R.K.N.D., Phani, A.S., “Finite Element Modeling of Beams with Surface Energy Effects,” *Journal of Applied Mechanics* 78, 031014, 2011.

Lu, P., Lee, H.P., Lu, C., O'Shea, S. J., "Surface Stress Effects on the Resonance Properties of Cantilever Sensors," *Phys. Rev. B* 72 085405, 2005.

Ma, W., Cross, L.E., "Large Flexoelectric Polarization in Ceramic Lead Magnesium Niobate," *Applied Physics Letters*, 79(19), 4420-4422, 2001.

Ma, W. and Cross, L.E., "Flexoelectric Polarization in Barium Strontium Titanate in the Paraelectric State," *Applied Physics Letters*, 81(19), 3440-3442, 2002.

Ma, W., Cross, L.E., "Strain-gradient Induced Electric Polarization in Lead Zirconate Titanate Ceramics," *Applied Physics Letters*, 82(19), 3923-3925, 2003.

Ma, W. and Cross, L.E., "Flexoelectricity of Barium Titanate," *Applied Physics Letters*, 88, 232902, (2006).

Madden, J. D. W., Vandesteeg, N. A., Anquetil, P. A., Madden, P. G. A., Takshi, A., Pytel, R. Z., Lafontaine, S. R., Wieringa, P. A., Hunter, I. W., "Artificial Muscle Technology: Physical Principles and Naval Prospects," *IEEE Oceanic Engineering Society*, 29(3), 706-728, 2004.

Majdoub, M.S., Maranganti, R. and Sharma, P., "Understanding the Origins of The Intrinsic Dead Layer Effect in Nanocapacitors," *Physical Review B*, 79, 115412, 2009.

Majdoub, M.S., Sharma, P. and Cagin, T., "Enhanced Size-Dependent Piezoelectricity And Elasticity in Nanostructures Due to The Flexoelectric Effect," *Physical Review B*,77, 125424-1 – 125424-9, 2008; Majdoub, M.S., Sharma, P. and Cagin, T. *Physical Review B*, 79, 119904(E), 2009.

Majdoub, M.S., Sharma, P. and Cagin, T., "Dramatic Enhancement in Energy Harvesting For a Narrow Range of Dimensions in Piezoelectric Nanostructures," *Physical Review B*, 78, 121407 (R) ,2008; Majdoub, M.S., Sharma, P. and Cagin, T. *Physical Review B*, 79, 159901(E), 2009.

Maskevich, V.S., Tolpygo, K.V., "Investigation of Long-wavelength Vibrations of Diamond-type Crystals with an Allowance for Long-range Force," *Sov. Phys. JETP* 5, 435, 1957.

Maradudin, A.A., "Light Scattering and Nanoscale Surface Roughness," Springer Science+Business Media, New York, 2007.

Maranganti, R. and Sharma, P., "Atomistic Determination of Flexoelectric Properties of Crystalline Dielectrics," *Physical Review B*, 80, 054109, 2009.

Mashkevich, V. S., Tolpygo, K. B., "Electrical, Optical and Elastic Properties of Diamond Type Crystals," *Sov. Phys. JETP* 5, 3, 435, 1957.

McDowell, M.T., Leach, A.M., Gall, K., “Bending and Tensile Deformation of Metallic nanowires,” *Modelling and Simulation in Materials Science and Engineering*, v 16, n 4,045003, 2008.

Meyer, R. B., “Piezoelectric Effects in Liquid Crystals**,**” *Phys. Rev. Lett.* 22, 918-921, 1969.

Mi, C., Kouris, D., “The Role of Interface Stress for Nanoparticles Embedded in Films,” *JSME Journal of Solid Mechanics and Materials Engineering*, Vol.1(10),1219-1230, 2007.

Mi, C., Jun, S., Kouris, D.A. and Kim, S.Y., “Atomistic Calculations of Interface Elastic Properties in Non-coherent Metallic Bilayers,” *Physical Review B* 77, 7, 075425, 2008.

Miller, R. E., Shenoy, V. B., “Size Dependent Elastic Properties of Structural Elements,” *Nanotechnology* 11, 139–147, 2000.

Mogilevskaya, S. G., Crouch, S. L., LaGrotta, A. and Stolarski, H. K., “The Effects of Surface Elasticity and Surface Tension on the Transverse Overall Elastic Behavior of Unidirectional Nano-composites,” *Composites Science and Technology* 70, 3, 427-34, 2010.

Mogilevskaya, S.G., Crouch, S.L and, Stolarski, H.K., “Multiple Interacting Circular Nano-inhomogeneities with Surface/interface Effects,” *Journal of the Mechanics and Physics of Solids* 56, 6, 2298-327, 2008.

Muralt, P., "Micromachined Infrared Detectors Based on Pyroelectric Thin Films," *Rep. Prog. Phys.,* 64, 1339, 2001.

Naranjo, B., Gimzewski, J.K., Putterman, S., "Observation of Nuclear Fusion Driven by a Pyroelectric Crystal," *Nature* 434, 1115-1117, 2005.

Naumov, I, Bratkovsky, A.M., Ranjan, V, "Unusual Flexoelectric Effect in Two-Dimensional Noncentrosymmetric sp(2)-Bonded Crystals," *Physical Review Letters* 102, 21, 217601, 2009.

Novosolev, K. S., Geim, A. K., Morozov, S. V., Jiang, D., Zhang, Y., Dubones, S. V., Grigorieva, I. V., and Firsov, A. A., "Electric Field Effect in Atomically thin Carbon Films," *Science,* 306, 666-669, 2004.

Novosolev, K. S., Geim, A. K., Morozov, S. V., Jiang, D., Zhang, Y., Dubones, S. V., Grigorieva, I. V., and Firsov, A. A., "Two-Dimensional Gas of Massless Dirac Fermions in Graphene," *Nature,* 438, 197-200, 2005.

Nützenadel, C., Züttel, A., Chartouni, D., Schmid, G., and Schlapbach, L., "Critical Size and Surface Effect of the Hydrogen Interaction of Palladium Clusters," *Eur. Phys. J.* D8, 245, 2000.

Nye, J. F., "Physical Properties of Crystals: Their Representation by Tensors and Matrices," *Oxford University Press*; Reprint edition, 1985.

Park, H. S., "Quantifying the Size-dependent Effect of the Residual Surface Stress on the Resonant Frequencies of Silicon Nanowires if Finite

Deformation Kinematics Are Considered," *Nanotechnology* 20, 115701, 2009.

Park, H. S., Klein, P. A., "Surface Stress Effects on the Resonant Properties of Metal Nanowires: The Importance of Finite Deformation Kinematics and the Impact of the Residual Surface Stress," *J. Mech. Phys. Solids.* 56, 3144-3166, 2008.

Peng, X., Ganti, S., Alizadeh, S., Sharma, P., Kumar, S., Nayak, S., "Strain Engineered Photoluminescence of Silicon Nano-clusters," *Physical Review B* 74, 035339, 1-5, 2006.

Petrov, A. G., Flexoelectric model for active transport. In: "Physical and Chemical Bases of Biological Information Transfer," pp. Ill—125, Plenum Press, New York and London, 1975.

Petrov, A.G., "Mechanosensitivity of Cell Membranes. Role of Liquid Crystalline Lipid Matrix," *Liquid Crystals: Chemistry and Structure*, 3319, P 306-318, 1998.

Petrov, A.G., Spassova M., Fendler J.H., "Flexoelectricity and Photoflexoelectricity in Model and Biomembranes," Thin Solid Films 284, P 845-848, 1996.

Petrov, A. G., "Flexoelectricity of model and living membranes," *Biochim Biophys Acta* 1561: 1–25, 2002.

Petrov, A. G., “Electricity and Mechanics of Biomembrane Systems: Flexoelectricity in Living Membranes,” *Anal Chim Acta.* 568 (1-2), 70-83, 2006.

Petrov, A. G., “Flexoelectricity and Mechanotransduction,” (Invited Review), In: Current Topics in Membranes, *Mechanosensitive channels, O.P.Hamil, Ed., Elsevier/Academic Press* 58, 121-150, 2007.

Rafailov, P. M., Dettlaff-Weglikowska, U., “Observation of Flexoelectricity in a Mixture of Carbon Single Walled Nanotubes with a Nematic Liquid Crystal,” *Molecular Crystals and Liquid Crystals* 545, 1282-1290, 2011.

Plimpton, S., “Fast Parallel Algorithms for Short-range Molecular Dynamics,” *Journal Computational Physics*, 117, 1-19, 1995 *http://lammps.sandia.gov*.

Qi, W.H., “Size Effect on Melting Temperature of Nano-solids,” *Physica B*, 368, 46-50, 2005.

Raphael R.M., Popel A.S., Brownell W.E., “A Membrane Bending Model of Outer Hair Cell Electromotility,” *Biophysical Journal* 78, I 6, P 2844-2862, 2000.

Reddy, J. N., “Theory and analysis of elastic plates and shells,” *CRC Press*, 2007.

Renault, P. O., Le Bourhis, E., Villain, P., Goudeau, P., Badawi, K.F., Faurie, D., “Measurement of the Elastic Constants of Textured Anisotropic Thin Films from X-ray Diffraction Data,” *Appl. Phys. Lett.* 83, 473-475, 2003.

Ru, C.Q., “Simple Geometrical Explanation of Gurtin-Murdoch Model of Surface Elasticity with Clarification of its Related Versions,” *Science China-Physics Mechanics & Astronomy* 53, 3, 536-534, 2010.

Scarpa, F., Adhikari, S., Srikantha Phani, A., *Nanotechnology*, 20 , 065709 , 2009.

Schedin, F., Geim, A.K., Morozov, S.V., Hill, E.M., Blake, P., Katsnelson, M. I. et al., “Detection of Individual Gas Molecules Adsorbed on Graphene,” *Nat. Mater.*, 6 9, 652, 2007.

Schiavone, P. and Ru, C.Q, “Solvability of Boundary Value Problems in a Theory of Plane-strain Elasticity with Boundary Reinforcement,” *International Journal of Engineering Science* 47, 11-12, 1331-38, 2009.

Schmidt, D., Schadt, M., Helfrich, W., “Liquid-crystalline Curvature Elasticity,” *Naturforsch*, Z., A 27A, 277, 1972.

Sharma, N. D., Maranganti, R., Sharma, P., “On the Possibility of Piezoelectric Nanocomposites without using Piezoelectric Materials,” *Journal of the Mechanics and Physics of Solids*, 55, 2328–2350, 2007.

Sharma, P., “Size-dependent Elastic Fields of Embedded Inclusions in Isotropic Chiral Solids,” *International Journal of Solids and Structures* 41, 6317–6333, 2004.

Sharma, P., Ganti, S., “Interfacial Elasticity Corrections to the Elastic State of Quantum Dots,” *Physica Status Solidi (b)* 234, R10, 2002.

Sharma, P., Ganti, S., "The Size-dependent Elastic State of Inclusions in Non-local Elastic Solids," *Philosophical Magazine Letters* 72, 83, 745, 2003.

Sharma, P., Ganti, S., "Size-dependent Eshelby's Tensor for Embedded Nano-inclusions Incorporating Surface/Interface Energies," *Journal of Appl. Mech.*, 71, 663-671, 2004.

Sharma, P., Ganti, S., Bhate, N., "The Effect of Surfaces on the Size-Dependent Elastic State of (nano) Inhomogeneities," *Applied Physics Letters*,82, 535–537, 2003.

Sharma, N.D., Landis, C.M. and Sharma, P., "Piezoelectric Thin-film Superlattices without using Piezoelectric Materials," *Journal of Applied Physics*, 108, 024304, 2010.

Sharma, P., Wheeler, L. T., "Size-Dependent Elastic State of Ellipsoidal Nano-inclusions Incorporating Surface/Interface Tension," *Journal of Appl. Mech.*, 74, 447-454, 2007.

Shenoy, V.B., "Atomistic Calculations of Elastic Properties of Metallic fcc Crystal Surfaces," *Physical Review B*, 71, 094104, 2005.

Shim, J. H., Lee, B.J., Cho, Y. W., "Thermal Stability of Unsupported Gold Nanoparticle: a Molecular Dynamics Study," *Surface Science* 512, 3, 262, 2002.

Shodja, H.M. and Tehranchi, A., "A Formulation for the Characteristic Lengths of FCC Materials in First Strain Gradient Elasticity via the Sutton-Chen Potential," *Philosophical Magazine* 90, 14, 1893-1913, 2010.

Son, Y. W., Cohen, M. L., and Louie S. G., "Energy Gaps in Graphene Nanoribbons," *Phys. Rev. Lett.,* 97, 216803, 2006.

Spector, A., Deo, N., Grosh, K., Ratnanather, J., Raphael, R., "Electromechanical Models of the Outer Hair Cell Composite Membrane," *Journal of Membrane Biology* 209, 2-3, P 135-152, 2006.

Steigmann, D. J., "Analysis of Nonlinear Electrostatic Membranes," *Journal of Elasticity* 97, I 1, P 97-101, 2009.

Steigmann, D. J., Ogden, R. W., "Elastic Surface-Substrate Interactions," *Proc. Royal Soc. A* 453, 437-474, 1997.

Steward, E. G., C , Cook, B. P., Kellett, E. A., "Dependence on Temperature of the Interlayer Spacing in Carbons of Different Graphitic Perfection," *Nature*,1015 ,187, 1960.

Stoller, M. D., Park, S., Zhu, Y., An, J, Ruoff, R. S., "Graphene-Based Ultracapacitors," *Nano Lett,* 8 (10), 3498, 2008.

Streitz. F.H., Cammarata, R.C., sieradzki, K., "Surface-Stress Effects on Elastic Properties in Thin metal films," *Physical Review B* 49, 10699-10706, 1994.

Sun, C. T., Zhang, H., "Size-Dependent Elastic Moduli of Platelike Nanomaterials," *J. Appl. Phys.* 93, 1212–1218, 2003.

Stuart, S. J., Tutein, A. B., Harrison, " A Reactive Potential for Hydrocarbons with Intermolecular Interactions," *J. A., J. Chem. Phys.,* 112, 6472-6486, 2000.

Sveshnikov, A. A., "Problems in Probability Theory, Mathematical statistics and Theory of Random Functions," 1978.

Tagantsev, A.K. "Piezoelectricity and Flexoelectricity in Crystalline Dielectrics," *Physical Review B*, 34, 5883-5889, 1986.

Tagantsev, A.K. "Electric Polarization in Crystals and its Response to Thermal and Elastic Perturbations," *Phase Transitions*, 35, 119-203, 1991.

Tagantsev, A.K., Meunier, V., Sharma, P. "Novel Electromechanical Phenomena at the Nanoscale: Phenomenological Theory and Atomistic Modeling," *MRS Bulletin*, 34(9), 643-647, 2009.

Tian, L., Rajapakse, R.K.N.D., "Elatic Field of an Isotropic Matrix with a Nanoscale Elliptical Inhomogenity," *International Journal of Solids and Structures* 44, 24, 7988-8005, 2007.

Tian, L., Rajapakse, R.K.N.D., "Analytical Solution for Size-Dependent Elastic Field of a Nanoscale Circular Inhomogeneity," *ASME J. Appl. Mech.,* 74, 568-574, 2008.

Tichy, J., Erhart, J., Kittinger, E., Privratska, J., "Fundamentals of Piezoelectric Sensorics," *Springer* 2010

Tombros, N., Jozsa, C., Popinciuc, M., Jonkman, H.T., Van Wees, B.J., *Nature*, 448 , 571, 2007.

Katsnelson, M.I., “Graphene: Carbon in Two Dimensions,” *Mater Today* 10 1–2, 20–27, 2007

Villain, P., Beauchamp, P., Badawi, K. F., Goudeau, P., Renault, P. O., “Atomistic Calculation of Size Effects on Elastic Coefficients in Nanometersized Tungsten Layers and Wires,” *Scripta Mater*., 50, 1247–1251, 2004.

Villain, P., Goudeau, P., Renault, P. O., Badawi, K. F., “Size Effect on Intragranular Elastic Constants in Thin Tungsten Films,” *Appl. Phys. Lett.* 81, 4365-4367, 2002.

Voorhees, P.W., Johnson, W.C., “The Thermodynamics of Elastically Stresses Crystals,” Solid State Physics and Appications 59, 1-201, 2004.

Wang, G.F. and Feng, X.Q., “Effects of Surface Elasticity and Residual Surface Tension on the Natural Frequency of Micro Beams,” *Applied Physics Letters.* 90, 231904, 2007.

Wang, X., Song, J., Zhang, F., He, C., Zheng, H., and Wang, Z. K., “Electricity Generation based on One-Dimensional Group-III Nitride Nanomaterials,” *Adv. Mater.,* 22, 2155-2158, 2010.

Wang, Y., Weissmuller, J., Duan, H.L., “Mechanics of Corrugated Surfaces,” *Journal of the Mechanics and Physics of Solids* 58, 10, 1552-1566, 2010.

Wang, Z.Q., Zhao, Y.P. and Huang, Z.P., "The Effects of Surface Tension on the Elastic Properties of Nano-structures," *International Journal of Engineering Science* 48, 2, 140-50, 2010.

Weissmuller, J., Cahn, J.W., "Mean Stresses in Microstructures Due to Interface Stresses," *Acta Materialia* 45, 5, 1899-1906, 1997.

Weissmuller, J., Duan, H., "Cantilever Bending With Rough Surfaces," *Phys. Rev. Lett.* 101, 146102-1-146102-4, 2008.

Whatmore, R. W., "Pyroelectric Devices and Materials," *Rep. Prog. Phys.* 49, 1335, 1986.

Williams, P.L., Mishin, Y., Hamilton, J.C., "An Embedded-atom Potential for the Cu-Ag System," *Modelling Simulation Material Science Engineering*, 14, 817, 2006.

Workum, K. V.,de Pablo, J. J., "Local Elastic Constants in Thin Films of an FCC Crystal," *Phys. Rev. E* 67, 031601, 2003.

Yoon, D., Son, Y. W., Cheong, H., "Negative Thermal Expansion Coefficient of Graphene Measured by Raman Spectroscopy," *Nano Lett.* 11 (8), 3227, 2011.

Zubko, P., Catalan, G., Buckley, A., Welche, P.R.L. and Scott, J.F. "Strain-Gradient Induced Polarization in $SrTiO_3$," *Physical Review Letters*, 99, 167601, 2007.